Cosmopolitan abyssal lineages? A systematic study of East Pacific deep-sea squat lobsters (Decapoda: Galatheoidea: Munidopsidae)

Authors: Rodríguez-Flores, Paula C., Seid, Charlotte A., Rouse, Greg W., and Giribet, Gonzalo

Source: Invertebrate Systematics, 37(1) : 14-60

Published By: CSIRO Publishing

URL: https://doi.org/10.1071/IS22030

RESEARCH PAPER
https://doi.org/10.1071/IS22030

Invertebrate Systematics

Cosmopolitan abyssal lineages? A systematic study of East Pacific deep-sea squat lobsters (Decapoda: Galatheoidea: Munidopsidae)

Paula C. Rodríguez-Flores[A,*], Charlotte A. Seid[B], Greg W. Rouse[B] and Gonzalo Giribet[A]

For full list of author affiliations and declarations see end of paper

***Correspondence to:**
Paula C. Rodríguez-Flores
Department of Organismic and Evolutionary Biology, Museum of Comparative Zoology, Harvard University, 26 Oxford Street, Cambridge, MA 02138, USA
Email: paularodriguezflores@g.harvard.edu

Handling Editor:
Shane Ahyong

Received: 1 July 2022
Accepted: 9 November 2022
Published: 11 January 2023

Cite this:
Rodríguez-Flores PC *et al.* (2023)
Invertebrate Systematics
37(1), 14–60. doi:10.1071/IS22030

ABSTRACT

Munidopsid squat lobsters are among the most abundant decapods at abyssal depths and the most diverse squat lobster group in the East Pacific region. During recent cruises along the East Pacific, many deep-sea squat lobsters were collected. Among these, we described five new munidopsid species supported both by morphological characters and molecular phylogenetics: *Munidopsis girguisi* **sp. nov.**, *M. nautilus* **sp. nov.**, *M. testuda* **sp. nov.**, *M. cortesi* **sp. nov.** and *M. hendrickxi* **sp. nov.** We also report new records of several *Munidopsis* species across the East Pacific that increase the species distribution ranges. Here, we reconstructed the phylogenetic relationships of the East Pacific species in relation to other Galatheoidea using one nuclear and two mitochondrial gene fragment(s); we also performed single locus species delimitation analyses to explore the species status of various East Pacific munidopsid taxa. The new taxa were photographed, illustrated and imaged with micro-computed tomography. The phylogenetic results show that: (1) *Janetogalathea californiensis*, previously included in the family Galatheidae, nests within Munidopsidae; (2) the phylogenetic position of *Phylladiorhynchus* and *Coralliogalathea* as belonging in Galatheidae is not supported; and (3) *Munidopsis* is paraphyletic, agreeing with recent systematic hypotheses. Short genetic distances and species delimitation analyses suggested that a clade mostly constituted by abyssal species might include fewer species than currently considered, as species show a wider geographic range than previously considered, conforming with traditional hypotheses of cosmopolitanisms in abyssal species.

ZooBank: urn:lsid:zoobank.org:pub:CED9EB18-7061-47A7-B2FF-7F1DAFCC7B12.

Keywords: crustaceans, long-distance dispersal, microCT, mitochondrial genes, morphology, new species, species delimitation, taxonomy.

Introduction

Squat lobsters in the family Munidopsidae are deep-sea dwellers, nearly absent from shallow waters, and represent the most abundant group of decapods at abyssal depths (Baba *et al.* 2008; Macpherson *et al.* 2010; Schnabel *et al.* 2011*a*). Munidopsids currently comprise nearly 300 species in 4 genera: *Galacantha* A. Milne-Edwards, 1880, *Leiogalathea* Baba, 1969, *Munidopsis* Whiteaves, 1874 and *Shinkaia* Baba & A.B. Williams, 1998 (Dong *et al.* 2021; Rodríguez-Flores *et al.* 2022*a*). Within this family, the global genus *Munidopsis* is the most speciose, with 270 species described to date. Additional species are added nearly every year (e.g. Rodríguez-Flores *et al.* 2018, 2022*a*; Dong *et al.* 2019, 2021; Marin 2020), suggesting that a great deal of diversity remains to be discovered. Munidopsids occur in deep-sea benthos across a latitudinal gradient in both hemispheres (Baba 2005) but few records are attributed to Antarctic waters (García Raso *et al.* 2008). Several species occur on seamounts, in cold-water coral reefs or as commensals of deep-sea echinoderms, whereas others are found in habitats supporting chemosynthesis such as hydrothermal vents, cold seeps or whale falls (Baba 2005; Macpherson 2007). Only *Munidopsis serricornis* (Lovén, 1852) inhabits open water shallower than 100 m, in Norway, and *M. polymorpha* Koelbel, 1892, occurs in shallow lava tubes in

Lanzarote, Canary Islands, and these represent the species that occur at the shallowest depths in the family (Baba *et al.* 2008). Sampling these squat lobsters, as for other deep-sea fauna, is costly both in terms of time and funding. Moreover, several *Munidopsis* species are rare, known from only a few localities, few individuals or even only from the holotype (Rodríguez-Flores *et al.* 2022*a*). These factors have contributed to incomplete knowledge of species diversity and distribution patterns, making the assessment of intraspecific variation and consequent establishment of the basis for species delimitation within *Munidopsis* difficult.

Munidopsis species display high morphological disparity including several adaptations to life in the deep sea. The carapace is devoid of the typical striation of other galatheoidean squat lobsters, pigmentation is usually lacking and all species have reduced ocular orbits. Phylogenetic analyses have suggested that the genus *Munidopsis* is paraphyletic or polyphyletic (Ahyong *et al.* 2011; Rodríguez Flores 2021). Indeed, the sequential addition of taxa previously not included in the squat lobster tree of life has challenged the taxonomic status of several families, revealing that the current formal classification needs revision (Schnabel *et al.* 2011*b*; Rodríguez-Flores *et al.* 2022*b*). For example, members of *Leiogalathea* have an external habitus like that of the members of the squat lobster family Galatheidae, with well-developed eyes, a carapace dorsally covered by setose short striae and a triangular broad-on-base rostrum. However, previous studies (Ahyong *et al.* 2011; Schnabel *et al.* 2011*b*; Bracken-Grissom *et al.* 2013) placed *Leiogalathea* as the sister group to all other munidopsid taxa and this is currently classified within Munidopsidae. Given this fact, morphological convergence and homoplasy have contributed to a confusing taxonomic classification of squat lobsters, highlighting that systematics based solely on external characters of the carapace and rostrum should be cautiously considered

Studies on the biogeography of deep-sea squat lobsters have shown that the East Pacific diversity is apparently poor compared to that of the West Pacific basin (Macpherson *et al.* 2010; Schnabel *et al.* 2011*a*). Nevertheless, Munidopsidae remains the most diverse family of squat lobsters in this region, with more than 50 of the 73 known galatheoidean species from the East Pacific (Baba and Wicksten 2019). Other squat lobsters are poorly represented; for example Galatheidae includes only two species, *Janetogalathea californiensis* (Benedict, 1902), a common species occurring along the northern East Pacific, and *Galathea paucilineata* Benedict, 1902, only known from a damaged specimen collected in Galapagos. Two species of *Phylladiorhynchus* Baba, 1969 were recorded from Corral and Valparaiso in Chile but the systematic status in Galatheidae is dubious (Rodríguez-Flores *et al.* 2021, 2022*b*). Over 30 *Munidopsis* species from the East Pacific Munidopsidae represent East Pacific endemics, whereas the remaining species are found in the West and East Pacific, and few of these are distributed across the East Pacific and Atlantic (Jones and Macpherson 2007; Baba *et al.* 2008). Nine Munidopsidae species have been found in association with hydrothermal vents or cold seeps along the East Pacific including the endemic *Munidopsis lentigo* Williams & Van Dover, 1983, that is only known from the northern East Pacific Rise near Baja California. Several studies suggest that species with an abyssal distribution recorded from abyssal plains and seamounts have wider geographic ranges than species with bathyal distributions and those living in hydrothermal vents or cold seeps (Etter *et al.* 2005; McClain and Hardy 2010; Etter *et al.* 2011). Additionally, previous studies on squat lobsters have suggested rapid radiation or retardation in the molecular evolution of some deep-sea lineages (Machordom and Macpherson 2004; Cabezas *et al.* 2012; Rodríguez-Flores *et al.* 2020) coupled with a recent deep-sea colonisation. Therefore, poor genetic structure has been observed in bathyal and abyssal lineages of squat lobsters with cosmopolitan distributions whereas species from the continental shelf tend to have deeper genetic structure and display allopatry.

Thanks to an increased effort in deep-sea exploration during the past few decades (e.g. Hatch *et al.* 2020; Marlow *et al.* 2022; O'Hara *et al.* 2020; Salinas-de-León *et al.* 2020), the availability of deep-sea squat lobster material in museum collections has increased considerably. During the revision of squat lobster material recently sampled along the East Pacific, new taxa and records were identified. In an integrative taxonomic framework, we describe new deep-sea munidopsid squat lobsters from the East Pacific. We also reconstruct the phylogenetic relationships among East Pacific species based on two mitochondrial markers and one nuclear fragment (cytochrome *c* oxidase subunit I, *16S* rRNA and *28S* rRNA), aiming to explore the systematic position of the East Pacific munidopsids and *Janetogalathea californiensis*, currently in Galatheidae. Finally, we test species hypotheses within Munidopsidae based on morphology and single locus species delimitation methods to (1) test the taxonomic status of these species; (2) explore molecular and morphological diversity within the family; and (3) infer the effect of depth range in the geographic speciation pattern of this lineage.

Methods

Sampling

Museum specimens were collected during various oceanographic cruises. These included several expeditions by Charlotte A. Seid and Greg W. Rouse during the past decade that aim to explore and characterise East Pacific deep-sea (>200 m) biodiversity through the use of remotely operated vehicles (ROVs: *Doc Ricketts*, *Hercules*, *SuBastian* and *Tiburon*) and the human occupied vehicle (HOV) *Alvin*. During these expeditions, specimens were collected using suction samplers, hydraulic manipulators or other submersible-

deployed devices. Specimens were maintained alive in chilled seawater, photographed using a handheld camera or photomicroscope, sampled for genetics into 95% ethanol for long-term storage at −20°C and vouchered for morphology (treated with 10% seawater formalin or 95% ethanol for at least 24 h and subsequently transferred to 50% ethanol for long-term archival).

Morphological examination

Specimens were examined using a Leica MZ 12.5 stereomicroscope. Drawings were made using a camera lucida and digitised with a Wacom Intuos Pro tablet. Terminology used for the species descriptions followed Baba *et al.* (2009, 2011). Size was indicated by postorbital carapace length. Rostrum length was taken from the base (frontal margin) to the tip of the rostrum; rostrum width was taken as the width of the base. Measurements of appendages were taken on dorsal (pereopod 1), lateral (antennule, pereopods 2–4) and ventral (antenna) midlines. Ranges of morphological and meristic variations were included in the description. Abbreviations used were as follows: Mxp, maxilliped; P1, pereopod; 1 (cheliped); P2–4, pereopods 2–4 (walking legs 1–3); M, male; F, female; ov., ovigerous. Type material of *Munidopsis quadrata* Faxon, 1893, *M. carinipes* Faxon, 1893, *M. margarita* Faxon, 1893 and *M. townsendi* Benedict, 1902 was examined and illustrated. All specimens were deposited in the Invertebrate Zoology collection at the Museum of Comparative Zoology (MCZ IZ), Cambridge, MA, USA; the Invertebrate Zoology collection at the California Academy of Sciences (CASIZ), San Francisco, CA, USA; the Benthic Invertebrate Collection at Scripps Institution of Oceanography (SIO-BIC), University of California San Diego, La Jolla, CA, USA; the Invertebrate Zoology collection at the Smithsonian National Museum of Natural History (USNM), Washington, DC, USA; the Museo de Zoología, Universidad de Costa Rica (MZUCR), San José, Costa Rica; and the Muséum national d'Histoire naturelle (MNHN), Paris, France.

Micro-CT imaging

Only new species with an intact external morphology were scanned, to avoid further damage to the types. We mounted specimens in plastic vials, without staining, dry and using polypropylene cotton. We used 15-mL Falcon tubes or 1.5-mL Eppendorf tubes, depending on the size of the specimens, sealed with Parafilm.

Micro-computed tomography (micro-CT) scans were conducted in a SkyScan 1273 scanner (Bruker MicroCT, Kontich, Belgium). The scanner was equipped with a Hamamatsu 130/300 tungsten X-ray source 40–130 kV and a 6-megapixel (3072 × 1944) flat-panel X-ray detector. Scanning parameters were as follows: source current, 100 µA; source voltage, 75 kV; exposure time, 1000 ms; frames averaged, 2–6; rotation step, 0.3; frames acquired over 180° = 960; no filter; no binning; activated flat field correction; and scanning time, 50–120 min. Computer images were reconstructed using the software NRecon (ver. 1.6.6.0, Bruker MicroCT, Kontich, Belgium). To enhance image contrast and compensate for ring and streak artefacts, the following reconstruction parameters were set: no smoothing; ring artefact correction, 5–11; and activated beam hardening correction. Three-dimensional-rendering was performed using CTvox software (ver. 2.2, Bruker).

DNA extraction, amplification and sequencing

Specimens used for DNA extraction were dissected under a stereomicroscope. Tissue subsampled from the 5th pereopod was digested overnight using the DNeasy Blood & Tissue kit (Qiagen) following the manufacturer's protocol. Partial sequences of the mitochondrial gene cytochrome *c* oxidase subunit I (*COI*), *16S* ribosomal RNA and nuclear *28S* ribosomal RNA were amplified by polymerase chain reaction (PCR) using the following combination of primers: LCO 1490/HCO 2198 (Folmer *et al.* 1994) or alternatively a squat-lobster-specific primer 3′ from LCO 1490, tenuiCOIFwint/HCO 2198 (Rodríguez-Flores *et al.* 2019*a*); 16Sa/16Sbr (Palumbi 1991) or 16S1471/16S1472 (Crandall and Fitzpatrick 1996); and 28SBR/28Sphyf2 (Palero 2008; Rodríguez-Flores *et al.* 2022*b*). PuReTaq Ready-To-Go (RTG) PCR Beads (Cytiva) were employed for the DNA amplification, following these cycle conditions: 5 min of initial denaturation at 95°C followed by 35 cycles of 30 s of denaturation at 95°C, 45 s of annealing at 45–50°C, 1 min of extension at 72°C and a 10-min final extension at 72°C. Purification of the amplicons was carried out using ExoSAP-IT (Affymetrix). Sanger sequencing of both forward and reverse strands was performed by GeneWiz (Cambridge). Forward and reverse DNA sequences obtained for each specimen were checked and assembled using Sequencher (ver. 5.4, Gene Codes Corporation, Ann Arbor, MI, USA). The presence of pseudogenes was checked using either Sequencher or the web tool EXPASY (https://web.expasy.org/translate/) translating the nucleotide sequences to amino acids under the invertebrate mitochondrial genetic code. Ribosomal gene sequences were aligned with MAFFT (Katoh *et al.* 2002) using the iterative method L-INS, recommended for sequences with conserved domains flanked by long variable regions, such as in the dataset analysed here, especially for the *28S* rRNA gene. A posteriori manual checking and correction of the alignments was carried out in AliView (ver. 1.26, see https://ormbunkar.se/aliview/; Larsson 2014). The alignment of the concatenated gene fragments was built in PAUP (ver. 4.0a, build 169, see https://paup.phylosolutions.com/; Swofford 2003). We also calculated the uncorrected genetic distance (*p*) between the new species and closest relatives using PAUP.

Phylogenetic analyses

Phylogenetic analyses were performed using two different data sets: (1) concatenated data of 152 taxa and (2) *COI*

data alone that included a larger number of terminals available in public databases, with 212 sequences of 82 named species. We first retrieved sequences from previous publications from the NCBI database (Ahyong *et al.* 2011; Bracken-Grissom *et al.* 2013; Rodríguez-Flores *et al.* 2018, 2019*a*, 2022*a*, 2022*b*; Dong *et al.* 2019, 2021). In the first dataset (1), we included wide taxonomic sampling across Galatheoidea (Galatheidae, Munididae, Munidopsidae and Porcellanidae), providing a phylogenetic framework to test the systematic position of the East Pacific species. We rooted the tree with the Lithodidae *Paralithodes camtschaticus* (Tilesius, 1815) (see Supplementary Table S1 for details on the taxonomic sampling). For the second dataset (2) we selected *Janetogalathea californiensis* (Benedict, 1902) as the outgroup for Munidopsinae (*sensu* Ahyong *et al.* 2011). We ran MrBayes (ver. 3.2.1, see https://nbisweden.github.io/MrBayes/download.html; Huelsenbeck and Ronquist 2001) for the Bayesian inference (BI) analyses. We selected a partition scheme by gene and codon for *COI* in the concatenated dataset and by codon in the *COI* dataset, according to the results of Model Selection in W-IQ-TREE online (ver. 1, see http://iqtree.cibiv.univie.ac.at/; Trifinopoulos *et al.* 2016) based on a Bayesian information criterion (BIC). For the MrBayes analyses we set the parameters of the likelihood model as 'mixed' for the nucleotide substitution model and the rates as 'invgamma'. Four Markov Chains Monte Carlo (MCMC) were run for 5×10^7 generations and sampling trees and parameters every 5000 generations for the estimation of the posterior probabilities. The initial 25% of the generations were discarded as burn-in. Bayesian analyses were run in the CIPRES portal (see http://www.phylo.org/; Miller *et al.* 2010). We also ran maximum likelihood analyses (ML) to compare both ML and BI results. The ML tree was inferred with W-IQ-TREE online (ver. 1; Trifinopoulos *et al.* 2016). Bootstrap support values were calculated with 1000 pseudoreplicates and the other parameters were set as default. Nodes were considered supported when bootstrap values (Bs) were higher than 70% and posterior probability (pP) higher than 0.95. Phylogenetic trees were plotted and edited in FigTree (ver. 1.4.4, see http://tree.bio.ed.ac.uk/software/figtree/). Posterior probabilities from the Bayesian Inference and bootstrap support from ML were included in the final tree.

Single locus species delimitation analyses

To test species hypotheses, we ran single locus species delimitation analyses using the *COI* dataset. The choice of this marker was based on utility in taxonomy and species delimitation in crustaceans, and broad data availability for further comparisons (i.e. Jones and Macpherson 2007). We employed several heuristic methods for these analyses: (1) distance-based methods: Assemble Species by Automatic Partitioning method (ASAP) (Puillandre *et al.* 2021) and Automatic Barcode Gap Discovery for primary species delimitation (ABGD); and (2) tree-based methods based on the Phylogenetic Species Concept: the Poisson Tree Process (PTP) (Zhang *et al.* 2013) and generalised mixed Yule coalescence (GMYC) (Fujisawa and Barraclough 2013). We compared the results of these methods with currently accepted species.

ASAP is an exploratory tool to identify the best partitions of species by implementation of a hierarchical clustering algorithm that is based on pairwise genetic distances. ASAP efficiently builds species partitions from single locus sequence alignments (Puillandre *et al.* 2021). We ran ASAP through the online server (see https://bioinfo.mnhn.fr/abi/public/asap/asapweb.html). We selected simple distances (*p*-distances) as the substitution model to compute the distances. The probability under the group split was set to 0.01. The ABGD method delimits species in terms of the barcode gap between the intraspecific and interspecific genetic distances. This method detects the barcoding gap as the first significant gap beyond a given limit as proxy of species partition (Puillandre *et al.* 2012). ABGD was run online (see https://bioinfo.mnhn.fr/abi/public/abgd/abgdweb.html). We set the parameter values as follows: $P_{min} = 0.001$; $P_{max} = 0.1$; steps = 10, Nb bins = 20. The parameter X (relative gap width) was initially set to 2.0 and subsequently modified according to the exploration analyses. The model of evolution was simple *p*-distance, based on a barcode gap of 2%.

The PTP model infers species boundaries by modelling speciation or branching events based on the number of substitutions in a given gene tree (Zhang *et al.* 2013). bPTP adds Bayesian support (BS) values to delimited species on the input tree file. As input, we used the unrooted ML tree obtained with IQTREE. We ran the analyses for 5×10^5 MCMC generations with a thinning set at 500, burn-in = 25% and removing outgroups to improve the delimitation results. The analyses were carried using the web tool platform bPTP server (see http://species.h-its.org/ptp/). We checked MCMC convergence after the run.

GMYC is a species delimitation method that uses a speciation and neutral coalescent model (Yule 1925; Hudson 1991). GMYC was run in R (ver. 4.1.2, R Foundation for Statistical Computing, Vienna, Austria, see https://www.R-project.org/) by using the 'splits' package (ver. 1.0-20, see http://r-forge.r-project.org/projects/splits). We obtained an ultrametric tree in BEAST (ver. 2.6, see https://www.beast2.org/; Bouckaert *et al.* 2019) for the GMYC analyses, using the package Beast Model test to select the substitution model fitting the data. We set a Relaxed log normal clock for the clock model since this allows rate heterogeneity among branches. As our purpose was only to obtain an ultrametric tree and not calibrate the molecular clock, we set the clock rate to 1.0. We set the tree prior to the Birth–Death model with a Birth rate distribution uniform (Lower = 0.0, Upper = 1000.0) and a Death rate distribution uniform (Lower = 0.0, Upper = 1.0.). Chain length for the MCMC run was 10 000 000 generations logging every 1000 generations. A maximum clade credibility tree was obtained, after discarding 25% of the trees, using TreeAnnotator (ver. 2.1.2,

see https://www.beast2.org/treeannotator/; Drummond and Rambaut 2007). The bGMYC analysis was first run with the resulting maximum clade credibility (MCC) tree and subsequently with 100 randomly selected trees from the 7500 post-burn-in trees in the bGMYC package (ver. 1.0.2, see https://nreid.github.io/software/; Reid and Carstens 2012). We used the following uniform priors: Yule process rate change (0–5), coalescence process rate change (0–1.5), and threshold parameter or number of taxa (1–16). Then, a scale for these parameters (1, 1, 0.2) was fixed. The results were plotted to check for convergence.

Haplotype networks were built for selected clades including East Pacific samples in taxa with taxonomic uncertainty or potential species complexes. Haplotype networks were built with the R package pegas (ver. 1.1, see https://cran.r-project.org/package=pegas; Paradis 2010) using a parsimony network with the function haploNet. Maps for *Munidopsis* species were drawn in R by using the packages ggplot 2 (ver. 3.4.0, see https://ggplot2.tidyverse.org/; Kahle and Wickham 2013), rnaturalearthdata (ver. 0.1.0, see https://cran.r-project.org/package=rnaturalearthdata; South and South 2016) and gridExtra (ver. 2.3, B. Auguie, A. Antonov and M. B. Auguie, see https://cran.r-project.org/package=gridExtra).

Results

The overall results of our phylogenetic analyses and morphological examination converged on the presence of 5 new species in the eastern Pacific: *Munidopsis girguisi* **sp. nov.**, *Munidopsis nautilus* **sp. nov.**, *Munidopsis testuda* **sp. nov.**, *Munidopsis hendrickxi* **sp. nov**. and *Munidopsis cortesi* **sp. nov.** Results of our analyses on morphological and molecular data suggest the need for establishing the following synonymies: *Munidopsis alfredolaguardai* Hendrickx & Ayón-Parente, 2013 and *M. townsendi* Benedict, 1902 are proposed as junior synonyms of *Munidopsis aspera* (Henderson, 1885); and *Munidopsis asiatica* Marin, 2020 is here proposed as a junior synonym of *Munidopsis similis* Smith, 1885. *Janetogalathea californiensis* is recovered as sister of *Leiogalathea* within the Munidopsidae clade, therefore this taxon should be reassigned from Galatheidae.

Phylogenetic results

According to model finder in IQ-TREE the best scheme and models obtained fitting our data were GTR+F+G4 for the first codon position, TN+F+I+G4 for the second and TIM3e+I+G4 for the third codon for *COI*, TVM+F+I+G4 for *16S* rRNA and TVMe+I+G4 for *28S* rRNA.

Results of ML and BI analyses yielded trees with congruent topologies. Munidopsidae was recovered as monophyletic with high support (Bs = 96% and pP = 1.00) (Fig. 1). Galatheidae was recovered as non-monophyletic

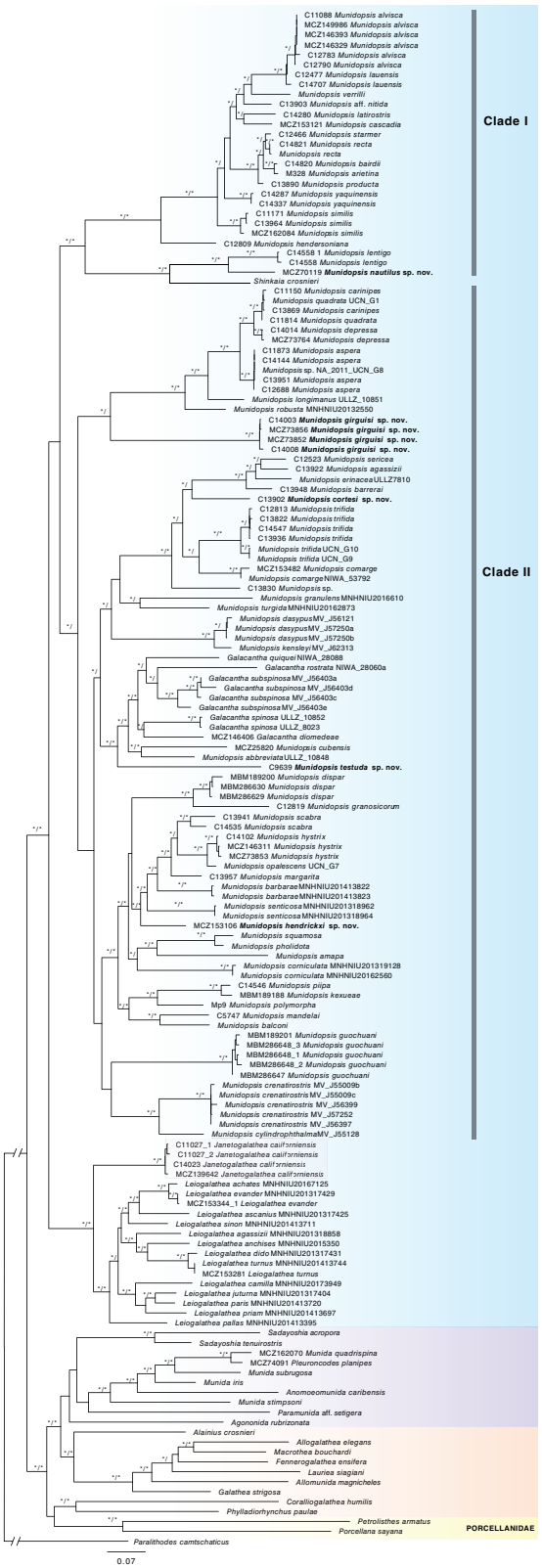

Fig. 1. Phylogenetic hypothesis of the concatenated data set (*COI* + *16S* rRNA + *28S* rRNA) resulting from the ML analysis. Tip labels in bold indicate new taxa. Asterisks indicate supported nodes: ML bootstrap support >70%/Bayesian posterior probability >0.95.

since the genera *Coralliogalathea* Baba & Javed, 1974 and *Phylladiorhynchus* (both currently in Galatheidae) formed a clade unrelated to the remainder of the Galatheidae. This clade was sister group to Porcellanidae (although without support: Bs < 70% and pP < 0.95), both being sister group to a clade including Munididae + Galatheidae (excluding *Coralliogalathea* and *Phylladiorhynchus*) with relatively high support (Bs = 91% and pP = 0.96).

We did not obtain high support for the monophyletic clade including the family Munididae (Bs < 70% and pP < 0.95) although the clade with Munididae and most Galatheidae was well supported. The family Munidopsidae was recovered as sister group to the clade that includes the other galatheoids. This latter clade received a Bs = 71% and a pP = 1.00.

Within Munidopsidae, *Munidopsis* was recovered as polyphyletic, since *Galacantha* and *Shinkaia* were clustered within the genus. A clade including all the samples of *Leiogalathea* and *Janetogalathea* was recovered with maximal support. This clade was the sister group to the remaining Munidopsidae species and this grouping also received maximal support. The clade with the remaining Munidopsidae did not receive high support, and was split into what we have named Clade I and Clade II (see Fig. 1). Clade I, which received maximal support, included mostly bathyal and abyssal species (e.g. *Munidopsis alvisca* Williams, 1988; *M. bairdii* (Smith, 1884); *M. recta* Baba, 2005; *M. verrilli* Benedict, 1902; *M. starmer* Baba & de Saint Laurent, 1992; and *M. producta* Baba, 2005). Many internal relationships within Clade I were poorly supported. Clade I divided into two early subgroups, one composed of *Munidopsis lentigo* and *Munidopsis nautilus* **sp. nov.**, and one with the remaining species. *M. hendersoniana* Faxon, 1893 was sister group to the remaining species within the latter clade.

Clade II included the remaining Munidopsidae species analysed (Fig. 1), most of which inhabit shelf and slope depths. Most of the deep relationships within this clade were poorly supported; however, some species-groups with congruent morphology were recognised with the molecular data, for example the *aspera*-group including species with elongated ocular peduncles [*M. carinipes* Faxon, 1893; *M. quadrata* Faxon, 1893; *M. depressa* Faxon, 1893; *M. aspera* (Henderson, 1885); *M. longimanus* (A. Milne Edwards, 1880); and *M. robusta* (A. Milne Edwards, 1880)]; the *crenatirostris*-group [*M. crenatirostris* Baba, 1988 + *M. cylindrophthalma* (Alcock, 1894)]; the genus *Galacantha*; the *dasypus*-group (*M. dasypus* Alcock, 1894 + *M. kensleyi* Ahyong & Poore, 2004); and the *polymorpha*-group (*M. polymorpha* + *M. piipa* Marin, 2020 + *M. kexueae* Dong, Gan & X Li, 2021).

For the most part, the new species described below were scattered across the phylogeny and not closely related. *Munidopsis girguisi* **sp. nov.** clustered as the sister taxon of the *aspera*-group but with low support (Bs = 88% and pP < 0.95). *Munidopsis cortesi* **sp. nov.** was included in the *trifida*-group constituted by species with a trifid rostrum: e.g. *M. erinacea* (A. Milne-Edwards, 1880); *M. agassizii* Faxon, 1893; *M. barrerai* Bahamonde, 1964; *M. comarge* Taylor, Ahyong & Andreakis, 2010; and *M. trifida* Henderson, 1885; however, the systematic position as sister group of the clade including *M. sericea* Faxon, 1893 + *M. agassizii* + *M. erinacea* was poorly supported (Bs = 82% and pP < 0.95). *Munidopsis hendrickxi* **sp. nov.** is related to the clade including *M. scabra* Faxon, 1893; *M. hystrix*; *M. opalescens* Benedict, 1902; *M. barbarae* (Boone, 1927); *M. margarita*; and *M. senticosa* Rodríguez-Flores, Macpherson & Machordom, 2018. *Munidopsis testuda* **sp. nov.** was sister group to a clade including *M. abbreviata* (A. Milne-Edwards, 1880) + *M. cubensis* Chace, 1942 plus all the *Galacantha* species. This grouping was highly supported (Bs = 98% and pP = 1).

Phylogenetic analyses of the *COI* fragment alone showed shallow divergences and wide distributional species ranges within the clade including bathyal and abyssal species (Clade I), contrasting with the deep divergences and allopatric distribution within the clade mostly containing species from the continental shelf and slope (Clade II) (Fig. 2). However, in a few cases *Munidopsis* species hypotheses were not supported by species delimitation analyses.

Species delimitation results

The different species delimitation analyses recovered largely congruent results but some methods tended to propose more species than others (see Fig. 2). ASAP recovered 10 species partition schemes, of which the best partition recovered 64 groups from the originally proposed 82 species including the outgroup. ABGD recovered 7 partitions when setting the parameter $X = 1$ after exploring the data and found the barcode gap width around this threshold. The initial species partition hypotheses found 57 groups (Partition with prior maximal distance $P = 1.29 \times 10^{-2}$; Barcode gap distance = 0.080; Distance Simple Dist MinSlope = 1.000000). The recursive analyses delimited up to 79 species, finding in all cases a barcode gap of ~0.08. bPTP results estimated a number of groups or species between 75 and 107 (mean 88) but only 79 of these presented support values higher than 50%. GMYC results were similar to the bPTP results, estimating 82 species with a confidence interval of 80–85 and a maximum likelihood of the GMYC model of 1438.268.

All these methods were congruent in suggesting that clade I (Fig. 2) comprised fewer species than currently accepted, i.e. all methods grouped multiple available names as single species. The clade including the mostly bathyal and abyssal species *Munidopsis arietina* Alcock & Anderson, 1894, *M. bairdii*, *M. bracteosa* Jones & Macpherson, 2007, *M. recta*, *M. scotti* Jones & Macpherson, 2007, *M. antonii* (Filhol, 1884) and *M. exuta* Macpherson & Segonzac, 2005 was resolved as a single species by all methods. The clade including *M. vrijenhoeki* Jones & Macpherson, 2007, *M. nitida* (A. Milne-Edwards, 1880) and *M. spinifrons*

Fig. 2. Phylogenetic hypotheses based on the *COI* data alone resulting from the Bayesian analysis, with results from the species delimitation analyses (ASAP, ABGD, bPTP, GMYC); a grey box indicates that the specimens are not part of the species hypothesis of the black bar. Tip labels in bold indicate new taxa. Colours indicate geographic distribution as specified on the map. Gradients of depth and habitat are also indicated. Asterisks indicate supported nodes: ML bootstrap support >70%/Bayesian posterior probability >0.95.

Dong, Xu, Li & Wang, 2019 was resolved as a single species by the distance-based methods but as four or five species by the tree-based methods. The hydrothermal vent species *M. alvisca* Williams, 1988 from the East Pacific, *M. lauensis* Baba & de Saint Laurent, 1992 and *M. myojinensis* Cubelio, Tsuchida, Hendrickx, Kado & Watanabe, 2007 from the

West Pacific were considered a single species in all analyses and therefore this study supports the idea of a single species broadly distributed across hydrothermal vent sites across the Pacific and Indian Oceans; this is evidenced by the morphological conservatism between *M. lauensis* and *M. alvisca* that makes these species morphologically indistinguishable once multiple specimens per population are examined. An inability to distinguish species on a molecular basis occurs in *M. similis* and *M. asiatica*, two species that are extremely similar, and *M. albatrossae* Pequegnat & Pequegnat, 1973 and *M. aries* (A. Milne-Edwards, 1880), where the three specimens sampled from the Atlantic, East and West Pacific are not distinguished as different species. Additional species not supported by our species delimitation analyses include *M. quadrata* and *M. carinipes* (by all methods) and some methods also include *M. depressa* with these two species. Additionally, *M. piipa* and *M. kexueae* Dong, Gan & Li, 2021 are shown as a single species by some methods but not by GMYC, and *M. kensleyi* and *M. dasypus* are sometimes supported as one species and sometimes as two or three species. By contrast, *M. scabra* from California and Costa Rica, and *Galacantha subspinosa* Macpherson, 2007 (all sequences from GenBank) appear as multiple species.

Haplotype networks

We reconstructed haplotype networks for the following selected clades: *M. aspera*; *M. quadrata* + *carinipes*; *M. piipa* + *M. kexueae*; and *M. similis* + *M. asiatica* (Fig. 3, 4). For *Munidopsis aspera* we included haplotypes from six individuals and a sequence from GenBank identified as *Munidopsis* sp. (from Chile) that nested within *M. aspera*. We found six haplotypes from these seven sequences, five of which were unique, and one of which was shared among individuals from Magellan Strait and the Gulf of California. These haplotypes were connected by a single mutational step. We found unique haplotypes for each of the six specimens analysed for *M. quadrata* and *M. carinipes* with a distance between haplotypes of three to five mutational steps. The haplotype network did not segregate the haplotypes among the two species sampled. For *Munidopsis piipa* from the Bering Sea and California, and *M. kexueae* from the West Pacific, haplotypes were also unique for each specimen and the haplotype network clearly separated the *M. kexueae* specimen from *M. piipa*, with 19 mutational steps between the two groups of haplotypes. This contrasted with some of the species delimitation analyses (Fig. 2) that found *M. kexueae* nested within *M. piipa* or assigned the four specimens as a single species. In the case of *Munidopsis similis* and *M. asiatica*, we found unique haplotypes for each specimen analysed, with a minimum distance between connected haplotypes of 2 and a maximum of 9 mutational steps. Interestingly, two of the most extreme haplotypes were from specimens from nearby localities in California. However, *Munidopsis asiatica* from the Sea of Okhotsk, NW Pacific, only differed from a specimen from the Pacific of Costa Rica by two mutational steps. Although all the samples from the Gulf of Mexico formed a group, one of the Pacific samples appeared closer to these than to the other Pacific samples.

Permits

Specimen collection and field operations in Costa Rica were performed under the following permits issued by CONAGEBIO (Comisión Nacional para la Gestión de la Biodiversidad), INCOPESCA (Instituto Costarricense de Pesca y Acuicultura) and SINAC (Sistema Nacional de Áreas de Conservación) under MINAE (Ministerio de Ambiente y Energía), Government of Costa Rica: INCOPESCA-CPI-003-12-2018, R-070-2018-OT-CONAGEBIO, SINAC-CUSBSE-PI-R-032-2018, SINAC-SE-CUS-PI-R-035-2017. In accordance with the Nagoya Protocol on Access and Benefit Sharing, DNA sequencing for this project was authorised by the Contract for the Grant of Prior Informed Consent between MINAE-SINAC-ACMC and Jorge Cortés Nuñez for the Basic Research Project: 'FK190106 – Cuantificación de los vínculos biológicos, químicos y físicos entre las comunidades quimiosintéticas con el mar profundo circundante.'

Systematics

GALATHEOIDEA Samouelle, 1819

MUNIDOPSIDAE Ortmann, 1898

Genus ***Janetogalathea*** Baba & Wicksten, 1997

Janetogalathea californiensis (Benedict, 1902) family **Munidopsidae** stat. nov.

(Fig. 5*a*, *b*.)

Galathea californiensis Benedict, 1902

Material examined

Non-type specimens. USA: off San Diego, California, leg. Harim Cha, Kent Trego, R/V *New Horizon* student cruise; 28.x.2007, 32.67500°N, 117.36330°W, 175–300 m: 1 M 24.1 mm, 1 F 14.9 mm (SIO-BIC C11027). — USA: Crespi Knoll, off California, leg. Emily McLaughlin, Jessica Pruitt, R/V *Falkor*, ROV *SuBastian* dive S0169 Slurp 2, 13.x.2018, 33.09770°N, 117.86790°W, 484.2 m: 1 F 5.5 mm (SIO-BIC C14023). — USA: California, leg. E/V *Nautilus*, ROV Hercules dive H1534, Stn NA074-027-01, 14.vii.2018, 33.95930°N, 119.47540°W, 172.4 m: 1 F 9.5 mm (MCZ IZ-139642).

Diagnosis

Modified from Macpherson and Baba (2011). Carapace with transverse striae usually granulated with numerous short

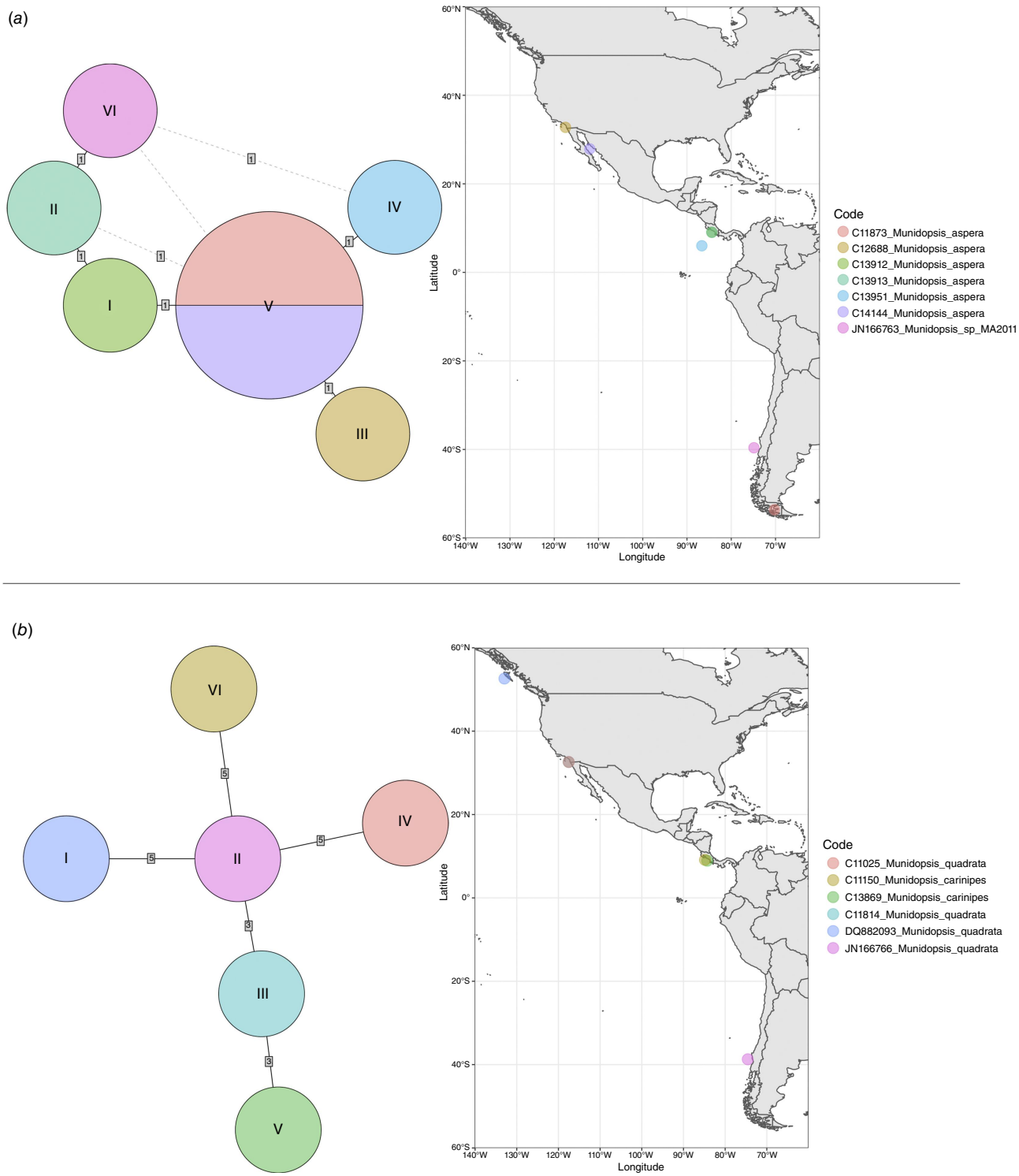

Fig. 3. Haplotype networks with haplotype distributions for (*a*) *Munidopsis aspera* and (*b*) *M. quadrata* + *M. carinipes*.

setae and scattered stiff long setae, laterally with 4–6 spines, cervical grooves distinct. Rostral spine flattish, subtriangular, lateral margin usually with 3–4 lateral spines, proximal small. With a pair of epigastric spines. Frontal margins slightly oblique. Orbit not distinctly excavated, without outer orbital angle. Anterolateral spine of carapace strong. Branchial margin with 4 spines. Abdominal somites 2–4 with 2 transverse ridges, unarmed. Telson incompletely subdivided. Sternite 3 narrow, expanded laterally, sternite 4 subtriangular. Eyes large, movable, cornea strongly dilated. Article 1 of antennule

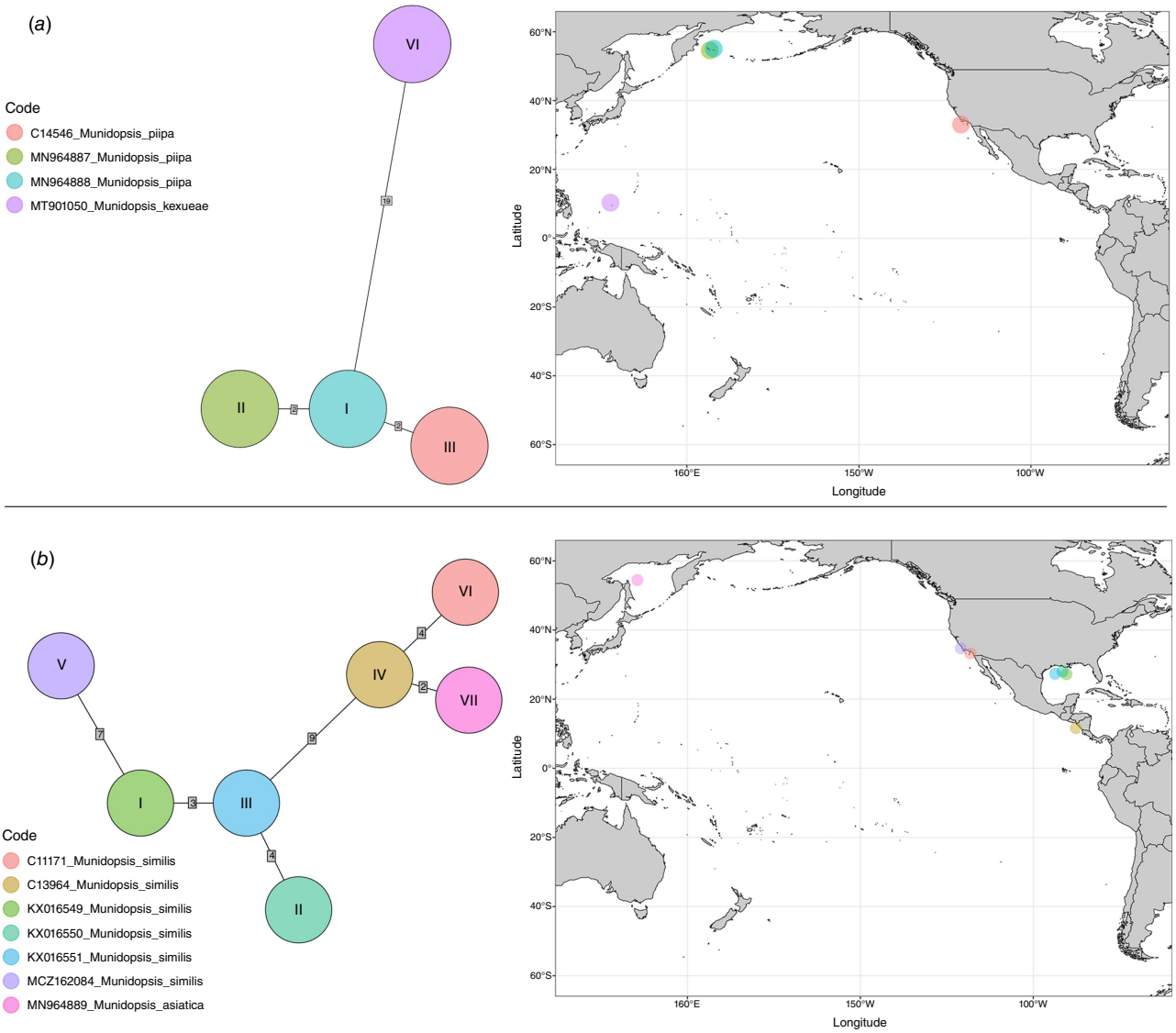

Fig. 4. Haplotype networks with haplotype distributions for (*a*) *Munidopsis piipa* + *M. kexuae* and (*b*) *M. similis* + *M. asiatica*.

with 3 well-developed spines. Article 1 of antenna with distomesial spines short, fused with orbit. Short and thick flagellum on Mxp1. Mxp3 merus as long as ischium, subrhomboidal in lateral view. P1 slender, elongate. P2–4 long and slender; dactyli slender, curving, flexor margin with spine-like setae. Epipods absent from all pereopods.

Colouration

Carapace and abdomen reddish or light orange. P1–4 light orange.

Distribution

Baja California, Gulf of California, Mexico Channel Islands, California, USA. From 89- to 3993-m depth (see comments in Hendrickx 2021 and Hendrickx *et al.* 2011, regarding *J. californiensis* geographic distribution).

Genetic data

COI, *16S* rRNA and *28S* rRNA.

Remarks

Janetogalathea californiensis is now included in the family Munidopsidae due to evidence from molecular phylogenetics placing this as sister group of *Leiogalathea*, according to nuclear and mitochondrial data. We investigated the presence of the chief synapomorphy of Munidopsidae, the absence of a short or reduced flagellum on the exopod of the Mxp1. The Mxp 1 exopod presents a short, thick pseudoflagellum, as in *Leiogalathea* (Ahyong *et al.* 2010). However, the validity of this character as a synapomorphy for Munidopsidae is questionable. Both *Leiogalathea* and *Janetogalahea* also share the presence of a broad triangular

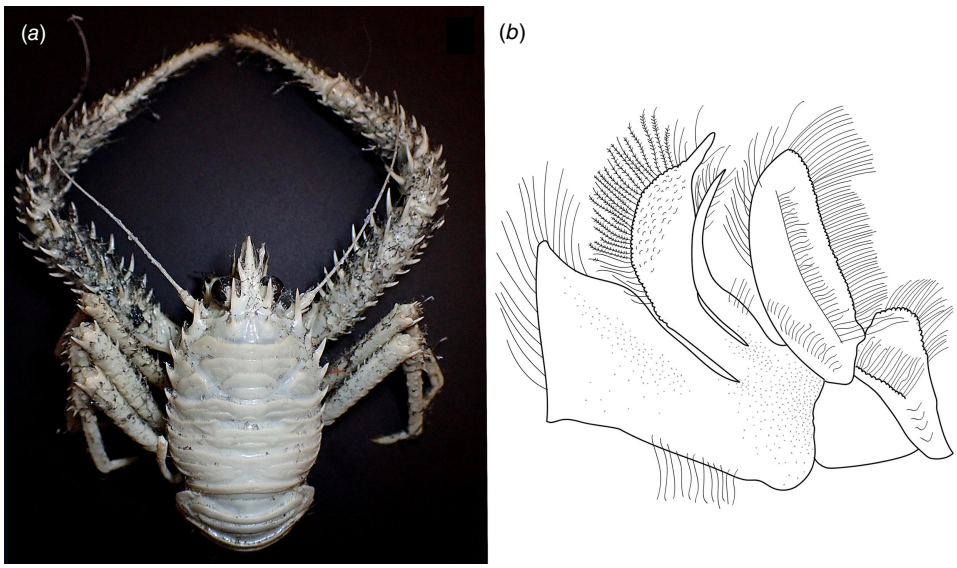

Fig. 5. *Janetogalathea californiensis* (Benedict, 1902). (*a*) Mxp1, lateral view, California (MCZ IZ-139642). (*b*) General habitus, dorsal view, 1 M (SIC BIO C11027) San Diego, CA, USA.

or subtriangular rostrum, a well-developed cornea and a carapace with few to several transverse setose striae. *Janetogalathea* and *Leiogalathea* could arguably form a clade that could be assigned family rank, showing morphological convergence with squat lobsters in the family Galatheidae but this will be addressed in future studies.

The wide bathymetric distribution and dubious morphological identification of specimens from the Galapagos Islands (Arnés-Urgellés *et al.* 2020; Hendrickx 2021) suggest that *Janetogalathea californiensis* could constitute a species complex. A deeper study including genetic data across the species range should be conducted to test this hypothesis.

Genus ***Munidopsis*** Whiteaves, 1874

Munidopsis aspera (Henderson, 1885)

(Fig. 6*a–j*, 7*a–e*, Supplementary Fig. S1.)

Elasmonotus asper Henderson, 1885

Munidopsis townsendi Benedict, 1902, **syn. nov.**

Munidopsis alfredolaguardai Hendrickx & Ayón-Parente, 2013, **syn. nov.**

Material examined

Holotype (*M. townsendi*). ECUADOR: Galapagos Islands, Santa Cruz and San Cristobal Islands, leg. USFC Steamer *Albatross*, Stn 2818, field number USFC/A2818, 0.48330°S, 89.90830°W, 15.iv.1888, 717 m: ov. F 8.1 mm (USNM 26167).

Non-type specimens. Magellan Strait, A. Milne-Edwards det., Saint Laurent re-det.: 2 ov. F 10.2–10.9 mm (MNHN Ga301).

Magellan Strait, leg. Nerida Wilson, Greg Rouse, R/V *Nathaniel Palmer*, Stn SM1b-3, 10.iv.2013, 53.6022°S, 70.2456°W to 53.6025°S, 70.2322°W, 270–285 m: 1 M 13.4 mm, 1 ov. F 12.3 mm (SIO-BIC C11873).

ECUADOR: east of Galapagos Islands, leg. USFC Steamer *Albatross*, Stn 3402, 28.iii.1891, 0.95833°S, 89.05833°W, 421 fms (769.9 m): 1 M 6.5 mm, 3 ov. F 7.5–7.8 mm, 2 F 7.5–8.3 mm (MCZ IZ CRU-4557). — ECUADOR: east of San Salvador Island, Galapagos Islands, leg. USFC Steamer *Albatross*, Stn 3406, 3.iii.1891, 0.26666°S, 90.35833°W, 551 fms (1008 m): 1 M 4.8 mm, 1 F 5.1 mm (MCZ IZ CRU-4558).

COSTA RICA: The Thumb, leg. Greg Rouse, Allison Miller, R/V *Falkor*, ROV *SuBastian* dive S0217 B4-3, 10.i.2019, 9.04915°N, 84.39308°W, 1065 m; specimen not measured (SIO-BIC C13912), juvenile (SIO-BIC C13913). — COSTA RICA: Seamount 8, leg. Greg Rouse, Avery Hiley, R/V *Falkor*, ROV *SuBastian* dive S0226 Q7, 21.i.2019, 6.00765°N, 86.64906°W, 1310 m: 1 ov. F 11.2 mm (SIO-BIC C13951).

MEXICO: Guaymas Basin, Gulf of California, leg. Greg Rouse, Sigrid Katz, R/V *Western Flyer*, ROV *Doc Ricketts* dive D381, 11.iv.2012, 27.89591°N, 111.96700°W, 1064 m: 1 M 8.8 mm (SIO-BIC C14144).

USA: Pioneer Seamount, off San Francisco, California, leg. Craig McClain, David Clague, R/V *Western Flyer*, ROV *Tiburon* dive T1100, 18.vi.2006, 37.36141°N, 123.39300°W, 1229–1513 m: 1 M 6.75 mm (SIO-BIC C11953). — USA: off San Diego, California, leg. Greg Rouse and students, R/V *Robert Gordon Sproul*, otter trawl within oxygen minimum zone, 5.viii.2017, 32.7553°N, 117.4546°W, 570 m: 1 M 11.2 mm (SIO-BIC C12687), 1 ov. F 10.1 mm (SIO-BIC C12688), 1 M 11.2 mm (SIO-BIC C12524). — USA: off San Diego, California, leg. Greg Rouse, Avery Hiley and students, R/V *Robert Gordon Sproul*, SP1825, Stn 3 otter trawl, 2.ix.2018, 32.76463°N, 117.45417°W to 32.77180°N, 117.45325°W, 500 m: 1 ov. F 11.1 mm (SIO-BIC C13703). — USA: off San Diego, California, leg. Gabriella Berman, Sonja Huc, R/V *Robert Gordon Sproul*, SP2115 otter trawl, 7.viii.2021, 32.73467°N, 117.45100°W to 32.80017°N, 117.41567°W, 500 m: 1 ov. F 10 mm (SIO-BIC C14526).

Description

Carapace

Slightly longer than broad, widest at midlength; convex from side to side. Dorsal surface densely covered by acute denticles and denticulated tubercles, each denticle or tubercle with few short setae, hepatic and anterior branchial areas with denticles and some acute denticles. Regions well delineated by deep furrows, anterior and posterior

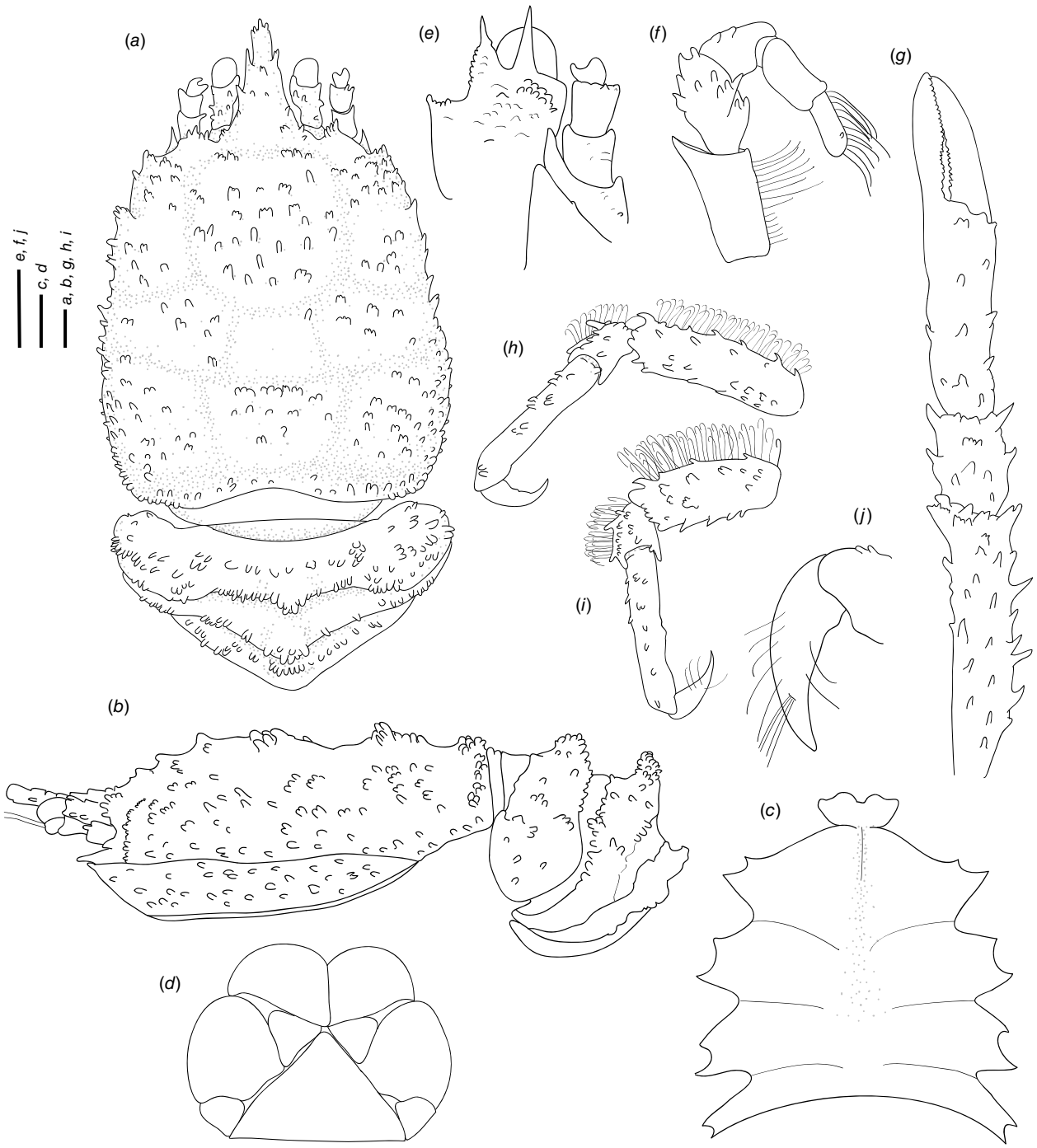

Fig. 6. Line drawings of *Munidopsis aspera* Henderson, 1885, ov. F 10.9 mm (MNHN-Ga301), Magellan Strait. (*a*) Carapace and abdomen, dorsal view. (*b*) Carapace and abdomen, lateral view. (*c*) Sternal plastron. (*d*) Telson. (*e*) Cephalic region, showing antennular and antennal peduncles, ventral view. (*f*) Right Mxp3, lateral view. (*g*) Left P1, dorsal view. (*h*) Left P2, lateral view. (*i*) Left (unattached) P4, lateral view. (*j*) Left P2 dactyli. Scale bars: 1 mm.

cervical grooves distinct. Gastric region flattened. Posterior margin armed with tubercles, preceded by elevated ridge. Rostrum triangular to spiniform, setose, width 0.2–0.3× anterior width of carapace, directed slightly upwards, denticles and tubercles on margin and dorsal surface, 0.3× carapace length, 1.3–1.6× as long as broad. Frontal margin slightly concave behind ocular peduncle, blunt outer orbital angle above antennal peduncle, orbit delimited by several outer orbital denticles or tubercles. Lateral margins convex; anterolateral angle armed with acute tubercles; branchial margins, tuberculated, denticulated. Pterygostomian flap surface covered by denticles and granules, anterior margin blunt.

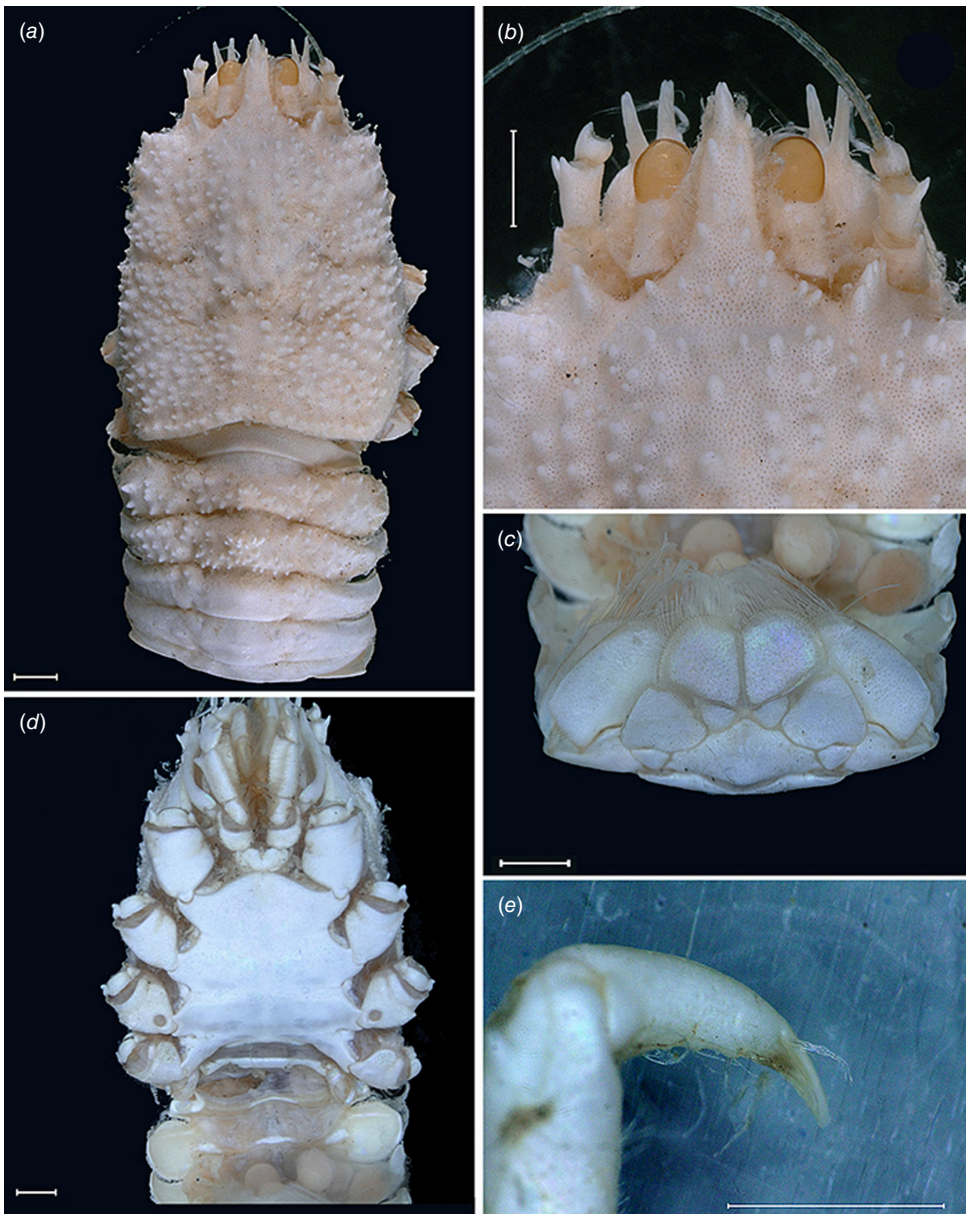

Fig. 7. *Munidopsis townsendi* Benedict, 1902, Galapagos, holotype (USNM 26167). (*a*) Carapace and abdomen, dorsal view. (*b*) Anterior carapace and rostrum, dorsal view. (*c*) Telson. (*d*) Sternal plastron. (e) Unattached leg dactyli. Scale bars: 1 mm.

Sternum

Slightly longer than broad, maximum width at sternite 6. Sternite 3 broad, 2.2–2.6× wider than long, anterolaterally rounded, often serrated, anterior margin with median notch flanked by 2 lobes. Sternite 4 narrowly elongate anteriorly, anterior margin smooth; surface depressed in midline, smooth; greatest width 2.5–3.2× that of sternite 3, and 2.0–2.7× wider than long.

Abdomen

Tergites with tubercles and denticles in all surfaces, tergites 2–4 armed with a median broad spine covered by tubercles, tergites 2–3 with 1 elevated transverse ridge; tergites 4–6 lacking ridges; tergite 6 with weakly developed posterolateral lobes and nearly transverse posteromedian margin. Telson composed of 9 plates; 1.4–1.5× as wide as long.

Eye

Eyestalk movable; peduncle elongated, densely covered by denticles and small tubercles, narrower than cornea length; cornea ovoid, length 0.7–0.9× that of peduncle; epistomial spine (below antennal spine, ventral to frontal margin) absent.

Antennule

Article 1 of peduncle with subequal dorsolateral and distolateral spines, distolateral margin proximally armed with denticles; distomesial margin with denticles.

Antenna

Peduncle not exceeding eye, armed with denticles and granules; article 1 with distomesial spine and distolateral spine, distomesial spine reaching end of article 2. Article 2 unarmed or with minute distomesial and distolateral spine. Article 3 unarmed or with small lateral spine or with prominent distal denticles; article 4 unarmed.

Mxp3

Surface with granules and denticles. Ischium 1.3× longer than merus measured on extensor margin, distal margin serrated; flexor margin of merus with one prominent spine and several denticles, extensor margin with 3–4 spines including distal spine.

P1

Moderately slender, females 1.7–2.0, males 2.5–2.7× longer than carapace, cylindrical, with numerous tubercles and denticles. Merus 2.4–2.8× carpus length, with denticles and spines on all surfaces. Carpus 1.3–1.5× longer than broad, unarmed or with rows of spines on mesial, lateral margins and some distal stout spines. Palm with row of spines on all surfaces, moderately slender, 2.6× longer than carpus, 2.6–2.8× longer than broad. Fingers unarmed or armed with proximal small spines or denticles, 0.7–0.9× longer than palm, opposable margins nearly straight, not gaping, spoon-shaped; fixed finger without denticulate carina on distolateral margin.

P2–4

Moderately slender, coarsely tuberculated and denticulated in all surfaces, with fine distally curved setae on meri and carpi, cylindrical in cross section, slightly decreasing in size posteriorly. P2 merus moderately slender, 0.5–0.6× carapace length, nearly 4.0× longer than high and 1.5× length of P2 propodus. P2–4 meri decreasing in length posteriorly (P3 merus 0.9× length of P2 merus, P4 merus 0.9× length of P3 merus); extensor margin with granules and denticles along entire border, distal part cylindrical ending in 1–2 thick spines; flexor margin tuberculated; P2–4 carpi with 0–3 thick spines on extensor margin, acute tubercles on lateral sides; P2–4 propodi with acute tubercles on extensor margin and lateral sides, distal flattened, ending in 3 denticles, 5.2–6.0× as long as high, flattened in cross section, unarmed; dactyli short, 0.4–0.5× length of propodi; distal claw short, moderately curved; flexor margin distally strongly curved, unarmed.

Epipods

Absent from pereopods.

Eggs

Approximately 10–55 round eggs of 1 mm each.

Colouration

Body and pereopods whitish to light brownish, with light orange eyes.

Distribution

California, Gulf of California, to Strait of Magellan, from 166- to 1398-m depth.

Genetic data

COI, *16S* rRNA and *28S* rRNA.

Remarks

Munidopsis aspera was described from Port Churruca, Magellan strait, Chile (Henderson 1885), with additional records from Galapagos (Ecuador), Cocos Islands (Costa Rica) (Faxon 1895) and California (Schmitt 1921; Luke 1977). The species was poorly illustrated in the literature (Wicksten 2012) but considered widely distributed across the East Pacific (Baba *et al.* 2008). *Munidopsis townsendi* Benedict, 1902 was described from Galapagos and only the anterior part of the carapace and rostrum, and the left P1 were illustrated (Benedict 1902). *Munidopsis alfredolaguardai* was described from the Baja California Peninsula in the SW Gulf of California (Hendrickx and Ayón-Parente 2013) and later recorded from Chile (Guzman and Sellanes 2015). *Munidopsis alfredolaguardai*, *M. aspera* and *M. townsendi* are similar morphologically but undertaking a definitive comparison among species was difficult because of the absence of proper illustrations of *M. aspera* and *M. townsendi*. We analysed the morphology and genetics from material from the full range of *M. aspera*, including material from the type locality (Magellan Strait), Galapagos and Gulf of California, and the type of *M. townsendi*. We found morphological variation among specimens across the range of the species in carapace size, spinulation on cheliped palms, the number and size of the external denticles and tubercles on carapace, pereiopods, ocular peduncles and antennal articles. However, we did not elucidate genetic structure genetic differences across the distribution range for all the markers analysed (Fig. 1–3*a*), nor morphological differences between *M. aspera* and *M. townsendi* and an illustrated description of *M. alfredolaguardai* (Hendrickx and Ayón-Parente 2013; Guzman and Sellanes 2015). We therefore conclude that *M. alfredolaguardai* and *M. townsendi* are junior synonyms of *M. aspera*.

Munidopsis aspera belongs to a group of species sharing a frontal margin without delimited orbit, telson with 9–10 plates, eye movable, unarmed, with peduncle longer than cornea and epipods absent from all pereiopods. This group of species includes *M. quadrata* and *M. carinipes* from the Northern East Pacific, *M. longimanus* from the Gulf of Mexico and the Caribbean Sea, *M. robusta* from the Caribbean Sea, *M. depressa* from California, *M. abdominalis* (A. Milne Edwards, 1880) from the

Caribbean Sea, *M. alaminos* Pequegnat & Pequegnat, 1970 from the Gulf of Mexico, *M. brevimana* (A. Milne Edwards, 1880) from the Caribbean Sea and *M. riveroi* Chace, 1939 from the Gulf of Mexico and the Caribbean Sea. *Munidopsis aspera* is easily distinguished from the remaining species of the group by having the flexor margin of the dactyli unarmed, and the carapace, pereopods, ocular peduncles and antennal articles densely covered by denticles and tubercles.

Munidopsis barrerai Bahamonde, 1964

Material examined

Non-type specimens. COSTA RICA: Las Gemelas Seamount, near Isla del Coco, leg. Greg Rouse, Avery Hiley, R/V *Falkor*, ROV *SuBastian* dive S0225 S7, 20.i.2019, 4.97945°N, 87.45870°W, 637 m: 1 F 14.5 mm (SIO-BIC C13948).

Genetic data

COI, *16S* rRNA and *28S* rRNA.

Distribution

Chile, Perú from 280- to 800-m depth and Costa Rica at 637-m depth.

Remarks

Munidopsis barrerai is newly recorded from Costa Rica. The general morphology of the specimen collected from Costa Rica agrees with the species described by Bahamonde (1964) and Guzman and Sellanes (2015). Unfortunately we did not have material from Chile for genetic comparisons between populations.

Munidopsis carinipes Faxon, 1893

(Fig. 8*a–g*, Supplementary Fig. S2.)

Material examined

Lectotype. PANAMA: Gulf of Panama, Azuero Peninsula, Morro de Puercos, leg. USFC Steamer *Albatross*, Stn 3353, 23.ii.1891, 7.10416°N, 80.56666°W, 695 fms (1271 m): 1 M 10.1 mm (MCZ IZ CRU-4561).

Paralectotype. Same collecting data as lectotype: 1 M 6.1 mm, 1 ov. F 8.2 mm (MCZ IZ-163058).

Non-type specimens. COSTA RICA: Jaco Scar, leg. Elena Perez, Jake Bailey, R/V *Atlantis*, HOV *Alvin* dive 4509, 3.iii.2009, 9.1172°N, 84.8425°W, 1459 m: 1 M 10.5 mm (SIO-BIC C11150). — COSTA RICA: Mound 11, leg. Victoria Orphan, Hang Yu, R/V *Atlantis*, HOV *Alvin* dive 4988, naturally occurring wood fall, 3.xi.2018, 8.92208°N, 84.30446°W, 1010 m: 1 M 9.9 mm (SIO-BIC C13869). — COSTA

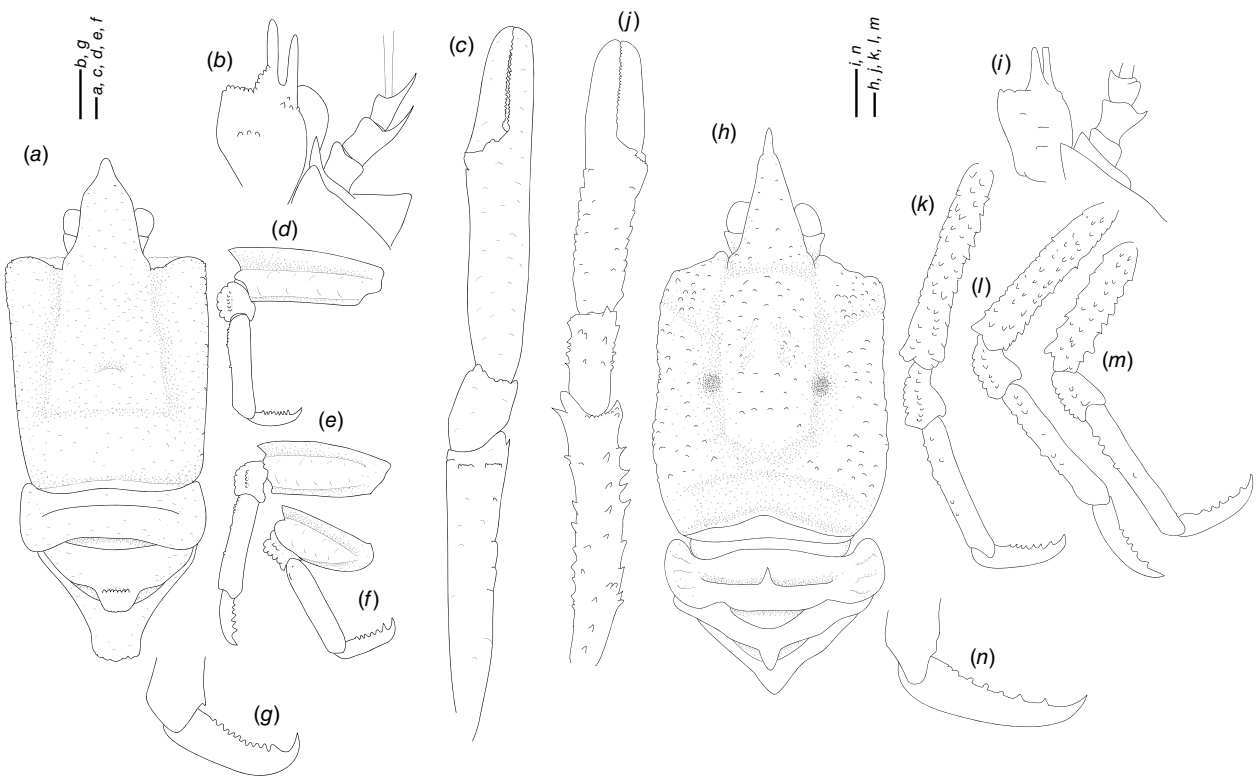

Fig. 8. (*a–g*) Line diagrams of *Munidopsis carinipes* Faxon, 1893, M 10.09 mm, lectotype (MCZ IZ CRU-4561), Panama. (*h–n*) Line diagrams of *Munidopsis quadrata* Faxon, 1893 M 9.8 mm, lectotype (MCZ IZ CRU-4560), Mexico. (*a*, *g*) Carapace and abdomen, dorsal view. (*b*, *i*) Cephalic region, showing antennular and antennal peduncles, ventral view. (*c*, *j*) P1, dorsal view. (*d*, *k*) Left P2, lateral view. (e, *l*) Left P3, lateral view. (*f*, *m*) Left P4, lateral view. (*g*, *n*) Left P2 dactyl. Scale bars: 1 mm.

RICA: Mound 12, leg. Greg Rouse, Allison Miller, R/V *Falkor*, ROV *SuBastian* dive S0215 B3-7, 8.i.2019, 8.93313°N, 84.30750°W, 1011 m: 1 ov. F 10.0 mm (SIO-BIC C13916).

Diagnosis

Carapace dorsally smooth, porose, laterally unarmed, with deep dorsal furrows, cervical grooves indistinct. Rostrum broadly triangular, lateral margins subparallel, unarmed. Frontal margins slightly oblique, slightly concave behind ocular peduncle. Orbit not distinctly excavated, outer orbital angle blunt. Anterolateral angle unarmed. Branchial margin unarmed. Abdominal somites with transverse ridge, somites 3–5 armed with a broad spine. Telson divided into 9 plates. Sternite 3 moderately broad, anterolateral angles produced, sternite 4 subtriangular. Eyes unarmed, movable, epistomial spine absent. Article 1 of antennule with well-developed dorsolateral and distolateral spines. Article 1 of antenna with distomesial spine. Mxp3 merus subrhomboidal in lateral view. P1 slender, elongate, unarmed, fixed finger without denticulate carina on distolateral margin. P2–4 stout, unarmed; meri strongly carinated, with a ridge in extensor and flexor margin; dactyli moderately slender, curving, flexor margin with cuticular teeth along all margin decreasing proximally. Epipods absent from all pereopods.

Eggs

Approximately 20–35 eggs, 1 mm in diameter.

Colouration

Body and pereopods whitish, with light orange eyes.

Distribution

East Pacific, Panama and Costa Rica from 915- to 1459-m depth.

Genetic data

COI, *16S* rRNA and *28S* rRNA.

Remarks

Munidopsis carinipes belongs to a group of species sharing a frontal margin without a delimited orbit, telson with 9–10 plates, eye movable, unarmed, with peduncle longer than cornea, and epipods absent from all pereopods. The closest species is *M. quadrata* Faxon, 1893 from the Northeast Pacific. See the differences in the Remarks of that species.

Munidopsis girguisi sp. nov.

(Fig. 9*a–k*, 10*a*, *b*, *g*, 11*a*, *d*, Supplementary Fig. S3.)

ZooBank: urn:lsid:zoobank.org:act:5FAD0D92-72A1-492E-B4D0-B2ABAD807F70

Material examined

Holotype. USA: California, leg. E/V *Nautilus*, ROV Hercules dive H1455, Stn NA066-152, 8.viii.2015, 33.66222°N, 118.56974°W, 535 m: 1 M 18 mm (MCZ IZ-73856).

Paratypes. Same collecting data as holotype: 1 M 4 mm, 1 F 10 mm (MCZ IZ-163059). — USA: California, leg. E/V *Nautilus*, ROV Hercules dive H1455, Stn NA066-145, 8.viii.2015, 33.66009°N, 118.57134°W, 558 m: 1 F broken 7 mm (MCZ IZ-73852). — USA: Point Dume, off Malibu, California, leg. Charlotte Seid, Emily McLaughlin, R/V *Falkor*, ROV *SuBastian* dive S0163, Slurp 1, 8.x.2018, 33.94187°N, 118.84381°W, 719 m: 14 M 11.6–16.7 mm, 4 ov. F 12.3–15.6 mm, 3 F 9.9–11.2 mm (ethanol-treated specimens, SIO-BIC C14008), 4 M 16.6–20.0 mm 2 ov. F 12.3–13.4 mm (formalin-fixed specimens, SIO-BIC C14008).

Non-type specimens. USA: California, leg. E/V *Nautilus*, ROV Hercules dive H1455, Stn NA066-151, 8.viii.2015, 33.66017°N, 118.56964°W, 554.6 m: 1 M 3 mm, 1 F 4.7 mm (MCZ IZ-73844). — USA: California: seep, leg. E/V *Nautilus*, ROV Hercules dive H1455, Stn NA066-150, 8.viii.2015, 33.6604°N, 118.5695°W, 554 m: 1 M 4.5 mm, 1 F 2.0 mm (broken) (MCZ IZ-74029). — USA: Point Dume, off Malibu, California, leg. Charlotte Seid, Emily McLaughlin, R/V *Falkor*, ROV *SuBastian* dive S0164, Slurp 4, 9.x.2018, 33.94186°N, 118.843986°W, 723 m, 1 ov. F 12.3 mm (SIO-BIC C14010). — USA: Point Dume, off Malibu, California, leg. Charlotte Seid, Emily McLaughlin, R/V *Falkor*, ROV *SuBastian* dive S0164, Slurp 3, 9.x.2018, 33.94187°N, 118.84376°W, 723 m, 2 M 14.5–15.6 mm (formalin-fixed specimens, SIO-BIC C14012), 5 M 12.3–15.6 mm, 1 ov. F 13.4 mm, 1 F 12.3 mm (ethanol-treated specimens, SIO-BIC C14012). — USA: Redondo Knoll, off California, leg. Charlotte Seid, Emily McLaughlin, R/V *Falkor*, ROV *SuBastian* dive S0167, 11.x.2018, 33.68120°N, 118.57140°W to 33.6898°N, 118.57497°W), 498–578 m: 1 F 6.7 mm (SIO-BIC C14038). —USA: Santa Monica Mound and Fossil Hill, off California, leg. Greg Rouse, R/V *Western Flyer*, ROV *Doc Ricketts* dive D1250, 7.ii.2020, 33.83851°N, 118.69038°W to 33.84447°N, 118.68830W, 623–863 m, 1 M 16.7 mm (SIO-BIC C14442), 1 M 12.3 mm 3 ov. F 11.2–14.5 mm (SIO-BIC C14443). — USA: Santa Monica Mound, off California, leg. Greg Rouse, R/V *Western Flyer*, ROV *Doc Ricketts* dive D1252, 8.ii.2020, 33.79938°N, 118.64631°W to 33.79947°N, 118.64698°W, 789–807 m, 1 ov. F 10.0 mm (SIO-BIC C14445). — USA: Lasuen Knoll, off California, leg. Greg Rouse, Nicolas Mongiardino Koch, R/V *Falkor*, ROV *SuBastian* dive S0449, SCB-236, slurp 2, 2.viii.2021, 33.38816°N, 118.00555°W, 382 m, 1 M 13.4 mm (SIO-BIC C14553). — USA: Lasuen Knoll, off California, leg. Greg Rouse, Nicolas Mongiardino Koch, R/V *Falkor*, ROV *SuBastian* dive S0449, SCB-235, 2.viii.2021, 33.38818°N, 118.00556°W, 382 m, 2 F 9.9–8.8 mm (SIO-BIC C14554). — USA: Rosebud whalefall, off San Diego, California, leg. Greg Rouse, R/V *Western Flyer*, ROV *Doc Ricketts* dive D1253, 9.ii.2020, 32.77687°N, 117.48807°W, 845 m: 1 M 13.4 mm (SIO-BIC C14437). — USA: California, leg. Robert C. Vrijenhoek, R/V *Western Flyer*, ROV *Doc Ricketts* dive D476, 21.v.2013, 33.843400°N, 118.68900°W, 664 m, 6 M 5.4–10.8 mm, 3 ov. F 11.5–12.3 mm, 4 F 7.0–11.4 mm (USNM 1463927). — USA: California, leg. Robert C. Vrijenhoek, R/V *Western Flyer*, ROV *Doc Ricketts* dive D631, 24.vi.2014, 33.90430°N, 118.73400°W, 535 m, 2 M 3.1–4.0 m, 2 F 3.7–12.5 mm (USNM 1487201), 2 M 3.1–3.3 mm, 2 F 3.3–5.7 mm (USNM 1487195).

COSTA RICA: Jaco Summit, leg. Greg Rouse, Allison Miller, R/V *Falkor*, ROV *SuBastian* dive S0213, 6.i.2019, 9.17341°N, 84.80380°W, 730–820 m: 2 specimens not measured (tissue SIO-BIC C13897 ex MZUCR 3760-01).

Etymology

Named for Prof. Peter Girguis, Chief Scientist of the R/V *Falkor* 'Backyard Deep' cruise FK181005, during which most

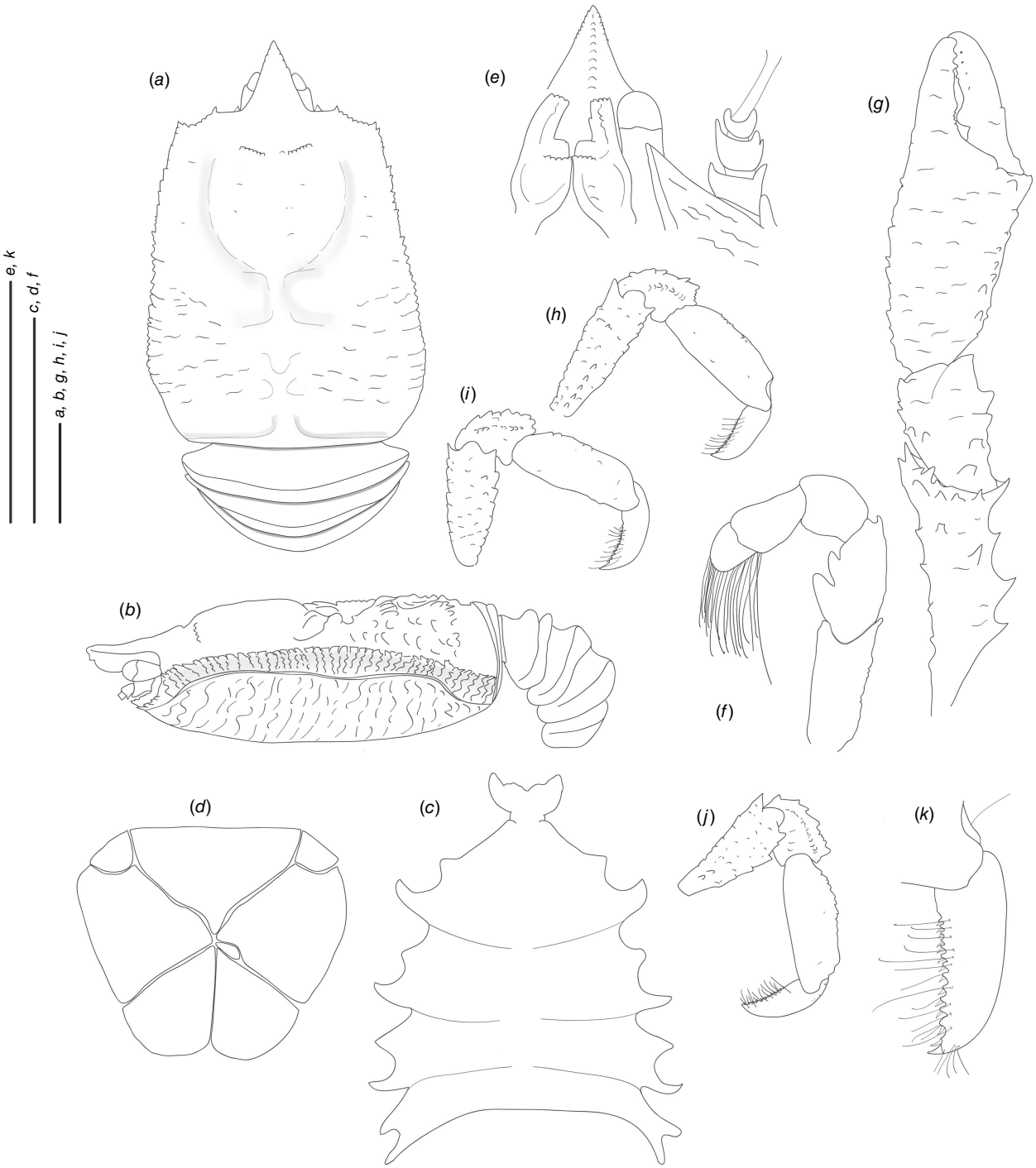

Fig. 9. Line diagrams of *Munidopsis girguisi* **sp. nov.**, M 18 mm, holotype (MCZ IZ-73856), California. (*a*) Carapace and abdomen, dorsal view. (*b*) Carapace and abdomen, lateral view. (*c*) Sternal plastron. (*d*) Telson. (e) Cephalic region, showing antennular and antennal peduncles, ventral view. (*f*) Left Mxp3, lateral view. (*g*) Left P1, dorsal view. (*h*) Right P2, lateral view. (*i*) Right P3, lateral view. (*j*) Right P4, lateral view. (*k*) Right P3 dactyli, lateral view. Scale bars: 1 mm.

of the paratypes were collected. The type locality off Los Angeles matches Prof. Girguis' 'Angeleno' origins. The presence of filamentous bacteria resonates with Prof. Girguis' research in deep-sea microbiology, and the tripoint carapace marking resembles the ABISS autonomous lander deployed by the Girguis lab on this cruise. We honor Prof. Girguis' enthusiasm for collecting these animals and his kind, inclusive leadership as Chief Scientist.

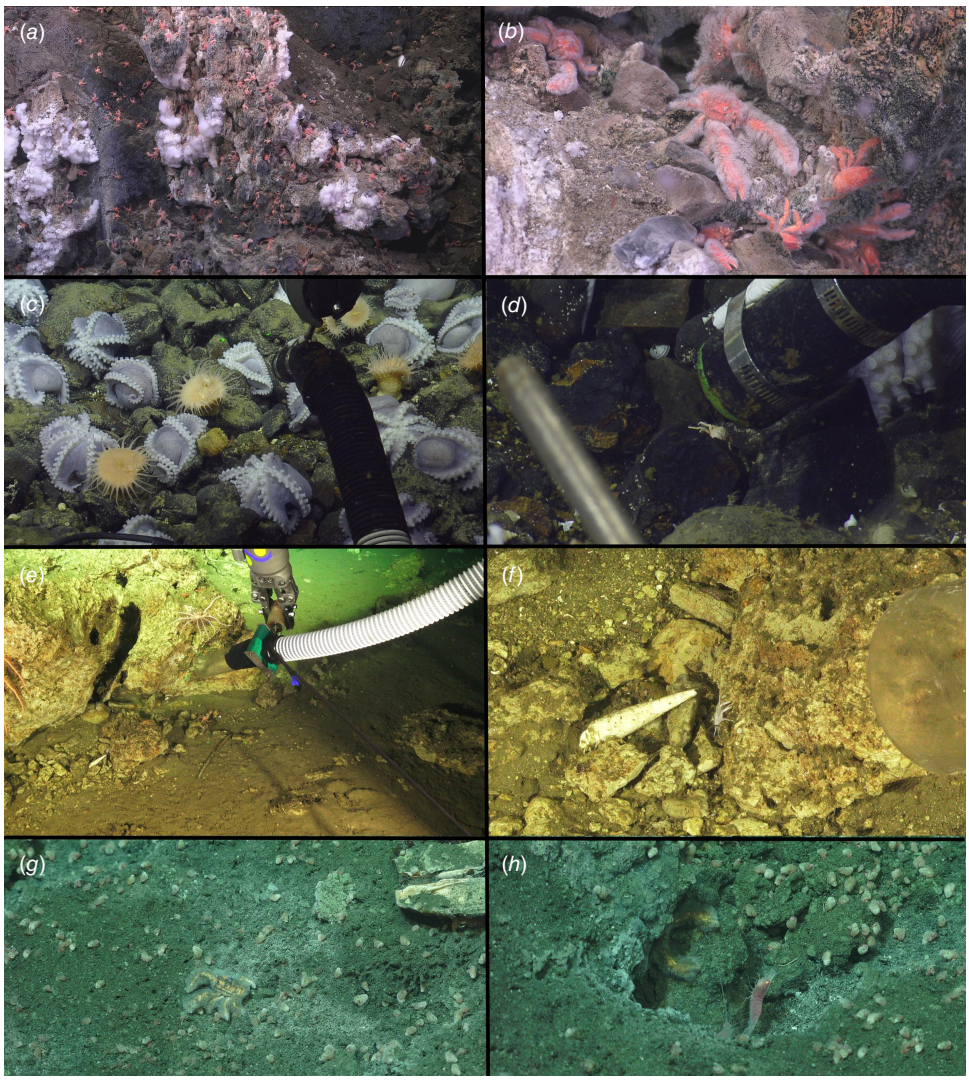

Fig. 10. *In situ* images. (*a*, *b*) *Munidopsis girguisi* **sp. nov.**, California, dive S0449, SCB-236 (SIO-BIC C14553). (*c*, *d*) *Munidopsis hendrickxi* **sp. nov.**, California, Stn NA117-012-01-B-MCZ, holotype (MCZ IZ-153106). (e, *f*) *Munidopsis similis* Smith, 1885, Costa Rica, dive S0230 S3 (SIO-BIC C13964). (*g*–*h*) Costa Rica, dive S0213. (*g*) *Munidopsis girguisi* **sp. nov.** (SIO-BIC C13897). (*h*) *Munidopsis cortesi* **sp. nov.**, holotype (MZUCR 3761-01). Photo credits: ROV *SuBastian*/ Schmidt Ocean Institute (*a*, *b*, e–*h*) and Nautilus Live Ocean Exploration Trust (*c*, *d*).

Diagnosis

Carapace quadrangular, dorsally smooth, with pair of epigastric scales, with dorsal deep furrows and rugae, cervical grooves indistinct. Rostrum broadly triangular, lateral margins convergent, unarmed. Frontal margins slightly oblique. Orbit not distinctly excavated, outer orbital angle with a minute spine. Anterolateral angle armed with a small spine. Branchial margin serrated, unarmed. Pterygostomian flap with rugae. Abdominal somites unarmed. Telson divided into 7–8 plates. Sternite 3 anterolaterally rounded, anterior margin with median notch flanked by 2 lobes, sternite 4 subtriangular. Eyes unarmed, movable, epistomial spine present. Article 1 of antennule with dorsolateral process mesially concave. Article 1 of antenna with well-developed distolateral spine. Mxp3 merus subrhomboidal in lateral view. P1 moderately stout, with some spines, fixed finger without denticulate carina on distolateral margin. P2–4 stout, unarmed; meri carinated, propodi paddle-shaped; dactyli stout, curving, flexor margin with cuticular teeth along all margin decreasing proximally. Epipods absent from all pereopods.

Description

Carapace

Quadrangular, slightly longer than broad, widest at posterior part; slightly convex from side to side. Dorsal

Fig. 11. Three-dimensional renderings of Micro-computed tomography X-ray images. (*a*, *d*) *Munidopsis girguisi* **sp. nov.**, M 18 mm, holotype (MCZ IZ-73856). (*b*, e) *Munidopsis hendrickxi* **sp. nov.**, M 9.1 mm, holotype (MCZ IZ-153106). (*c*, e) *Munidopsis cortesi* **sp. nov.**, ov. F 5.2 mm, holotype (MZUCR 3761-01). Three-dimensional reconstructions available from MCZbase.

surface smooth, with two epigastric produced scales, hepatic and anterior branchial areas with scarce rugae; posterior cardiac and intestinal region with few rugae. Regions well delineated by deep furrows, anterior and posterior cervical grooves indistinct. Gastric region slightly elevated. Posterior cardiac region constricted by lateral furrows, forming notches; posterior margin unarmed, preceded by deep transverse depression. Rostrum broadly triangular, dorsally concave, width 0.15–0.25× anterior width of carapace, horizontal, lateral margins coarsely serrated, ventrally convex and carinated, 0.2–0.3× carapace length, 1–1.5× as long as broad. Frontal margin serrated, oblique behind ocular peduncle, blunt outer orbital angle above antennal peduncle, outer orbital spine and process (antennal spine) minute. Lateral margins carinated, with numerous rugae, preceded by a depression, nearly straight proximally, oblique distally;

anterolateral spine minute. Pterygostomian flap surface with large and short rugae, anteriorly acute.

Sternum

Slightly longer than broad, maximum width at sternite 6. Sternite 3 moderately broad, 1.8–2.5× wider than long, anterolaterally rounded, anterior margin with median notch flanked by 2 lobes. Sternite 4 narrowly elongate anteriorly; surface depressed in midline, smooth; greatest width 2–3× that of sternite 3 and 2.0× wider than long.

Abdomen

Unarmed; tergite 2 with 2 elevated transverse ridges, smooth; tergites 3–5 lacking posterior ridge; tergite 6 with weakly produced posterolateral lobes and nearly transverse posteromedian margin. Telson composed of 7–8 plates, 1.2× as wide as long.

Eye

Eyestalk movable, partially concealed by rostrum; peduncle smooth, longer than cornea length; cornea subglobular; lateral surface contiguous to epistomial spine, ventral to frontal margin.

Antennule

Article 1 of peduncle with dorsolateral process mesially concave, distally serrated; distomesial margin produced and squamate.

Antenna

Peduncle not exceeding eye; article 1 with strong distolateral spine, distomesial angle unarmed, not reaching end of article 2, partially concealed by pterygostomian flap. Article 2 with well-developed distomesial and distolateral spines. Article 3 longer than article 2, with well-developed distomesial and distolateral spines, often double distolateral or distomesial spines. Article 4 unarmed. Flagellum longer than carapace.

Mxp3

Surface smooth. Flexor margin of merus with 2 spines, proximal larger, small distal spine; extensor margin with 1 distal spine. Ischium slightly longer than merus measured on extensor margin, unarmed. Crista dentate, finely denticulate. Dactylus, propodus and carpus unarmed.

P1

Moderately stout, with some granules and scales, females 1.7–1.9, males 1.8–2.2× longer than carapace. Merus 1.9–2.0× carpus length, with some spines at all surfaces, mesial stronger, including a few distal stout spines, dorsal margin proximally carinated. Carpus 1.5–1.8× longer than broad, with few spines at all surfaces, distal spines absent. Palm stout, slightly longer than carpus, 1.5–1.7× longer than broad, with row of small spines on mesial and lateral margins. Fingers unarmed, 0.7–0.9× longer than palm, opposable margins nearly straight, slightly gaping, spooned; fixed finger without denticulate carina on distolateral margin.

P2–4

Stout, coarsely granulated, devoid of setae, slightly decreasing in size posteriorly. P2 merus stout, 0.3–0.5× carapace length, nearly 3.0× longer than high and 1.1–1.2× length of P2 propodus. P2–4 meri decreasing in length posteriorly (P3 merus 0.8 length of P2 merus, P4 merus 0.9 length of P3 merus); extensor margin of P2–4 meri carinated, with small spines along entire border, distal part flattish ending in thick spine; flexor margin granulate ending in a thick spine; carpi with one small spine on extensor margin, granulated carina along lateral side; P2–4 propodi paddle-shaped, 2.6–2.7× as long as high, flattened in cross-section, extensor margin granulated; dactyli 0.6–0.7× length of propodi; distal claw short, moderately curved; flexor margin distally curved, with 11–13 min dactylar teeth decreasing in size proximally, each with slender corneous spine, ultimate tooth closer to dactylar angle than to penultimate tooth.

Epipods

Absent from pereopods.

Eggs

Approximately 10–45 eggs, 0.6–1 mm in diameter.

Colouration

Carapace and pereopods pink or varying shades of orange; carapace with a white tripoint marking on many of the California specimens.

Distribution

California and Costa Rica from 381- to 845-m depth.

Genetic data

COI, *16S* rRNA and *28S* rRNA.

Remarks

This new species appears to be covered by filamentous bacteria on the carapace, abdomen and chelipeds when alive but these bacteria were missing after fixation. Other squat lobster species living in hydrothermal vents and cold seeps exhibit this kind of epibiotic bacteria (e.g. Goffredi *et al*. 2008). *Munidopsis girguisi* sp. nov. resembles *Munidopsis denudata* Macpherson, 2007 from the Solomon Islands and *M. inermis* Faxon, 1893 from Panama. However, the new species is easily distinguished from these species by the following characters:

- The new species has deep furrows on the dorsal surface of the carapace and rugae on the pterygostomian flap, whereas these surfaces are smooth in *M. denudata* and in *M. inermis*.

- The frontal margin of the carapace is unarmed in *M. denudata* and *M. inermis* whereas this is armed with a minute antennal spine in the new species.
- The anterolateral angle is unarmed in *M. denudata* and *M. inermis* whereas this angle is armed with a small spine in the new species.
- The new species has an acute triangular rostrum whereas *M. denudata* has a broadly triangular rostrum.
- The flexor margin of the Mxp3 is armed with one strong proximal spine and one small distal spine in *M. denudata* whereas this margin is armed with two proximal spines in the new species.
- P1–4 have spines in the new species, whereas these are unarmed in *M. denudata* and *M. inermis*.
- The dactyli flexor margin is unamred in *Munidopsis inermis* whereas this margin is armed with minute spines in the new species.

Munidopsis granosicorium Williams & Baba, 1989

(Fig. 12*a–k*.)

Material examined

Non-type specimens. COSTA RICA: Parrita Seep, leg. Lisa Levin, Kris Krasnosky, R/V *Atlantis*, HOV *Alvin* dive 4924, 7.vi.2017, 9.03168°N, 84.62100°W, 1402 m: 1 ov. F 6.1 mm (SIO-BIC C12819).

Description

Carapace

As long as broad, widest at midlength; heavily sculptured, ridged longitudinally; convex from side to side. Dorsal surface densely covered by denticles and tubercles, each denticle or tubercle with a few short setae, epigastric denticles strongly serrated, hepatic and anterior branchial areas with denticles and some acute granules. Regions well delineated by deep furrows including distinct anterior and posterior cervical grooves. Gastric region elevated, with a longitudinal ridge interrupted by cervical groove. Cardiac region elevated, including prominent longitudinal ridge. Intestinal region with longitudinal ridge, preceded by a depression. Posterior margin unarmed, preceded by transverse depression. Rostrum narrowly triangular, width 0.23× anterior width of carapace, directed slightly upwards, few spines on margin, dorsally carinate, 0.33× carapace length, 1.4× as long as broad. Basis of rostrum armed with pair of minute spines in line with base of eye, peri-epigastric. Frontal margin slightly concave behind ocular peduncle, blunt outer orbital angle above antennal peduncle, outer orbital spine and process (antennal spine) absent. Lateral margins nearly straight; anterolateral angle unarmed; branchial margins unarmed. Pterygostomian flap surface covered by denticles and granules, anterior margin blunt, unarmed.

Sternum

1.2× longer than broad, maximum width at sternite 7. Sternite 3 broad, 2× wider than long, anterolaterally rounded, anterior margin with median lobe flanked by 2 lobes. Sternite 4 narrowly elongated anteriorly, anterior margin serrated; surface depressed in midline, smooth; greatest width 3× that of sternite 3 and 2.0× wider than long.

Abdomen

Tergites with granules, tergites 2–4 armed with a median broad spine, tergites 2–3 with 2 elevated transverse ridges, lateral part of dorsal surfaces covered by granules and scales; tergites 4–6 lacking posterior ridge; tergite 6 with weakly produced posterolateral lobes and nearly transverse posteromedian margin. Telson composed of 8 plates; 1.2× as wide as long.

Eye

Eyestalk immovable; peduncle small, shorter than cornea length; cornea globular, prominent, exposed; epistomial spine absent.

Antennule

Article 1 of peduncle with subequal dorsolateral and distolateral spines, dorsolateral double, distolateral proximally armed with denticles; distomesial margin granulate.

Antenna

Peduncle slightly exceeding eye, armed with denticles and granules; article 1 with distomesial spine, distolateral with granules and denticles. Article 2 with well-developed distomesial and distolateral spine, lateral margin with produced denticles. Article 3 with a small lateral spine, distolateral and distomesial angles unarmed. Article 4 unarmed.

Mxp3

Surface with granules and denticles. Ischium as long as merus measured on extensor margin, distal margin serrated; flexor margin of merus with 4 spines decreasing in size distally, distal margin armed with one spine; extensor margin with distal spine.

P1

Moderately slender, with numerous granules and denticles, each scale with few short setae, 1.6× longer than carapace. Merus 1.75× carpus length, with few distal stout spines. Carpus 1.8× longer than broad, with rows of spines on mesial, lateral margins, mesial stronger, distal spines stout. Palm with row of spines on all surfaces, slightly longer than carpus, 1.6× longer than broad. Fingers armed with a small spine on midlength margins, as long as palm, opposing margins nearly straight, not gaping, spooned; fixed finger without denticulate carina on distolateral margin.

P2–4

Moderately slender, coarsely tuberculated or denticulated on all surfaces, with fine distally curved setae in

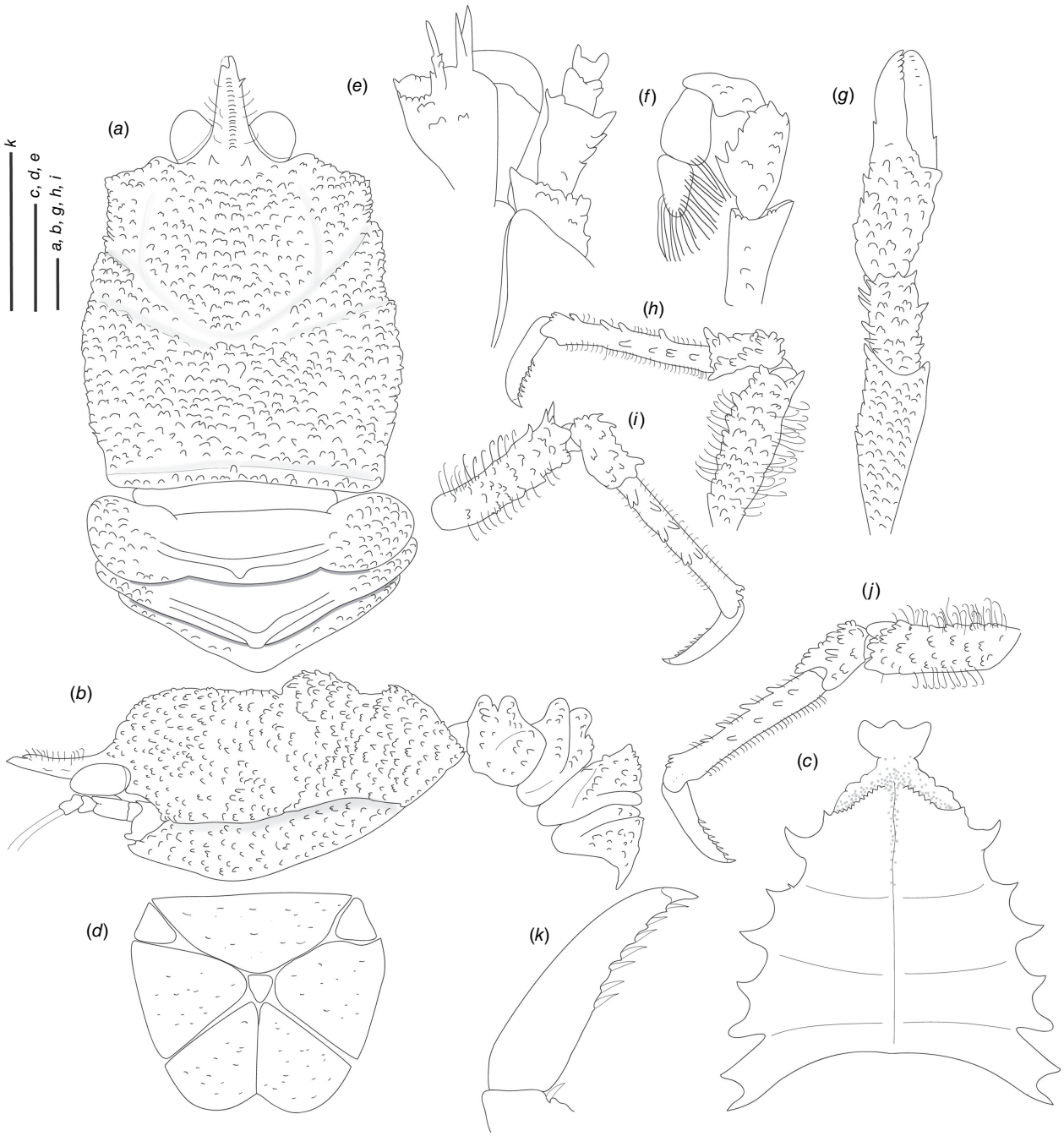

Fig. 12. Line diagrams of *Munidopsis granosicorium* Williams & Baba, 1989, ov. F 6.1 mm (SIO-BIC C12819), Costa Rica. (*a*) Carapace and abdomen, dorsal view. (*b*) Carapace and abdomen, lateral view. (*c*) Sternal plastron. (*d*) Telson. (e) Cephalic region, showing antennular and antennal peduncles, ventral view. (*f*) Left Mxp3, lateral view. (*g*) Left P1, dorsal view. (*h*) Right P2, lateral view. (*i*) Right P3, lateral view. (*j*) Right P4, lateral view. (*k*) Right P3 dactyli, lateral view. Scale bars: 1 mm.

meri, short setae in propodi, cylindrical in cross-section, slightly decreasing in size posteriorly. P2 merus moderately slender, 0.5× carapace length, nearly 2.2× longer than high and 0.9× length of P2 propodus. P2–4 meri decreasing in length posteriorly (P3 merus 0.9× length of P2 merus, P4 merus 0.95× length of P3 merus); extensor margin with granules and denticles along entire border, distal part cylindrical ending in 1–2 thick spines; flexor margin granulated, ending in thick spine; P2–4 carpi with denticles and spines on extensor margin, acute tubercles on lateral sides; P2–4 propodi with acute tubercles on extensor margin and lateral sides, distal flattened, ending in 3 flattened denticles, 7.2–7.6× as long as high, trianguloid in cross-section, unarmed; dactyli 0.5–0.6× length of propodi; distal claw

short, moderately curved; flexor margin distally curved, with 7–8 min teeth only at distal-half margin, ultimate tooth closer to dactylar angle than to penultimate tooth.

Epipods
Present on P1–3.

Eggs
2 eggs of 1.9–2 mm in diameter.

Colouration
Carapace and pereopods whitish, with brownish setae. Eyes and Mpx3 light orange. Eggs light orange.

Distribution

Vancouver Island, Washington at 2020-m depth. Newly registered from Costa Rica at 1402-m depth.

Genetic data

COI, *16S* rRNA and *28S* rRNA.

Remarks

The specimen described from Costa Rica fits well with the description of *M. granosicorium* from Vancouver Island (Williams and Baba 1989). However, there is some morphological variation in the relative width of the rostrum, with this being lender in the Vancouver specimen and broader in the Costa Rica specimen. There are also fewer but large eggs in the specimens from Costa Rica compared to those from Vancouver, suggesting lecithotrophic larval cycle that in turn implies poor long distance dispersal ability (Baco *et al.* 2016). Given the geographical distance between the two known populations, these likely correspond to different species but an analysis of more material would be necessary to confirm this. *Munidopsis granosicorium* belongs to the group of species with the dorsal surface of the carapace covered by tubercles, granules or denticles, epigastric processes, the lateral margins of the carapace unarmed, a triangular rostrum, the frontal margin concave behind the ocular peduncle, eyes with the ocular peduncle short and fixed, without an eye-spine and the telson composed of 7–8 plates. This species closely resembles *M. follirostris* Khodkina, 1973 from Chile, *M. sonne* Baba, 1995 from Fiji, *M. tuberosa* Osawa, Lin & Chan, 2008 from southwestern Taiwan and the South China Sea, and *M. dispar* from the Mariana Trench. However, *M. granosicorium* is easily distinguished from these species by the following characters:

- *M. granosicorium* has the carapace heavily sculptured, with a longitudinal ridge on the gastric and cardiac regions, whereas the carapace lacks these longitudinal ridges in the other species.
- *M. granosicorium* has the rostrum broadly triangular whereas *M. follirostris, M. sonne* and *M. tuberosa* have the rostrum constricted between the eyes.
- The rostrum is dorsally carinated in *M. granosicorium* but the dorsal carina is absent in *M. tuberosa*.
- Abdominal somites 2–5 are armed with a median broad spine in *M. granosicorium* whereas these spines are absent in *M. dispar*, *M. sonne* and *M. tuberosa*.
- The lateral margin of the antennular peduncle is unarmed in M. *granosicorium*, whereas this is armed with small processes in *M. tuberosa*.
- *M. granosicorium*, *M. follirostris* and *M. sonne* have epipods in P1–3 whereas *M. dispar* lacks epipods on pereopods.

The closest species to *M. granosicorium* sequenced in this study is *M. dispar*. The genetic divergence for *M. dispar* and *M. granosicorium* ranged from 14.7 to 16.5% for *COI*. Unfortunately, we do not have genetic data for *M. follirostris*, *M. sonne* or *M. tuberosa*.

Munidopsis hendrickxi sp. nov.

(Fig. 10*c*, *d*, 11*b*, *e*, 13*a*–*k*.)

ZooBank: urn:lsid:zoobank.org:act:87A1B63B-878C-48EA-83DC-5B5690E0A7E6

Material examined

Holotype. USA: California, E/V *Nautilus*, ROV Hercules dive H1795, Stn NA117-012-01-B-MCZ: 14.x.2019, 35.51857°N, 122.63877°W, 3188 m: 1 M 9.1 mm (MCZ IZ-153106).

Etymology

Named after Michel Hendrickx, crustacean researcher at the Universidad Autonoma of Mexico, in recognition of dedication to the study of squat lobsters and other crustaceans from the Americas.

Diagnosis

Carapace dorsally covered by denticulate tubercles and scales, with dorsal deep furrows and rugae, cervical grooves distinct. Rostrum narrowly triangular, lateral margins subparallel, unarmed. Frontal margins slightly concave. Orbit slightly excavated, outer orbital angle with a blunt lobe. Anterolateral angle armed with a spine. Branchial margin unarmed. Abdominal somites unarmed. Telson divided into 7 plates. Sternite 3 anterolaterally produced, anterior margin serrated with a median acute lobe, sternite 4 narrowly subtriangular. Eyes unarmed, immovable, epistomial spine present. Article 1 of antennule with well-developed dorsolateral and distolateral spines, distolateral double. Article 1 of antenna with distomesial blunt process, distolateral with denticules. Mxp3 merus subrhomboidal in lateral view. P1 moderately slender, with some spines, fixed finger without denticulate carina on distolateral margin. P2–4 moderately slender, unarmed; meri carinated, dactyli

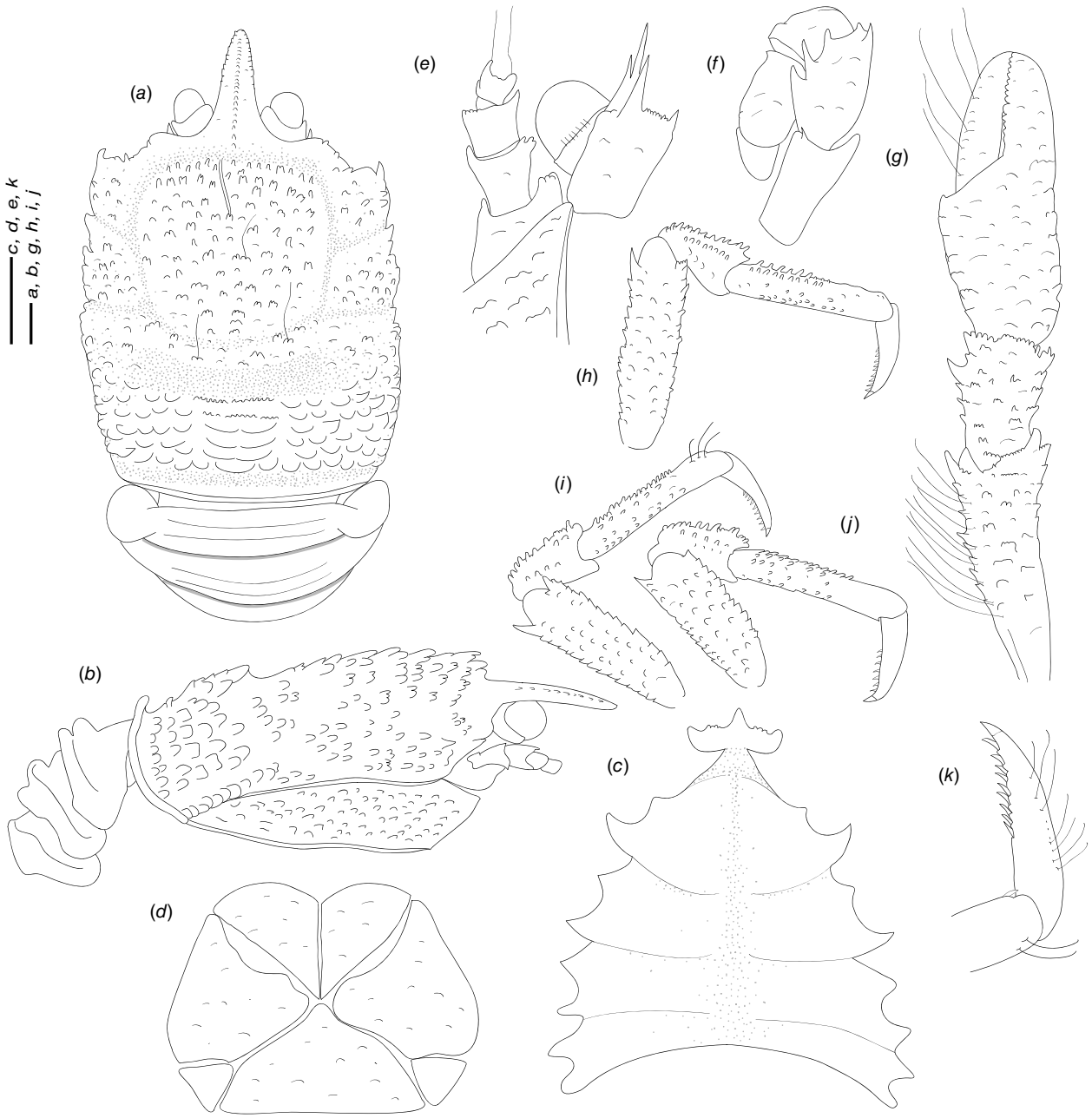

Fig. 13. Line diagrams of *Munidopsis hendrickxi* **sp. nov.**, 1 M 9.1 mm, holotype (MCZ IZ-153106), California. (*a*) Carapace and abdomen, dorsal view. (*b*) Carapace and abdomen, lateral view. (*c*) Sternal plastron. (*d*) Telson. (e) Cephalic region, showing antennular and antennal peduncles, ventral view. (*f*) Left Mxp3, lateral view. (*g*) Right P1, dorsal view. (*h*) Right P2, lateral view. (*i*) Right P3, lateral view. (*j*) Right P4, lateral view. (*k*) Right P4 dactyli, lateral view. Scale bars: 1 mm.

slender, curving, flexor margin with minute teeth along all margins decreasing proximally. Epipods present on P1–2.

Description

Carapace

Slightly longer than broad, widest at midlength; moderately convex from side to side. Dorsal surface covered by denticulate tubercles and scales, each tubercle and scale with a few short setae and some long, thick setae; hepatic and anterior branchial areas with scales and some acute tubercles; posterior cardiac and intestinal region covered by larger scales. Regions well delineated by furrows including distinct anterior and posterior cervical grooves. Gastric region slightly elevated. Posterior margin preceded by elevated ridge. Rostrum narrowly triangular, directed downwards slightly, distally covered with tubercles on lateral margins; dorsal surface longitudinally carinate, with

granules along midline, 0.3× as long as remaining carapace length, 1.7× longer than broad, 1.4× as long as broad. Frontal margin slightly concave behind ocular peduncle, outer orbital angle produced into blunt lobe above antennal peduncle, outer orbital spine and process (antennal spine) absent. Lateral margins straight; anterolateral spine well developed; anterior branchial margin with 2–3 small spines. Pterygostomian flap surface covered by granules and scales, anterior margin blunt, unarmed.

Sternum

As long as broad, maximum width at sternites 6 and 7. Sternite 3 broad, 2.6× wider than long, anterolaterally produced, anterior margin serrated with a median acute lobe. Sternite 4 narrowly elongate anteriorly; surface depressed in midline, smooth; greatest width 2.5× that of sternite 3 and 1.6× times wider than long.

Abdomen

Unarmed; tergites 2–3 with 2 elevated transverse ridges, lateral parts of dorsal surfaces smooth; tergites 4–6 lacking posterior ridge; tergite 6 with weakly produced posterolateral lobes and nearly transverse posteromedian margin. Telson composed of 7 plates; 1.3× as wide as long.

Eye

Eyestalk immovable; peduncle short and fixed, shorter than cornea length, wider than cornea width; cornea globular; lateral surface contiguous to small epistomial spine, ventral to frontal margin.

Antennule

Article 1 of peduncle with subequal dorsolateral and distolateral spines, distodorsal spine double; distomesial margin with spine distinct, slightly dentate.

Antenna

Peduncle exceeding eye; article 1 with distomesial blunt process, distolateral process with denticles. Article 2 with well-developed distolateral spine, distomesial surface with denticles. Article 3 with distomesial spine well-developed, distolateral angle with denticles. Article 4 unarmed. Flagellum longer than carapace.

Mxp3

Merus with 3 large spines along flexor margin, proximal larger; 2 small distal spines on extensor margin. Ischium as long as merus measured on extensor margin, with distal flexor and extensor spines. Crista dentata finely denticulate. Dactylus, propodus and carpus unarmed.

P1

Moderately slender, covered by denticles and scales, and fine, long setae, 1.9× longer than carapace. Merus 1.8× carpus length, with rows of spines on mesial, lateral margins and some distal stout spines. Carpus 1.5× longer than broad, with rows of spines on mesial, lateral margins and some distal stout spines. Palm unarmed, stout, slightly longer than carpus, 1.2× longer than broad. Fingers unarmed, 0.9× longer than palm, opposing margins straight, not gaping, spooned, fixed finger without denticulate carina on distolateral margin.

P2–4

Moderately slender, covered by denticles, devoid of setae, cylindrical in cross-section, slightly decreasing in size posteriorly. P2 merus moderately slender, 0.5× carapace length, nearly 3.5× longer than high and 1.2× length of P2 propodus. P2–4 meri decreasing in length posteriorly (P3 merus 0.9× length of P2 merus, P4 merus 0.8× length of P3 merus); extensor margin of P2–4 meri carinate, with denticles along entire border, distal part flattish ending in thick spine; flexor margin denticulate, distal spine strong; carpi with one thick distal spine on extensor margin, granulated carina along lateral side; P2–4 propodi 5.0–6.0 times as long as high, trianguloid in cross-section, armed with numerous denticles on flexor and extensor margins, and dorsal and ventral surface; dactyli 0.5–0.6× length of propodi; distal claw short, moderately curved; flexor margin distally curved, with 6–9 minute teeth only at distal-half margin, decreasing in size proximally, ultimate tooth at midlength between penultimate tooth and dactylar angle.

Epipods

Present on P1–2.

Colouration

Body light orange, whitish eyes.

Distribution

California, at ~3188-m depth.

Genetic data

COI, *16S* rRNA and *28S* rRNA.

Remarks

Munidopsis hendrickxi **sp. nov.** belongs to the group of species with the dorsal carapace surface covered in tubercles, granules or denticles, lateral margins of the carapace unarmed, rostrum triangular, frontal margin concave behind the ocular peduncle, eyes with the ocular peduncle short and fixed, lacking an eye-spine and the telson composed of 7–8 plates. The new species morphologically resembles *Munidopsis tuberosa* Osawa, Lin & Chan, 2008 from southwestern Taiwan and the South China Sea, and *M. dispar* from the Mariana Trench. However, the new species can be easily distinguished from the other by the following characters:

- The new species has a small spine on the anterolateral margin of the carapace, whereas this margin is unarmed in the other species.

- The new species has different tuberculation in the gastric area (denticles) from that in the cardiac area (long scales) whereas the carapace ornamentation is homogeneous in the other species.
- The new species has epipods on P1–2, whereas epipods are absent from the pereopods in *M. dispar* and present on P1–3 in *M. tuberosa*.

The new species and *M. dispar* diverge on 11.6–12.8% for *COI*. Unfortunately, there are no molecular data available for *M. tuberosa*.

Munidopsis hystrix Faxon, 1893

(Fig. 14*a–h*.)

Material examined

Lectotype. MEXICO: Nayarit, off Tres Marias Islands, leg. USFC Steamer *Albatross*, Stn 3425, 18.iv.1891, 21.31666°N, 106.40000°W, 680 fms (1244 m): 1 M 17.1 mm (MCZ IZ-CRU-4549).

Paralectotypes. Same collecting data as lectotype: 7 M 8.8–18.7 mm, 1 ov. F 16.4 mm, 2 F 8.8–12.2 mm (MCZ IZ-163060).

Non-type specimens. MEXICO: western slope of Concepcion Canyon, Guaymas Basin, leg. Greg Rouse, Sigrid Katz, R/V *Western Flyer*, ROV *Doc Ricketts* dive D383 A2, 12.iv.2012, 26.88295°N, 111.658622°W, 823 m: 1 M 8.9 mm (SIO-BIC C14357). — MEXICO: leg. E/V *Nautilus*, ROV Hercules dive H1665, Stn NA092-058, 13.xi.2017, 19.24652°N 110.87116°W, 819 m: 1 M 15.3 mm (MCZ IZ-146311).

USA: California, leg. E/V *Nautilus*, ROV Hercules dive H1455, Stn NA066-148, 8.viii.2015, 33.66012°N, 118.56919°W, 556 m: 1 F 8.5 mm (MCZ IZ-73853). — USA: California, leg. E/V *Nautilus*, ROV Hercules dive H1460, Stn NA067-011, 15.viii.2015, 33.45408°N, 118.67693°W, 702 m: 1 juvenile 2 mm (MCZ IZ-73638). — USA: California, leg. E/V *Nautilus*, ROV Hercules dive H1542, Stn NA075-002, 25.vii.2016, 33.74604°N, 118.61636°W, 795 m: damaged specimen (MCZ IZ-139982). — USA: Santa Monica Mound, off California, leg. Emily McLaughlin, Jessica Pruitt, R/V *Falkor*, ROV *SuBastian* dive S0172, Slurp 4, 15.x.2018, 33.83468°N, 118.67614°W, 780 m: 1 F 11.20 mm (SIO-BIC C14031). — USA: Emery Knoll, off California, leg. Emily McLaughlin, Jessica Pruitt, R/V *Falkor*, ROV *SuBastian* dive S0175, Slurp 4, 17.x.2018, 33.03611°N, 118.39808°W, 665 m: 1 F 3.5 mm (SIO-BIC C14037). — USA: off San Diego, California, leg. Greg Rouse and students, R/V *Robert Gordon Sproul* SP1913, otter trawl, 14.vii.2019, 32.8093°N, 117.4673°W to 32.8739°N, 117.5154°W, 700 m: 1 ov. F 19.9 mm (SIO-BIC C14102), 1 M 20 mm (SIO-BIC C14111). — USA: Forty Mile Bank, off San Diego, California, leg. Greg Rouse, Kaila Pearson, E/V *Nautilus*, ROV *Hercules* dive H1845, cruise NA124, 3.xi.2020, 32.60044°N, 118.02825°W to 32.59787°N, 118.01624°W, 1111–650 m: 1 F 11.1 mm (SIO-BIC C14470).

Diagnosis

Carapace spinose, dorsally covered by small spinules and setose scales, dorsal deep furrows, cervical grooves indistinct. Gastric region covered with spines, 1–2 pairs of well-developed epigastric spines, median cardiac spine well developed, preceded by a deep depression. Rostrum narrowly triangular, dorsally carinated, margin armed with 2–3 well-developed spines. Frontal margins concave. Orbit distinctly excavated, outer orbital angle delimited by antennal spine. Anterolateral angle armed with a strong spine. Anterior branchial margin armed with 3–4 well-developed spines; posterior branchial area dorsally armed with 3–4 pairs of well-developed spines, margin armed with small spines. Posterior carapace margin with 1–2 pairs of spines, preceded by a depression. Abdominal somites 2–4 with 2 transverse ridges, somite 2 armed with a pair of spines. Telson divided into 7 plates. Sternite 3 narrow, anterolateral angles produced, sternite 4 subtriangular. Eyes armed with dorsal spine, movable, epistomial spine absent. Article 1 of peduncle with well-developed dorsolateral and distolateral spines. Article 1 of antenna with distolateral spine. Mxp3 merus 0.5–0.6× longer than ischium, subrhomboidal in lateral view. P1 slender, elongate; meri and carpi with well-developed spines on all surfaces, fixed finger without denticulate carina on distolateral margin. P2–4 slender, spinose; dactyli slender, curving, flexor margin with teeth only at distal-half margin. Epipods absent from all pereopods.

Distribution

Galapagos Islands, Perú, Gulf of California, Baja California and California, from 436- to 1244-m depth.

Genetic data

COI, *16S* rRNA and *28S* rRNA.

Remarks

Munidopsis hystrix belongs to the group of species having a frontal margin with a delimited orbit, movable eye with small median spine projecting from upper surface, the abdomen armed with spines and the telson composed of 7–8 plates. This group of species includes *M. hystrix, M. opalescens* and *M. margarita* Faxon, 1893 from the East Pacific. These three species are morphologically and genetically similar. Differences relating to this complex are described in Remarks of *M. margarita*.

Munidopsis margarita Faxon, 1893

(Fig. 15*a–j*.)

Material examined

Lectotype. ECUADOR: Galápagos, Off Galapagos Islands, leg. USFC Steamer *Albatross*, Stn 3404, 28.iii.1891, 1.05000°S, 89.46666°W, 385 fms (704 m): M 7.5 mm (MCZ IZ CRU-4551).

Paralectotype. Same collecting data as lectotype: 1 F 6.5 mm (MCZ IZ-163061).

Non-type material. COSTA RICA: Seamount 6, leg. Greg Rouse, Avery Hiley, R/V *Falkor*, ROV *SuBastian* dive S0227, B3-7, 22.i.2019, 7.67944°N, 85.91141°W, 578 m: 1 F broken 8.9 mm (SIO-BIC C13957).

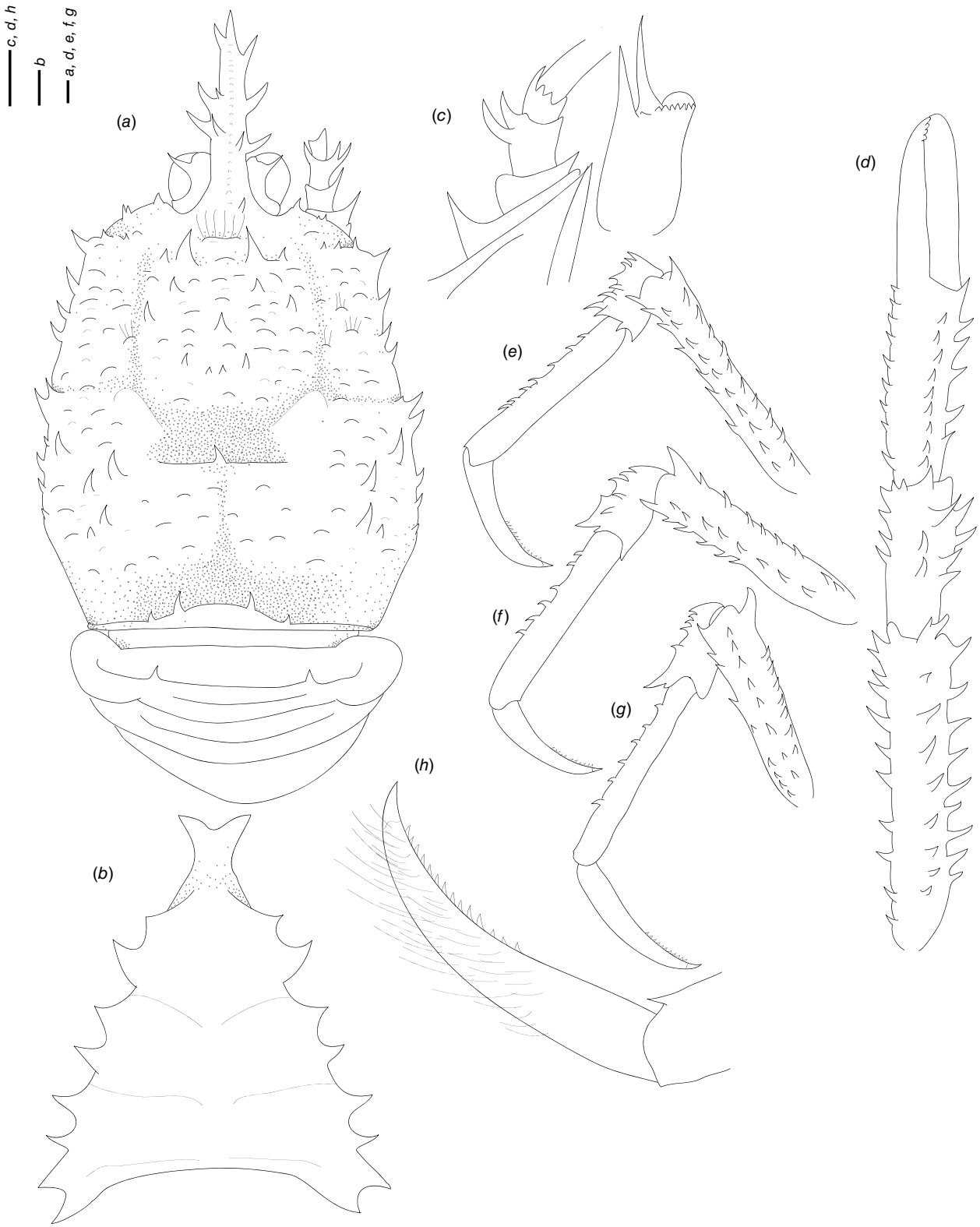

Fig. 14. Line diagrams of *Munidopsis hystrix* Faxon, 1893 M 17.1 mm, lectotype (MCZ IZ CRU-4549), Mexico. (*a*) Carapace and abdomen, dorsal view. (*b*) Sternal plastron. (*c*) Cephalic region, showing antennular and antennal peduncles, ventral view. (*d*) Right P1, dorsal view. (e) Right P2, lateral view. (*f*) Right P3, lateral view. (*g*) Right P4, lateral view. (*h*) Right P4 dactyli, lateral view. Scale bars: 1 mm.

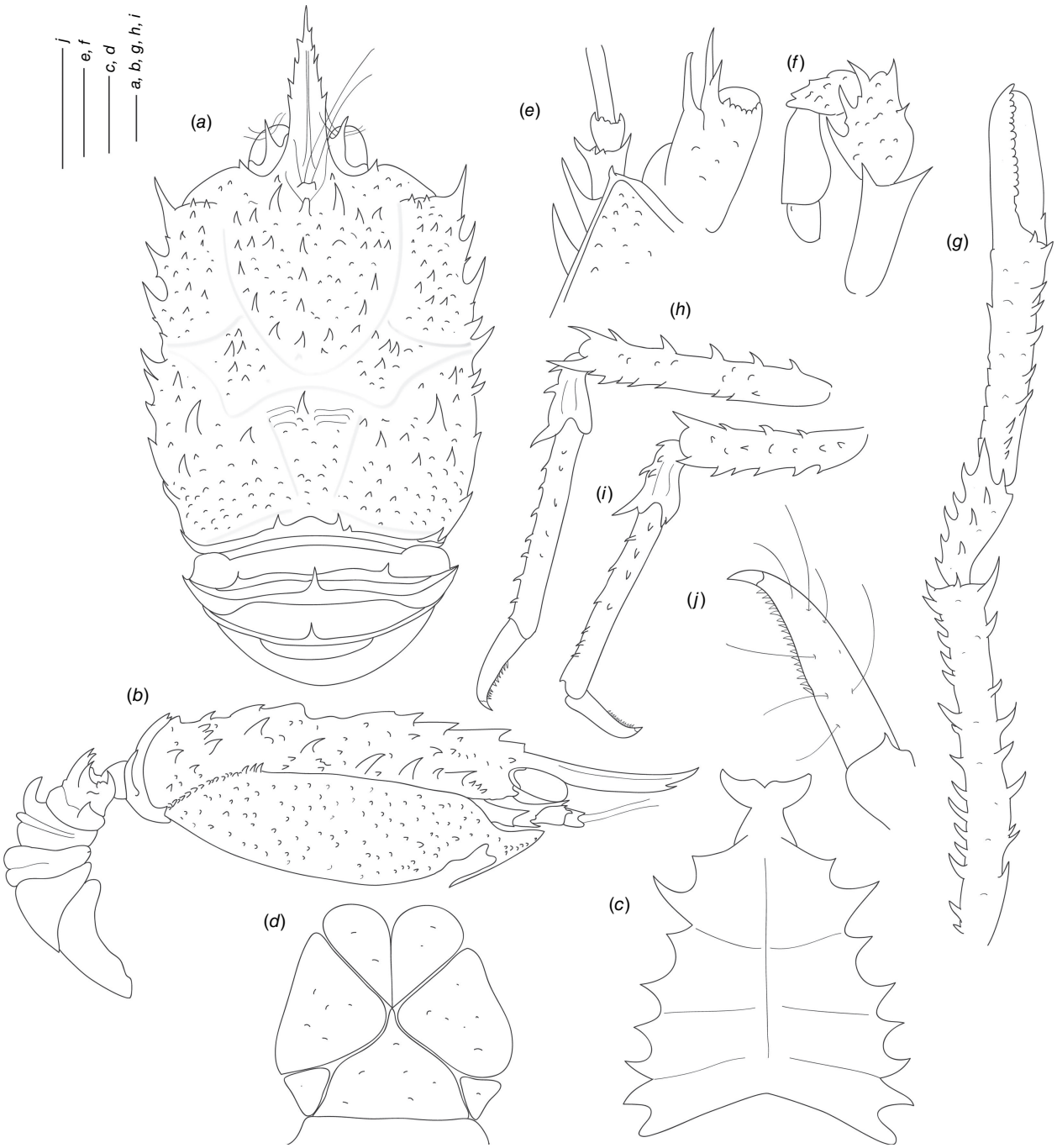

Fig. 15. Line diagrams of *Munidopsis margarita* Faxon, 1893, 1 F broken 8.9 mm (SIO-BIC C13957), Costa Rica. (*a*) Carapace and abdomen, dorsal view. (*b*) Carapace and abdomen, lateral view. (*c*) Sternal plastron. (*d*) Telson. (e) Cephalic region, showing antennular and antennal peduncles, ventral view. (*f*) Left Mxp3, lateral view. (*g*) Right P1, dorsal view. (*h*) Right P2, lateral view. (*i*) Right P3, lateral view. (*j*) Right P4, lateral view. (*k*) Right P4 dactyli, lateral view. Scale bars: 1 mm.

Description

Carapace

Spinose, slightly broader than long, widest at midlength; moderately flattened from side to side. Dorsal surface densely covered in spines and a few scales, each scale with a few setae; pair of epigastric spines strong, median processes with long setae, hepatic and anterior branchial areas with spinules; posterior cardiac and intestinal region covered with spinules and scales. Regions well delineated by deep furrows including distinct anterior and posterior cervical grooves. Gastric region elevated. Posterior margin armed

with 3 pairs of spines, 2 median pairs (median pair the strongest) and 1 lateral pair, close to the carapace margin, posterior margin preceded by a depression. Rostrum triangular, width 0.2× anterior width of carapace, directed slightly upwards, dorsally carinate, margin distally armed with 5 small spines; 0.4× carapace length, 1.8× as long as broad. Frontal concave behind ocular peduncle, blunt outer orbital angle above antennal peduncle, ending in a small outer orbital spine (antennal spine). Lateral margins straight; anterolateral spine strong; anterior branchial margin with 6 spines, each pair constituting a strong spine followed by a small spine; 5–6 branchial spines behind posterior branch of cervical groove. Pterygostomian flap surface covered in granules, anteriorly acute, armed with a strong spine.

Sternum

0.9× as long as broad, maximum width at sternite 7. Sternite 3 broad, 3.2× wider than long, anterolaterally rounded, anterior margin with median notch flanked by 2 lobes. Sternite 4 narrowly elongated anteriorly; surface depressed in midline, smooth; greatest width 2.3× that of sternite 3 and 1.7× wider than long.

Abdomen

Tergites 2–3 armed with posterolateral broad spines, tergite 2 with 3 spines and 2 elevated transverse ridges, tergite 3 armed with 1 median spine, tergites 3–6 lacking a posterior ridge; tergite 6 with weakly produced posterolateral lobes and nearly transverse posteromedian margin. Telson composed of 7 plates; 1.2× as wide as long.

Eye

Eyestalk movable; peduncle forming a median spine, projecting from upper surface and exceeding cornea, peduncle shorter than cornea length; cornea subglobular; epistomial spine absent.

Antennule

Article 1 of peduncle with subequal dorsolateral and distolateral spines; distomesial margin slightly produced and granulated.

Antenna

Peduncle slightly exceeding eye. Article 1 with strong distolateral spine, not reaching end of article 2. Article 2 with well-developed distolateral spine, distomesial margin granulated. Article 3 with well-developed distomesial and distolateral spine. Article 4 unarmed.

Mxp3

Surface with granules. Ischium as long as merus measured on extensor margin; flexor margin of merus with 3 strong spines subequal in size; extensor margin with 2 small spines.

P1

Slender, spinose, with numerous spines. Merus 2.7× carpus length, with rows of strong spines at lateral and mesial margins. Carpus 0.9× longer than broad, with rows of strong spines on dorsal, mesial and lateral surfaces. Palm armed with row of strong spines on mesial margin, lateral margin irregular, with few spines, slender, 2.3× longer than carpus, 1.2× longer than broad. Movable finger armed with a basal spine, 0.9× longer than palm, opposable margins nearly straight, not gaping, spooned; fixed finger without denticulate carina on distolateral margin.

P2–4

Slender, spinose, cylindrical in cross-section. P2 merus slender, 0.6× carapace length, 4× longer than high and 1.1× length of P2 propodus. P2–4 meri decreasing in length posteriorly (P3 merus 0.9× length of P2 merus, P4 merus 0.8× length of P3 merus); extensor margin of P2 and 4 meri with strong spines on all surfaces, distal part flattish, terminating in a thick spine; flexor margin with spines; carpi with spines on extensor margin, distal spine strong, carina along lateral side; P2 and 4 propodi 5.1–5.2× as long as high, trianguloid in cross-section, armed with small spines on lateral and extensor surfaces; dactyli 0.5× length of propodi; distal claw short, moderately curved; flexor margin distally curved, with 11–14 teeth at midlength, ultimate tooth at midlength between penultimate tooth and dactylar angle.

Epipods

Absent from pereopods.

Colouration

Carapace and eyes deep orange, P1–4 colourless.

Distribution

Previously known from Galapagos at 704-m depth. Newly registered from Costa Rica, at 578-m depth.

Genetic data

COI, *16S* rRNA and *28S* rRNA.

Remarks

Munidopsis margarita belongs to the group of species having a frontal margin with a delimited orbit, movable eye with small median spine projecting from upper surface, the abdomen armed with spines and the telson composed of 7–8 plates. This group includes *M. hystrix*, *M. opalescens* and *M. margarita*, and these are morphologically and genetically close. These species can be distinguished based on the following morphological characters:

- The spines on the carapace and rostrum margin are more prominent in *M. opalescens* and *M. margarita* than in *M. hystrix*.

- The rostrum is spiniform in *M. hystrix* but triangular in *M. opalescens* and *M. margarita*.
- *Munidopsis margarita* has abdominal tergites 2–3 armed with posterolateral spines, whereas these spines are absent in the other species.
- *Munidopsis margarita* has abdominal tergite 2 armed with 3 or more spines whereas this tergite is armed with a single median spine in the other species.

Genetic divergences among these species ranged from 6.8 to 10% for *COI*.

Munidopsis nautilus sp. nov.

(Fig. 16*a–j*, Supplementary Fig. S4.)

Zoobank: urn:lsid:zoobank.org:act:ADD10D8C-8E69-48E1-B0AD-EDB9D13FD62B

Material examined

Holotype. ECUADOR: off Galapagos Islands, leg. E/V *Nautilus*, ROV *Hercules*, ROV Hercules dive H1433, Stn NA063-016, ROV Hercules

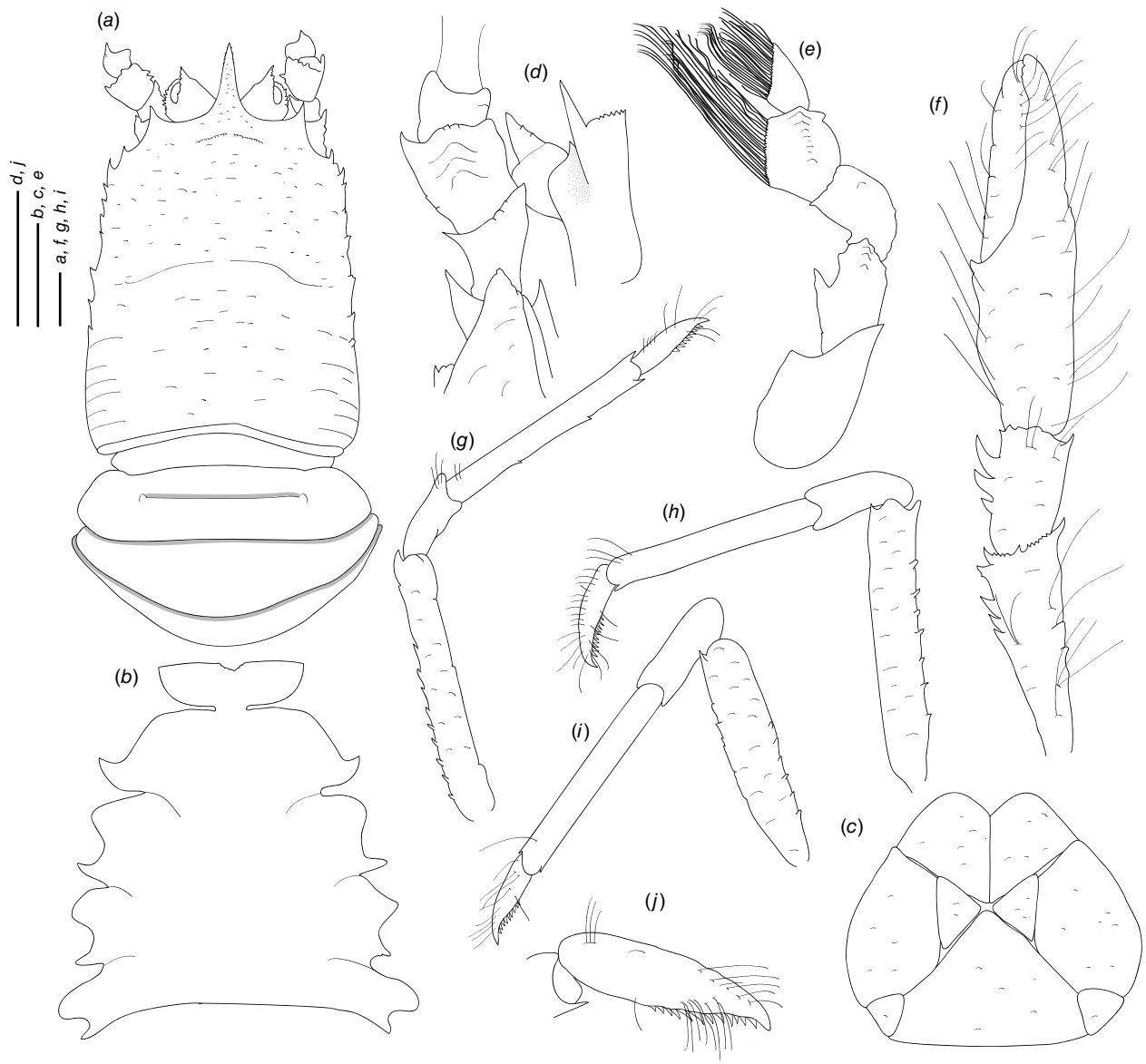

Fig. 16. Line diagrams of *Munidopsis nautilus* **sp. nov.**, ov. F 11.0 mm, holotype (MCZ IZ-70119), Ecuador: Galapagos. (*a*) Carapace and abdomen, dorsal view. (*b*) Sternal plastron. (*c*) Telson. (*d*) Cephalic region, showing antennular and antennal peduncles, ventral view. (e) Left Mxp3, lateral view. (*f*) Right P1, dorsal view. (*g*) Right P2, lateral view. (*h*) Right P3, lateral view. (*i*) Right P4, lateral view. (*j*) Right P4 dactyli, lateral view. Scale bars: 1 mm.

dive H1433, 20.vi.2015, 0.73720°N, 85.89091°W, 2600 m: 1 ov. F 11.0 mm (MCZ IZ-70119).

Etymology

Named after the Exploration Vessel *Nautilus* from which the exploration of the Galapagos Rift region was conducted, yielding these specimens. The name is a substantive in apposition.

Diagnosis

Carapace dorsally smooth, pair of epigastric scales, cervical grooves weakly distinct. Rostrum narrowly triangular, lateral margins subparallel, unarmed. Frontal margins concave. Orbit excavated, outer orbital angle with a spine. Anterolateral angle armed with a small spine. Branchial margin armed with spines. Abdominal somites unarmed. Telson divided into 9 plates. Sternite 3 anterolaterally blunt, anterior margin nearly straight with a median notch, sternite 4 widely triangular. Eyes unarmed, immovable, epistomial spine present. Article 1 of antennule with well-developed dorsolateral and distolateral spines. Article 1 of antenna with distomesial and distolateral spines. Mxp3 merus rectangular in lateral view, with dorsal carina. P1 moderately slender, with some spines, ventral pad in palm, fixed finger without denticulate carina on distolateral margin. P2–4 slender, unarmed; meri and propodi cylindrical, dactyli stout, curving, flexor margin with teeth along all margins decreasing proximally. Epipods absent from all pereopods.

Description

Carapace

1.2× longer than broad, widest posteriorly; weakly convex from side to side. Dorsal surface smooth, covered in small scales, each with a few short setae and some thick long setae; pair of epigastric produced and elevated scales. Regions not delineated, anterior and posterior cervical grooves weakly distinct. Mid-dorsal ridge medially interrupted. Posterior margin unarmed, angular, emarginated medially. Rostrum narrowly triangular, dorsally flattened, slightly directed downwards, 0.2× as long as remaining carapace length, 1.7× longer than broad, lateral margins serrated anteriorly. Frontal margin concave behind ocular peduncle, outer orbital angle produced into a spine above antennal peduncle, outer orbital spine strong, much larger (twice as large) than anterolateral spine. Lateral margins straight; anterolateral spine small; branchial margins armed with spines. Pterygostomian flap surface irregular, anterior margin acute.

Sternum

Slightly longer than broad, maximum width at sternite 7. Sternite 3 broad, 3.2× wider than long, anterolateral angle blunt, anterior margin nearly straight with a median notch. Sternite 4 narrowly elongated anteriorly; surface flattened, smooth; greatest width 2.9× that of sternite 3 and 1.8× wider than long.

Abdomen

Unarmed; tergite 2 with anterior transverse ridge, lateral partsof dorsal surfaces smooth; tergites 3–6 lacking ridges; tergite 6 with weakly produced posterolateral lobes and nearly transverse posteromedian margin. Telson composed of 9 plates; 1.2× as wide as long.

Eye

Eye immovable; flattened peduncle recovering all cornea surfaces, laterally and ventrally spinose, projected on dorsal surface in an acute triangular medial spine, exceeding midlength of rostrum, with serrated lateral margins; epistomial spine absent.

Antennule

Article 1 of peduncle with well-developed dorsolateral and small distolateral spines, distodorsal spine lateral margin strongly concave; distomesial margin dentate.

Antenna

Peduncle clearly exceeding eye. Article 1 with distomesial and distolateral spines. Article 2 with well-developed distolateral and distomesial spines, distal surface with dorsal carina. Article 3 with distomesial angle unarmed, distolateral spine well-developed, distal surface with denticles, dorsal surface carinated. Article 4 unarmed. Flagellum thick, longer than carapace.

Mxp3

Ischium as long as merus measured on extensor margin, with distal flexor and extensor spines. Crista dentata finely denticulate. Merus with 2 spines along flexor margin, proximal strong, distal small; extensor margin unarmed, dorsal surface carinated. Dactylus and carpus unarmed; propodus dorsal surface armed with a longitudinal carina.

P1

Slender, with few scales and long setae, 2.2× longer than carapace. Merus 1.9× carpus length, with row of well-developed spines on mesial margin and some distal stout spines, extensor margin serrated with few spines including strong distal spine. Carpus 1.5× longer than broad, with row of well-developed spines on mesial margin and some distal stout spines. Palm armed with distal spine mesial margin, slightly longer than carpus, pad of setae on ventral surface, 1.7× longer than broad. Fingers unarmed, 1.2× longer than palm, opposing margins straight, not gaping, spooned, fixed finger without denticulate carina on distolateral margin. Cheliped pad oval on ventral side of fixed finger.

P2–4

Slender, covered in setose scales, cylindrical in cross-section, slightly decreasing in size posteriorly. P2 merus slender, 2.0× carapace length, 6.5× longer than high and 1.2× length of P2 propodus. P3 meri longer than P2 and P4 (P3 merus 1.2× length of P2 merus, P4 merus 0.8× length of

P3 merus); extensor margin of P2–4 meri with spines along entire border, distal ending in thick spine in P2–3; flexor margin serrated, distal spine strong; carpi unarmed, lateral side smooth; P2–4 propodi 7.5–9.0× as long as high, cylindrical in cross-section, extensor margin unarmed, flexor margin armed with 0–3 spines, distal spine strong; dactyli highly setose, 0.38–0.4× length of propodi; distal claw short, moderately curved; flexor margin distally curved, with 11–12 teeth at distal half margin, ultimate tooth at midlength between penultimate tooth and dactylar angle.

Epipods
Absent from all pereopods.

Colouration
Unknown.

Distribution

Off Galapagos, at 2600-m depth.

Genetic data

COI and *28S* rRNA.

Remarks

The new species is morphologically similar to *M. lentigo* from the East Pacific Rise (Williams and Van Dover 1983). We have found the following morphological differences between both species:

- The new species presents produced epigastric scales whereas these epigastric scales are absent or weakly marked in *M. lentigo*.
- The spines on the branchial margin of the carapace are smaller than the outer orbital spine in the new species than in *M. lentigo*.
- The rostrum is narrowly triangular in the new species, whereas this is more strap-like in *M. lentigo*.

Unfortunately, we only have one specimen of the new species, therefore we cannot discuss intraspecific variation. However, *Munidopsis lentigo* and the new species are highly divergent genetically, with a genetic distance between 12 and 13% for *COI*.

Munidopsis piipa Marin, 2020

(Fig. 17*a–d*.)

Material examined

Non-type specimens. USA: California, Pioneer Seamount, 7.ii.1950, 37.35000°N, 123.41666°W, 1097–822.96 m: 1 F 20.6 mm (CAS-IZ 190354). — USA: California, Pioneer Seamount, 7.ii.1950, 37.349957°N, 123.430026°W, 805.–988 m: 1 M 10.5 mm (CAS-IZ 190356). — USA: Forty Mile Bank, off San Diego, California, leg. Greg Rouse and Nicolas Mongiardino Koch, R/V *Falkor*, ROV *SuBastian* dive S0446, SCB-172, 31.vii.2021, 32.6029°N, 118.02571°W, 1035 m: 1 F 13.4 mm (SIO-BIC C14546). — USA: California, leg. Robert C. Vrijenhoek, R/V *Western Flyer*, ROV *Tiburon* dive T665, 2.v.2004, 33.10070°N, 120.96000°W, 870 m, 1 specimen not sexed, not measured (USNM 1463979).

Distribution

Bering Sea (Piip submarine volcano) at 984-m depth, California, from 805- to 1097-m depth.

Genetic data

COI, *16S* rRNA and *28S* rRNA.

Remarks

Newly recorded for the East Pacific. *Munidopsis piipa* belongs to a group of species with a rostral spine short and spiniform, frontal margin of the carapace straight and telson with 10–12 plates. This group includes *Munidopsis ariadne* Macpherson, 2011 from the eastern Mediterranean, *Munidopsis goodridgii* Alcock & Anderson, 1899, *Munidopsis karukera* Macpherson, Beuck & Freiwald, 2016 from the Caribbean Sea, *Munidopsis maunga* Schnabel & Bruce, 2006, *Munidopsis milleri* Henderson, 1885 from the Philippines, *Munidopsis polymorpha* from shallow caves in the Canary Islands, *Munidopsis spinipes* MacGilchrist, 1905 from the Bay of Bengal and *Munidopsis kexueae* Dong, Gan & Li, 2021 from seamounts near the Yap Trench, West Pacific.

Munidopsis piipa closely resembles *M. kexueae* both morphologically and genetically. The descriptions of these species almost overlapped during the time of revisions and publication, therefore the species were not compared before our work. Phylogenetic and some species delimitation analyses do not support these species hypotheses, considering *M. piipa* and *M. kexueae* as a single taxon. However, haplotype networks demonstrate large genetic distances between the two species, with up to 4% of divergence for *COI* or 19 mutational steps (Fig. 4). The percentage of divergence between these species is low compared to other squat lobsters in the family, (e.g. Rodríguez-Flores *et al.* 2019*b*, *Leiogalathea*); although some species of the abyssal clade have been delimited based on similar genetic distance values (Jones and Macpherson 2007; Dong *et al.* 2019). According to the original species descriptions (Marin 2020; Dong *et al.* 2021), spinulation on the carapace margins and relative width of the rostrum are different in both taxa. However, these morphological and genetic differences could be part of intraspecific variation and population genetic structure, as very few specimens have been analysed to date. More data, including the analyses of more specimens, would be desirable to solve this taxonomic problem.

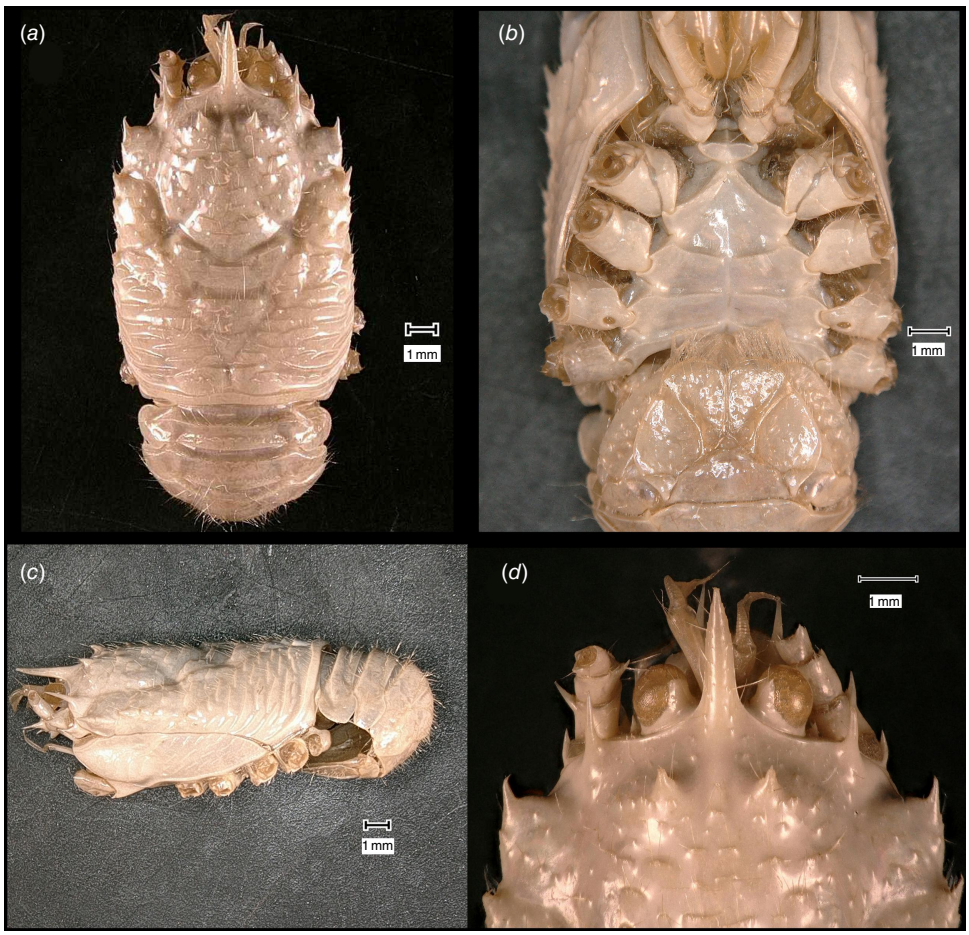

Fig. 17. *Munidopsis piipa* Marin, 2020, California (CASIZ 190356). (*a*) Carapace and abdomen, dorsal view. (*b*) Sternal plastron. (*c*) Carapace and abdomen, lateral view. (*d*) Anterior carapace and rostrum, dorsal view.

Munidopsis quadrata Faxon, 1983

(Fig. 8*j–n*, Supplementary Fig. S2.)

Material examined

Lectotype. MEXICO: Nayarit, off Tres Marias Islands, leg. USFC Steamer *Albatross*, Stn 3425, 18.iv.1891, 21.316660°N, 106.40000°W, 680 fms (1244 m): 1 M 9.8 mm (MCZ IZ CRU-4560).

Paralectotype. MEXICO: Nayarit, off Tres Marias Islands, leg. USFC Steamer *Albatross*, Stn 3424, 18.iv.1891, 21.25000°N, 106.38333°W, 676 fms (1236 m): 1 ov. F 9.9 mm (MCZ IZ CRU-4559).

Non-type specimens. USA: San Diego Trough, off California, leg. Robert Hessler, Spencer Luke, R/V *Melville*, Stn SIO69-486, 13.xii.1969, 32.41670°N, 117.49670°W, 1250 m: 6 M 6.6–10.0 mm (SIO-BIC C638). — USA: San Diego Trough, off California, leg. Harim Cha, Kent Trego and students, R/V *New Horizon*, otter trawl, 27.x.2007, 32.60330°N, 117.54180°W, 1210 m: 1 ov. F 9.9 mm (SIO-BIC C11814), 1 ov. F 7.8 mm (SIO-BIC C11025).

Diagnosis

Carapace granulated, dorsally covered in small granules, laterally unarmed, with dorsal deep furrows, cervical grooves indistinct. Gastric and cardiac region with a longitudinal protuberance. Rostrum triangular, broad base and lateral margins convergent, serrated, directed upwards. Frontal margins slightly oblique, slightly concave behind ocular peduncle. Orbit not distinctly excavated, outer orbital angle blunt. Anterolateral angle unarmed or armed with a small spine. Branchial margin unarmed. Abdominal somites with transverse ridge, somites 2–5 armed with a spine. Telson divided into 9 plates. Sternite 3 moderately broad, anterolateral angles produced, sternite 4 subtriangular. Eyes unarmed, movable, epistomial spine absent. Article 1 of peduncle with well-developed dorsolateral and distolateral spines. Article 1 of antenna with distomesial spine. Mxp3 merus 0.5–0.6× longer than ischium, subrhomboidal in lateral view. P1 slender, elongate; meri and carpi with small spines on all surfaces, fixed finger without denticulate carina on distolateral margin. P2–4 slender, spinose; dactyli moderately slender, curving, flexor margin with dactylar teeth along all margins decreasing proximally. Epipods absent from all pereopods.

Eggs
Approximately 35–55 eggs of 1 mm.

Colouration
Unknown.

Distribution

Northeast Pacific, from Mexico to Canada.

Genetic data

COI, *16S* rRNA and *28S* rRNA.

Remarks

Munidopsis quadrata belongs to a group of species with a frontal margin without delimited orbit, telson with 9–10 plates, eye movable, unarmed, with peduncle larger than cornea. The most closely related species is *M. carinipes* from Panama and Costa Rica. Indeed, there is no support for considering these species as different taxa according to molecular data (Fig. 2, 3*b*). However, both taxa are morphologically highly divergent, and the distribution ranges do not overlap. Both species are easily distinguished by the following characters:

- The anterolateral angle of the carapace is often armed with a small spine in *M. quadrata* whereas this angle is always unarmed in *M. carinipes*.
- The dorsal surface of the carapace is porose and smooth in *M. carinipes* whereas this is densely covered in granules in *M. quadrata*.
- Abdominal somite 2 is armed with a median broad spine in *M. quadrata* whereas this spine is absent in *M. carinipes*.
- Abdominal somites 3–5 are armed with a median small spine in *M. quadrata*, whereas these spines are much broader in *M. carinipes*.
- The rostral margins are subparallel in *M. carinipes* whereas these are convergent in *M. quadrata*.
- The P1 meri and carpi are spinose in *M. quadrata* whereas these are unarmed in *M. carinipes*.
- The P2–4 meri are dorsally and ventrally carinated and smooth in *M. carinipes*, whereas these are cylindrical in cross-section, spinose and not carinated in *M. quadrata*.
- The walking legs P2–4 are more slender in *M. quadrata* (propodus 6–7× as long as high) than in *M. carinipes* (propodus 4–5× as long as high).

All these morphological characters are consistent for all specimens examined from Panama and Costa Rica (*M. carinipes*), and from Mexico and California (*M. quadrata*). Therefore we decided to maintain the species status of both taxa, despite the lack of genetic support. Explanatory hypotheses for the molecular and morphological incongruence in this case would be: (1) recent speciation including incomplete lineage sorting for the analysed markers, (2) hybridisation or introgression between both species, or (3) extreme phenotypic variability. The lack of morphotypes of *M. carinipes* in *M. quadrata* populations and *vice versa* led to the prevalence of hypotheses (1) and (2) over hypothesis (3). To test these hypotheses, we would need broader population sampling and nuclear markers or ultimately genomic data.

Munidopsis similis Smith, 1885

(Fig. 8*e*, *f*, 18*a*–*f*.)

Munidopsis similis Smith, 1885

Munidopsis asiatica Marin, 2020, **syn. nov.**

Material examined

Holotype. USA: Nantucket Shoals, leg. United States Fish Commission, Albatross R/V, Stn 2192, 5.viii.1884, 39.77500°N, 70.24580°W, 1939 m, 1 ov. F 16.7 mm (USNM 8255).

Non-type specimens. USA: Gay Head–Bermuda transect, Atlantic Ocean, leg. R/V *Chain* 088, Howard L. Sanders, Stn 210A, 2.ii.1969, 39.716644°N, 70.766679°W, 2024 to 2064 m, 1 M 17.5 mm (MCZ IZ-81478). — USA: Hudson Canyon, leg. R/V *Knorr* 35, Stn 326, 18.xi.1973, 39.200000°N, 71.783333°W, 2288 to 2297 m: 3 M 12.3–22.1 mm, 1 ov. F 18.3 mm, 3 F 12.1–17.9 mm (MCZ IZ-127820). — USA: Hudson Canyon, Atlantic, leg. R/V *Knorr* 35, Stn 325, 18.xi.1973, 39.221611°N, 71.890043°W, 1919 to 1974 m: 1 M 14.5 mm (MCZ IZ-81527). — USA: rise off New England, Atlantic, leg. R/V *Atlantis II* 086, Stn 432, 41′ Gulf of Mexico shrimp trawl, 19.iii.1975, 39.52000°N, 70.33333°W, 2450 to 2350 m, 1 M 20.4 mm, 1 F 12.3 mm broken (MCZ IZ-39189). — USA: Atlantic Ocean, leg. R/V *Chain* 124, Stn 501, 4.vii.1975, 38.33666°N, 70.21833°W, 3287 to 3314 m: 1 M broken (MCZ IZ-81526).

USA: West Cortes Bank, California, leg. R/V *Atlantis II*, HOV *Alvin* dive 1508, cruise AT112, Leg 19, Stn MEA 85-5, 19.i.1985, 32.21823°N 119.25998°W, 1538–1678 m, 1 ov. F 12.1 mm (CAS-IZ 190355). — USA: San Diego Trough, off California, leg. Lisa Levin, Larry Lovell and students, R/V *Robert Gordon Sproul*, otter trawl, 2.x.2005, 32.60000°N, 117.50830°W, 1215 m: 1 M 11.2 mm (SIO-BIC C10923). — USA: San Diego Trough, off California, leg. Lisa Levin and students, R/V *New Horizon*, otter trawl, 31.x.2009, 32.59600°N, 117.48300°W, 1200 m: 1 not measured (SIO-BIC C11171). — USA: California, leg. E/V *Nautilus*, ROV Hercules dive H1829, Stn NA123-015-02-B-MCZ, 17.x.2020, 34.87917°N, 121.74157°W, 1295 m: 1 F 12.1 mm (MCZ IZ-162084).

COSTA RICA: Mound Jaguar, leg. Greg Rouse, Avery Hiley, R/V *Falkor*, ROV *SuBastian* dive S0230 S3, 25.i.2019, 9.65882°N, 85.88289°W, 1895 m: 1 M 5.8 mm (SIO-BIC C13964).

Diagnosis

Carapace with numerous short scales each with long, stiff setae, laterally with 3–4 spines, cervical grooves distinct. Rostral spine triangular, slender, often dorsally carinated, lateral margin often serrated. Pair of epigastric spines, often with additional small spines. Frontal margins slightly oblique. Orbit not distinctly excavated; outer orbital angle

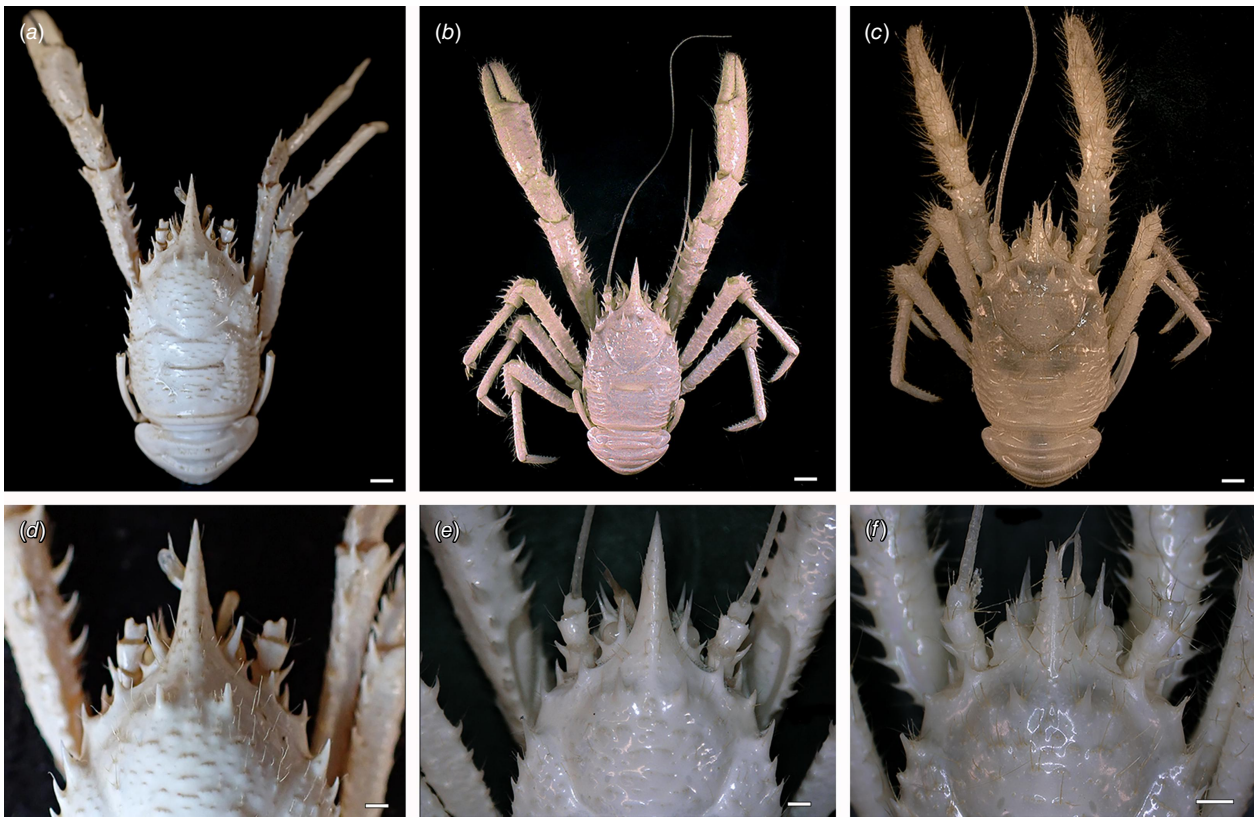

Fig. 18. *Munidopsis similis* Smith, 1885. (*a*, *d*) Holotype, Nantucket Shoals, Northwest Atlantic (USNM 8255). (*b*, *e*) Gay Head–Bermuda transect, Northwest Atlantic (MCZ IZ-81478). (*c*, *f*) California, East Pacific (MCZ IZ-162084). Scale bars: *a*, *b*, 2 mm; *c*–*f*, 1 mm.

produced into a strong antennal spine. Anterolateral spine of carapace strong. Branchial margin with 3–4 spines. Abdominal somites with transverse ridge, unarmed. Telson divided into 10 plates. Sternite 3 moderately broad, anterolateral angles produced, sternite 4 subtriangular. Eyes fixed, armed with mesial and lateral spines, mesial larger, epistomial spine absent. Article 1 of peduncle with well developed subequal dorsolateral and distolateral spines. Article 1 of antenna with distomesial spines and distolateral spines. Mxp3 merus as long as ischium, subrhomboidal in lateral view. P1 slender, elongate, spinose, fixed finger with denticulate carina on distolateral margin. P2 not reaching end of P1. P2–4 long and slender; dactyli moderately slender, curving, flexor margin with teeth along entire margin decreasing proximally. Epipods absent from all pereopods.

Colouration

Carapace, abdomen, eyes and pereopods whitish.

Distribution

Northwest Atlantic Ocean, Bering Sea and Northeast Pacific, including Costa Rica, from 1390- to 3314-m depth.

Genetic data

COI, *16S* rRNA and *28S* rRNA.

Remarks

Munidopsis similis was described from southern New England and recorded from the Middle Atlantic Bight, West of Iceland and the Gulf of Mexico (Smith 1885; Hansen 1908; Wenner 1982; Coykendall *et al.* 2017). Marin (2020) described a new taxon, *M. asiatica*, from the Bering Sea, reported as morphologically and genetically very similar to *M. similis* (see Marin 2020). We discovered new records of *M. similis* for the Northeast Pacific (USA and Costa Rica). Our analyses demonstrate a lack of genetic structure for *COI* among the Atlantic and East Pacific populations of *M. similis*, including the Bering Sea population corresponding to *M. asiatica*, therefore there is no molecular evidence for considering these as two separate taxa (Fig. 2, 4*b*). We found morphological variation at the individual level among and within the Atlantic and East Pacific populations in the relative width of the rostrum in relation to length, the presence or absence of a dorsal carina and the presence or absence of small additional spines on the epigastric and hepatic dorsal carapace (see

Supplementary Fig. S8). Variations within these characters were considered to be morphological differences between both species (Marin 2020). However, when several specimens of different populations are examined, this variation becomes intraspecific. Therefore, due to the lack of morphological and molecular support, we propose *M. asiatica* as a junior synonym of *M. similis*.

Munidopsis testuda sp. nov.

(Fig. 19*a–j*.)

ZooBank: urn:lsid:zoobank.org:act:9CD8FBD7-C6D7-410D-9D30-C367EDF0B7AF

Material examined

Holotype. ECUADOR: Galapagos Archipelago, leg. R/V *Thomas Washington*, Stn PLUM 02 WT, Rock Dredge D-08, 23.i.1990, 1.11683°N, 88.26283°W, 1000–917 m: ov. F 15.1 mm, 2 eggs (SIO-BIC C9639).

Etymology

From the Latin *testudo* (meaning 'turtle'), referring to Galapagos Islands but also the squamate carapace of the species, like a turtle shell.

Diagnosis

Carapace dorsally covered in granules and scales, wider scales at posterior, with dorsal deep furrows, cervical grooves distinct. Rostrum broad, dorsally elevated, spade-shaped, dorsally carinate, distally armed with 2 spines. Frontal margin nearly straight, spine below antennal angle. Orbit not excavated, outer orbital angle with a blunt lobe. Anterolateral angle armed with a spine. Branchial margin armed with a spine. Abdominal somites unarmed. Telson divided into 7 plates. Sternite 3 anterolaterally rounded, anterior margin with median lobe flanked by 2 lobes, sternite 4 narrowly subtriangular. Eyes unarmed, movable, epistomial spine present, cornea elongated. Article 1 of antennule with dorsolateral and distolateral spines, distolateral double. Article 1 of antenna with strong distomesial spine and distolateral spines. Mxp3 merus rectangular in lateral view. P1 stout, unarmed, fixed finger without denticulate carina on distolateral margin. P2–4 stout, unarmed; meri carinated, dactyli slender, curving, flexor margin with minute teeth along all margins decreasing proximally. Epipods present on P1–2.

Description

Carapace

Slightly broader than long, widest at midlength; moderately convex from side to side. Dorsal surface densely covered in granules and scales, each scale with a few short setae; hepatic and anterior branchial areas with scales and some acute granules; posterior cardiac and intestinal region covered in larger scales. Regions well delineated by deep furrows including distinct anterior and posterior cervical grooves. Gastric region slightly elevated. Posterior margin unarmed, preceded by elevated ridge. Rostrum broad, dorsally elevated, spade-shaped (lateral margins constricted between eyes), width 0.2× anterior width of carapace, directed slightly upwards, dorsally carinate, distally armed with 2 broad spines; 0.4× carapace length, 1.8× as long as broad. Frontal margin nearly straight behind ocular peduncle, blunt outer orbital angle above antennal peduncle, outer orbital spine and process (antennal spine) absent; spine below antennal angle, ventral to frontal margin, close to epistomial spine. Lateral margins straight; anterolateral spine broad; anterior branchial margin with one broad spine; one broad branchial spine behind posterior branch of cervical groove. Pterygostomian flap surface covered in granules and scales, anteriorly acute.

Sternum

0.9× as long as broad, maximum width at sternite 6. Sternite 3 broad, 3.2× wider than long, anterolaterally rounded, anterior margin with median lobe flanked by 2 lobes. Sternite 4 narrowly elongated anteriorly; surface depressed in midline, smooth; greatest width 2.3× that of sternite 3 and 1.7× wider than long.

Abdomen

Unarmed; tergite 2 with 2 elevated transverse ridges, lateral parts of dorsal surfaces covered in granules and scales; tergites 3–6 lacking a posterior ridge; tergite 6 with weakly produced posterolateral lobes and nearly transverse posteromedian margin. Telson composed of 8 plates; 1.5× as wide as long.

Eye

Eyestalk movable, partially concealed by rostrum; peduncle covered with a few granules, shorter than cornea length; cornea ovoid and elongated; lateral surface contiguous to epistomial spine, epistomial spine ventral to frontal margin.

Antennule

Article 1 of peduncle with subequal dorsolateral and distolateral spines; distomesial margin slightly produced and granulated.

Antenna

Peduncle slightly exceeding eye. Article 1 with strong distomesial spine and distolateral spines, not reaching end of article 2. Article 2 with well developed distomesial and distolateral spines, distomesial margin granulated. Articles 3–4 unarmed.

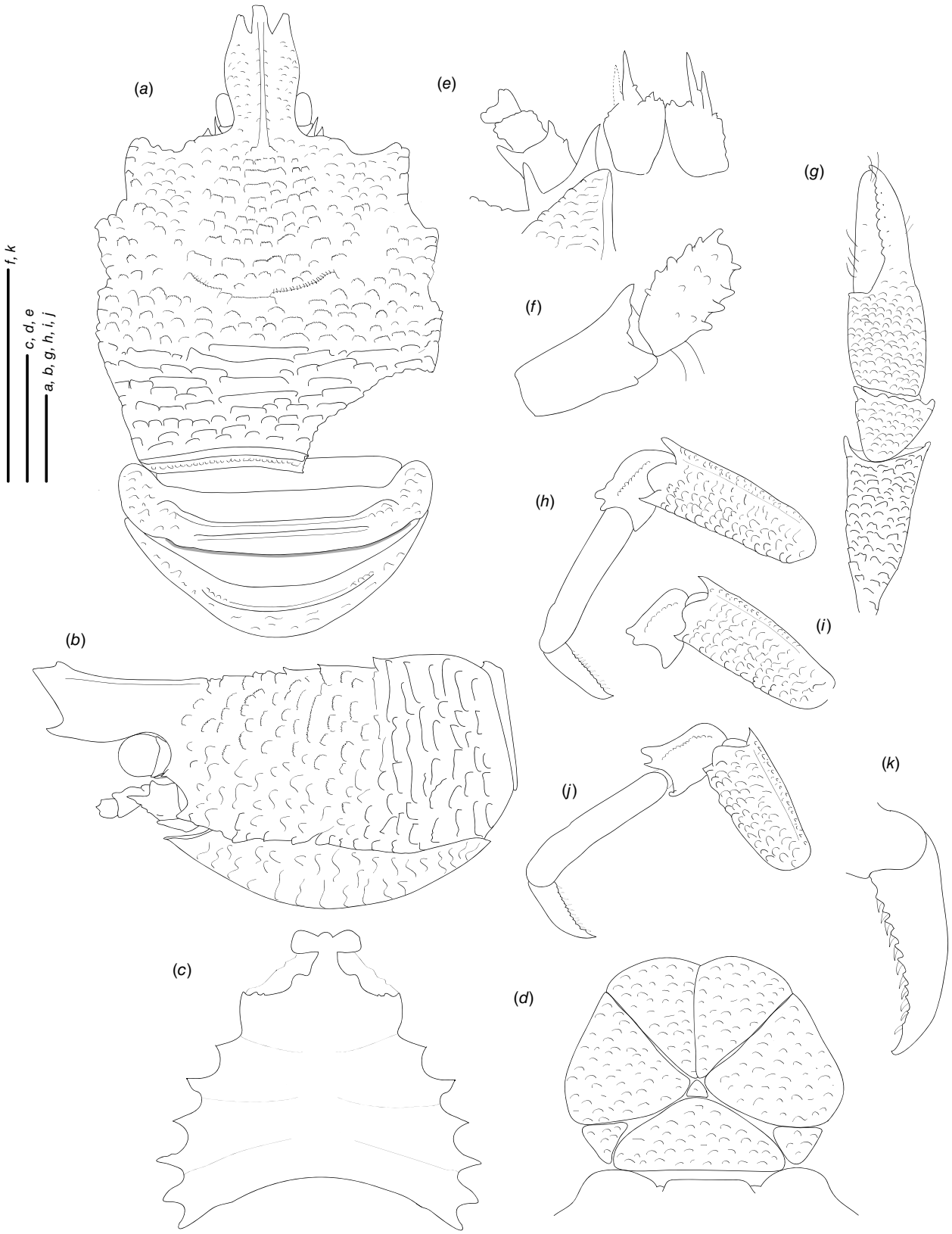

Fig. 19. (*Caption on next page*)

Fig. 19. Line diagrams of *Munidopsis testuda* **sp. nov.,** ov. F 15.1 mm, holotype (SIO-BIC C9639), Ecuador: Galapagos. (*a*) Carapace and abdomen, dorsal view. (*b*) Carapace and abdomen, lateral view. (*c*) Sternal plastron. (*d*) Telson. (e) Cephalic region, showing antennular and antennal peduncles, ventral view. (*f*) Left Mxp3, lateral view. (*g*) Right P1, dorsal view. (*h*) Right P2, lateral view. (*i*) Right P3, lateral view. (*j*) Right P4, lateral view. (*k*) Right P4 dactyli, lateral view. Scale bars: 1 mm.

Mxp3

Surface with granules. Ischium as long as merus measured on extensor margin; flexor margin of merus with 3 spines subequal in size and a smaller distal spine; extensor margin with 6 granules or blunt spines.

P1

Stout, with numerous minute granules and scales, each scale with few short setae, 1.3× longer than carapace. Merus 2.2× carpus length, with distal stout spines. Carpus 0.9× longer than broad, with some distal stout spines, a few acute granules along dorsal side. Palm unarmed, stout, slightly longer than carpus, 1.2× longer than broad. Fingers unarmed, 1.2× longer than palm, opposing margins nearly straight, not gaping, spooned; fixed finger without denticulate carina on distolateral margin.

P2–4

Stout, coarsely granulated, devoid of setae, cylindrical in cross-section, slightly decreasing in size posteriorly. P2 merus stout, 0.6× carapace length, 2.7× longer than high and 1.1× length of P2 propodus. P2–4 meri decreasing in length posteriorly (P3 merus 0.9× length of P2 merus, P4 merus 0.85× length of P3 merus); extensor margin of P2–4 meri carinate, with small granules along entire border, distal part flattish ending in thick spine; flexor margin granulated; carpi with one thick distal spine on extensor margin, granulated carina along lateral side; P2–4 propodi 5.1–5.2× as long as high, trianguloid in cross-section, unarmed; dactyli 0.5× length of propodi; distal claw short, moderately curved; flexor margin distally curved, with 11–12 dactylar teeth at entire margin, each with slender corneous spine, ultimate tooth closer to penultimate tooth than to dactylar angle.

Epipods

Present on P1–2.

Colouration

Unknown.

Distribution

Galapagos Islands, at 917–1000-m depth.

Genetic data

COI, *16S* rRNA and *28S* rRNA.

Remarks

The new species represents a highly divergent lineage that shares a trifid rostrum with the *trifida*-group (Fig. 1, 2): e.g. *M. trifida* from East Pacific, *M. ahyongi* Dong & Li, 2021 and *M. comarge* from the West Pacific. *M. testuda* **sp. nov.**, however, does not have a close relationship or share a common ancestor with this group of species (Fig. 1, 2) and differs from this group in having epipods on P1–2 instead of having pereopods without epipods or only in P1, and a carapace that is as long as broad instead of broader than long. The new species is closely related to *M. carolinensis* Dong & Li, 2021 from the Caroline Ridge in the tropical West Pacific and *M. expansa* Benedict, 1902 from off Florida and the Caribbean Sea. However, the new species can be distinguished from the other species by the following morphological characters:

- The rostrum is triangular in *M. carolinensis* and *M. expansa* whereas this is spade-shaped and constricted between the eyes in the new species.
- The scales on the carapace and pereopods are smaller and less dense in *M. carolinensis* and *M. expansa* than in the new species.
- The new species has an additional pair of spines apart from the epistomial spines, each lateral to the eyestalk and ventral to the frontal margin, whereas this pair of spines is absent in *M. carolinensis* and *M. expansa.*
- The new species has epipods on pereopods 1–2 whereas *M. carolinensis* has pereopods without epipods.

Munidopsis testuda **sp. nov.** and *M. carolinensis* diverge on 18% for *COI*. Unfortunately, no molecular data are available for *M. expansa*.

Munidopsis cortesi sp. nov.

(Fig. 20*g*, *h*, 16*a–j*.)

Zoobank: urn:lsid:zoobank.org:act:FDC547F3-F3AF-4E15-B2E4-8783972CBC61

Material examined

Holotype. COSTA RICA: Jaco Summit, leg. Greg Rouse, Allison Miller, R/V *Falkor*, ROV *SuBastian* dive S0213, Slurp 4, 6.i.2019, 9.17402°N, 84.79990°W, 742 m: ov. F 5.2 mm (tissue SIO-BIC C13902 ex MZUCR 3761-01).

Etymology

Named for Prof. Jorge Cortés Núñez, Universidad de Costa Rica, for his invaluable collaboration on deep-sea research and his efforts to create awareness of the deep regions of Costa Rica. We honour Prof. Cortés' academic retirement

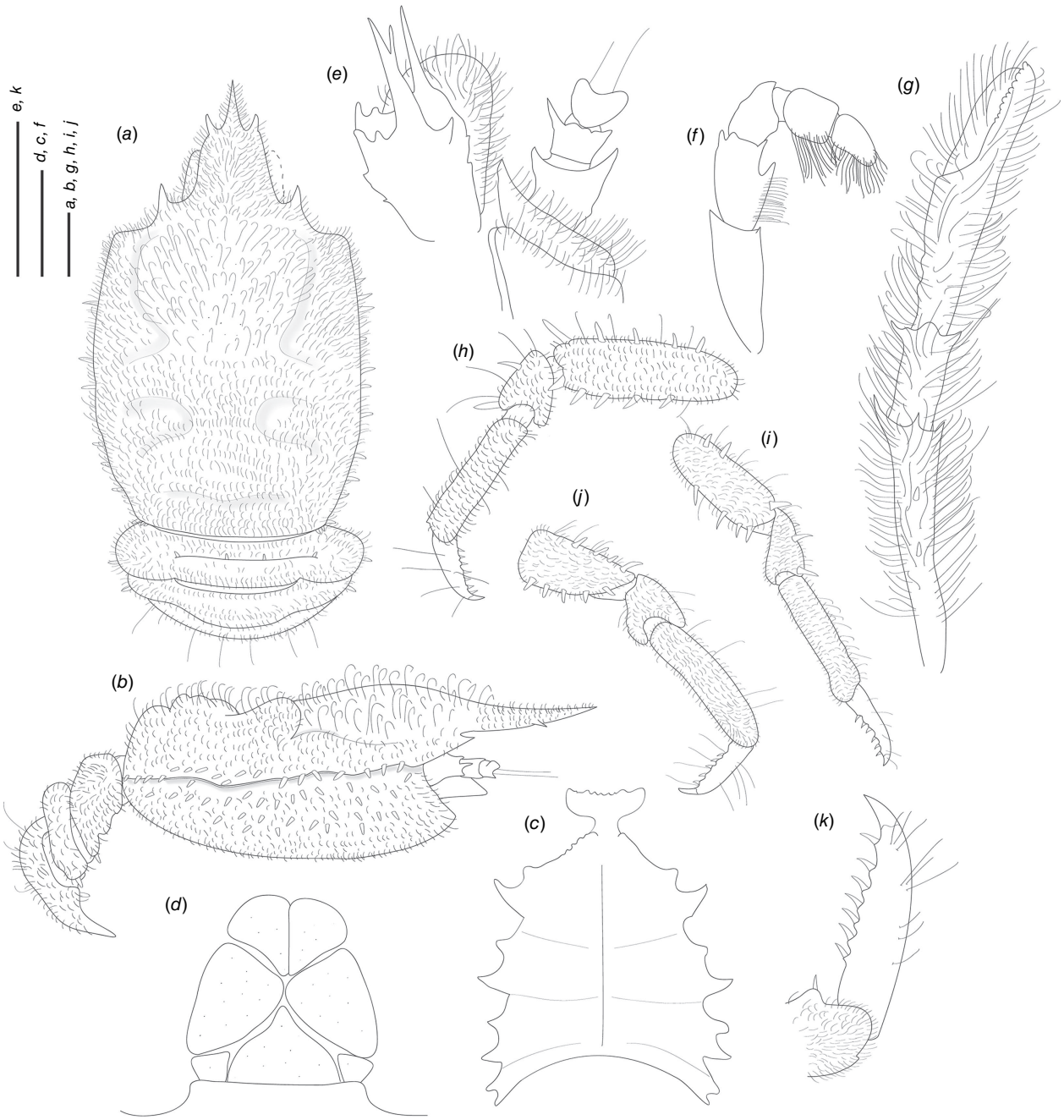

Fig. 20. Line diagrams of *Munidopsis cortesi* **sp. nov.**, ov. F 5.2 mm, holotype (MZUCR 3761-01), Costa Rica. (*a*) Carapace and abdomen, dorsal view. (*b*) Carapace and abdomen, lateral view. (*c*) Sternal plastron. (*d*) Telson. (*e*) Cephalic region, showing antennular and antennal peduncles, ventral view. (*f*) Left Mxp3, lateral view. (*g*) Right P1, dorsal view. (*h*) Right P2, lateral view. (*i*) Right P3, lateral view. (*j*) Right P4, lateral view. (*k*) Right P4 dactyli, lateral view. Scale bars: 1 mm.

after more than 40 years of research in marine biodiversity and ecology, and we celebrate his continued dedication to promoting ocean conservation.

Diagnosis

Carapace pubescent, dorsally smooth, with deep dorsal furrows, cervical grooves indistinct. Rostrum broadly triangular, trifid distally. Frontal margins concave. Orbit distinctly excavated, outer orbital angle with a strong spine. Anterolateral unarmed. Branchial unarmed. Abdominal somites 2–4 armed with posterolateral teeth, abdominal somite 3 armed with 4 teeth. Telson divided into 7 plates. Sternite 3 anterolaterally rounded, anterior margin with median serrated shallow notch flanked by 2 lobes, sternite 4 subtriangular. Eyes unarmed, movable, epistomial spine absent. Article 1 of antennule with

dorsolateral and distolateral spines. Article 1 of antenna with well-developed distomesial spine. Mxp3 merus subrhomboidal in lateral view. P1 slender, pubescent, fixed finger without denticulate carina on distolateral margin. P2–4 stout, pubescent; meri armed with acute teeth on flexor and extensor margins, propodi flattish in cross-section; dactyli slender, curving, flexor margin with cuticular teeth along all margins decreasing proximally. Epipods absent from all pereopods.

Description

Carapace

1.2× longer than wide; moderately convex from side to side; hirsute, dorsally unarmed, densely covered in short, fine setae, long distally curved setae on gastric region. Regions well delineated by deep furrows, cervical grooves indistinct. Gastric region slightly elevated. Posterior cardiac region elevated and constricted by lateral furrows, forming notches; posterior margin posteriolaterally armed with small teeth, preceded by deep transverse depression. Rostrum broad, width 0.3× anterior width of carapace, 0.4× carapace length; trifid distally; apex directed slightly upwards; lateral proximal margin weakly oblique, 1.4× as long as broad. Frontal margin concave behind ocular peduncle, antennal (outer orbital) spine strong. Lateral margins unarmed; slightly convex; widest at midlength, anterolateral angle unarmed. Pterygostomian flap densely covered with acute teeth, viewed in dorsal view, anterior margin blunt, unarmed.

Sternum

1.2× longer than broad, maximum width at sternite 5. Sternite 3 broad, 2.9× wider than long, anterolaterally rounded, anterior margin with median serrated shallow notch flanked by 2 lobes. Sternite 4 narrowly elongated anteriorly; surface depressed in midline, smooth; greatest width 2.7× that of sternite 3 and 2.0× wider than long.

Abdomen

Tergites with short, fine, dense setae; tergites 2–4 armed with posterolateral teeth; tergite 3 with elevated ridge, armed with 4 teeth; tergites 3–6 without elevated ridges; tergite 6 with posterior margin not produced. Telson composed of 7 plates, as wide as long.

Eye

Ocular peduncle unarmed; surface densely setose, movable, partially concealed by rostrum. Cornea subglobular, slightly wider than peduncle.

Antennule

Article 1 of peduncle with subequal dorsolateral and distolateral spines, distolateral spine bifid; distomesial margin with 2 pairs of blunt processes, distal surface dentate; distolateral margin armed with one spine.

Antenna

Peduncle exceeding eye; Article 1 with distomesial spine not reaching end of article 2, distolateral angle rounded. Articles 2–3 with well-developed distolateral spine, distomesial spine smaller. Article 4 unarmed. Flagellum longer than carapace.

Mxp3

Merus with 2 large spines along flexor margin, proximal larger than distal; small distal spine on extensor margin. Ischium longer than wide, with distal flexor and extensor spines. Crista dentata finely denticulate. Dactylus, propodus and carpus unarmed.

P1

Slender, densely covered in short, fine setae and long setae, 1.4× longer than carapace. Merus 2.4× carpus length, with some stout distal spines. Carpus 2.4× longer than broad, with some stout distal spines. Palm unarmed, slender, slightly longer than carpus, 2.6× longer than broad. Fingers unarmed, 0.85× longer than palm, opposing margins nearly straight, not gaping, spooned, fixed finger without denticulate carina on distolateral margin.

P2–4

Stout, densely covered in short fine setae and some long distally curved setae, cylindrical in cross-section, slightly decreasing in size posteriorly. P2 merus stout, 0.55× carapace length, nearly 3.1× longer than high and 1.3× length of P2 propodus. P2–4 meri decreasing in length posteriorly (P3 merus 0.7× length of P2 merus, P4 merus 0.9× length of P3 merus); extensor margin of P2–4 meri with acute teeth along entire border, distal part trianguloid; flexor margin with acute teeth along entire border, distal strongest; carpi P2–3 with two thick teeth on extensor margin, distal strongest, flexor margin unarmed; P2–4 propodi 4.3–4.4× as long as high, flattish in cross-section, unarmed; dactyli 0.7–0.9× length of propodi; distal claw short, moderately curved; flexor margin distally curved, with 6–8 dactylar teeth decreasing in size proximally, each with slender corneous spine, ultimate tooth at midlength between penultimate tooth and dactylar angle.

Epipods

Absent from pereopods.

Colouration

Carapace, abdomen and pereopods orange and brownish. Ocular orbits orange.

Distribution

Costa Rica at 742-m depth.

Genetic data

COI, *16S* rRNA and *28S* rRNA.

Remarks

Munidopsis cortesi **sp. nov.** belongs to a group of species sharing a flattened, distally trifid rostrum and unarmed carapace surface, and lacking pereopodal epipods. This group includes *M. acuminata* Benedict, 1902 from off South Carolina, north-western Atlantic; *M. alcocki* Ahyong, 2014 from the Indian Ocean, *M. aurantia* Lin & Chan, 2011 from Taiwan, *M. kareenae* Ahyong, 2013 from New Zealand, *M. modesta* Benedict, 1902 from Galapagos Islands, *M. nias* Ahyong, 2014 from the eastern Indian Ocean, *M. pubescens* Macpherson, 2007 from Madagascar, *M. serricornis* from the North Atlantic Ocean, *M. tuerkayi* Macpherson, Beuck & Freiwald, 2016 from the Caribbean Sea and *M. treis* Ahyong & Poore, 2004 from the West Pacific Ocean.

This new species is very different and easily distinguished from the other species of the group by the following characters:

- The new species has an unarmed anterolateral angle of the carapace and unarmed carapace margins whereas the other species have at least the anterolateral margin armed.
- The new species have acute teeth on the pterygostomian flap surface whereas these teeth are absent in the other species.
- The new species have acute teeth on the flexor and extensor margins of the meri of P2–4, whereas these teeth are absent in the other species, and in all of these, the flexor margins of the meri are unarmed.

Discussion

Phylogenetic relationships of squat lobsters

Our phylogenetic results reiterate that the phylogenetic relationships of squat lobsters are poorly known at many levels. Although not part of this study, there is lack of consensus in the literature on the phylogenetic position of Galatheoidea within Anomura (Ahyong *et al.* 2009; Schnabel *et al.* 2011*b*; Bracken-Grissom *et al.* 2013; Tan *et al.* 2018). Also, conflicting results on the relationships of the families within Galatheoidea were recovered depending on the set of data used and the taxon sampling employed in analyses (Schnabel *et al.* 2011*b*; Bracken-Grissom *et al.* 2013; Roterman *et al.* 2018; Palero *et al.* 2019). Moreover, the validity of the current classification at the family level is brought into question, including the polyphyly of Galatheidae and the conflicting placement of some galatheid genera (Ahyong *et al.* 2011; Schnabel *et al.* 2011*b*; Bracken-Grissom *et al.* 2013; Rodríguez-Flores *et al.* 2022*b*). Our phylogenetic analyses agree with those obtained by Rodríguez-Flores *et al.* (2022*b*), whose results did not support the monophyly of Galatheidae. The systematic placement of *Janetogalathea californiensis* obtained in this work supports the hypothesis of the existence of an overall high-level of convergence and homoplasy within the group (Machordom and Macpherson 2004; Cabezas *et al.* 2012). The genus was initially assigned to Galatheidae, on the bases of the striation of the carapace and the presence of a triangular rostrum that is broad at the base and has 3–4 marginal spines (Ahyong *et al.* 2010; Baba *et al.* 2011). However, the conflicting position of *Janetogalathea* and other genera (*Alainius* Baba, 1991, *Leiogalathea*) lacking a trispinous or trilobate rostrum indicates that these characters are not true synapomorphies of Galatheidae and could therefore be the result of evolutionary convergence or another type of homoplasy. The inclusion of *Leiogalathea* in Munidopsidae was supported by the synapormophy of Munidopsidae having a reduced flagellum in the first maxilliped in *Leiogalathea* or the flagellum being absent in the remaining species of the family (Ahyong *et al.* 2010; Baba *et al.* 2011). The flagellum is also reduced in *Janetogalathea* as expected given the phylogenetic position as sister group to *Leiogalathea*.

By contrast, the more diverse genera within Galatheoidea (*Munida* Leach, 1820, *Munidopsis* and *Galathea* Fabricius, 1793) are non-monophyletic. Several authors have proposed that *Munida* is a composite taxon (Machordom and Macpherson 2004; Rodríguez-Flores *et al.* 2019*a*; Miranda *et al.* 2020) that includes more than 15 putative genera (Machordom pers. comm.). This is also the case for *Munidopsis*; indeed, a phylogeny using two mitochondrial genes and over 30 munidopsid taxa proposed the paraphyletic status (Ahyong *et al.* 2011). Our results fully agree with those of Ahyong *et al.* (2011) in recovering *Munidopsis* as non-monophyletic (Fig. 1) but neither Ahyong *et al.* (2011) nor our study recovered highly supported deep relationships, probably due to the low number of characters employed in the analyses and saturation of the mitochondrial genes (e.g. Blouin *et al.* 1998) or the existence of an explosive radiation that is reflected in short internodes in a phylogeny (Whitfield and Lockhart 2007). In this sense, including more molecular and morphological characters, and a more thorough taxonomic sampling in the phylogenetic reconstructions, may confirm how many independent lineages can be delimited at genus level (Rodríguez-Flores *et al.* 2021). What is evident is the presence of unique combinations of morphological characters in the different clades that point towards the existence of different genus-level lineages within *Munidopsis*. For example, the clade including only bathyal or abyssal species (Clade I, Fig. 1, 2) includes species lacking external pigmentation and ocular spines (e.g. *M. aries*, *M. bairdii, M. alvisca*); the *trifida*-clade that includes *Munidopsis cortesi* **sp. nov.** consists of species that present a trispinous rostrum; and the clade including *M. lentigo* contains species with unique carapace morphology and a pad of setae on the ventral surface of pereopod 1. All these clades are highly divergent, suggesting ancient splitting during the evolutionary history of munidopsids. Therefore this evidence, together with the lack of monophyly makes considering *Munidopsis* as a complex including

several genus-level lineages reasonable. In conclusion, a great deal of work is needed to refine the squat lobster tree of life, ideally including more data and more complete taxon sampling to obtain a broader picture of the evolutionary history.

Species delimitation and speciation patterns

As a result of integrating molecular and morphological data for the East Pacific taxa, we have delimited five new species and propose three new junior synonyms.

Most species delimitation analyses have estimated a smaller number of species for the clade including only abyssal species within *Munidopsis* (Fig. 2) despite some of these being morphologically distinct. A total of 28 currently recognised species were analysed for this clade (Clade I), whereas some of these analyses only identified 12 species. Within clade I, a group of more than 10 species with very shallow divergences (*M. arietina*, *M. antonii, M. bracteosa, M. bairdi, M recta, M. exuta, M. scotti, M. producta* and *M. starmer*) (Fig. 2) is considered by some of the methods to be a single species. In clade I, there is also conflict in the morphological delimitation in 3 subclades that include pairs of allopatric species with very shallow divergences: (a) *M. aries* from the Atlantic + *M. albatrossae* from the Pacific, (b) *M. bairdii* from the Atlantic + *M. arietina* from the Pacific and (c) *M. alvisca* from the East Pacific + *M. myojinensis* + *M. lauensis* from the West Pacific (Macpherson and Segonzac 2005; Cubelio *et al*. 2007; Dong *et al.* 2019). Non-exclusive explanations for what may occur in this clade include the following: (1) original species descriptions are usually based on the morphological examination of only a few specimens due to the poor representation in collections (e.g. Jones and Macpherson 2007; Macpherson *et al.* 2016; Dong and Li 2021; Rodríguez-Flores *et al.* 2022*a*) that might have been a source of confusion regarding intraspecific variability and morphological differences among species. This general explanation could be applied to many other cases within *Munidopsis* apart from this clade; (2) large geographical distances between morphologically similar species that might lead to consideration of these as different taxa prior to the discovery of additional records that may suggest cosmopolitanism of a single morphotype; this could be the case for the pair of allopatric species *M. aries* vs *M. albatrossae* that are unclearly distinguished based on morphology but differ in geographical ranges (García Raso *et al.* 2008); (3) morphological disparity is high across *Munidopsis* (Rodríguez-Flores *et al.* 2022*a*) and also correlated with high intraspecific variation (see *M. antonii* in Baba 2005), and this high morphological disparity coupled with shallow divergences could be an indicator of a recent radiation of this clade; and (4) there might be a reduction in the rate of molecular evolution of the clade that results in shallow divergences when compared to other *Munidopsis* lineages, perhaps in relation to the adaptation to abyssal depths. In this sense, Rodríguez-Flores *et al.* (2022*b*) suggested that increased depth could reduce the rate of substitution in related squat lobsters. In this sense, there is evidence suggesting differences in functional loci in deep-sea fishes living at different depths (Gaither *et al*. 2018). Therefore, the effect of depth on the rate of molecular evolution of squat lobsters should be tested using thorough sampling, genomic data or a proxy of molecular evolution (e.g. CG content or transversion *v*. transition).

In any case some of these species likely constitute a single taxon with geographically structured genetic and morphological diversity. This may be the case for the clades mentioned earlier, and others, for example the species-group including *M. nitida*, *M. vrijenhoeki* and *M. spinifrons* from the Indian and Pacific oceans; and the species-group including M. *bermudezi* Chace, 1939 from the Atlantic and *M. cascadia* Ambler, 1980 from the East Pacific. We prefer not to make any taxonomic decisions in relation to any of these species, as a larger dataset including populations across all oceans, the study of intraspecific morphological variation and testing gene flow with nuclear markers should be considered to properly address these species hypotheses.

Limitations and caveats for these single-locus delimitation methods are broadly acknowledged (e.g. Sukumaran and Knowles 2017; Dellicour and Flot 2018). Population structure could be confounded with species divergences, especially for recent species. Introgression and other population processes such as incomplete lineage sorting could make species delimitation using a single mitochondrial locus difficult, in which case rapidly evolving nuclear genes can be much more informative. However, for deeply divergent species, single locus species delimitation seems to have relatively more power than for recently diverged ones (Rannala and Yang 2020). Another caveat of applying these methods to explore the species of Munidopsidae is that our data set contains many species, some of which are highly divergent with ancient speciation events and others of much more recent origin, and this prevents delimitation of all of these (Puillandre *et al.* 2021). Some of the methods might not be appropriate to analyse this set of data, for example there are many singletons that could not be suitable for these analyses. The nature of our data (many shallow and highly divergent species) resulted in a barcode gap that is barely discernible across the genetic distance data for ABGD; and other methods like bPTP or GMYC are probably over-splitting the real number of species (Dellicour and Flot 2018). Nonetheless, there is consensus in that we should consider different sources of data for species delimitation (e.g. Puillandre *et al.* 2012). Moreover, taking into account the agreement of several species delimitation methods (Dellicour and Flot 2018), the taxonomic status of the species included in this clade should be revised, including multiple sources of evidence and more robust data. However, some of the species considered in this clade

might be a single species attaining an abyssal cosmopolitan distribution. This conclusion seems to be congruent with the general idea of cosmopolitanism in the abyssal depth (McClain and Hardy 2010). This hypothesis should be tested further.

Biogeographical considerations

Interestingly, after removing *Janetogalathea* from Galatheidae, the family Galatheidae would be represented in the East Pacific only by *Galathea paucilineata* (Benedict, 1902) from Galapagos (if considering *Phylladiorhynchus* as non-Galatheidae following Rodríguez-Flores *et al.* 2022*b*; Fig. 1). According to the original description (Benedict 1902), this species would fit well within the genus *Leiogalathea*. However, the rostrum and some legs are unknown and until more material of this taxon can be examined, we cannot disprove that *G. paucilineata* might be a *Galathea* species, a member of *Leiogalathea* or even a species of *Janetogalathea* (Arnés-Urgellés *et al.* 2020). Irrespectively, the family Galatheidae is poorly represented in the Americas in comparison with the East Atlantic and the West Pacific (Schnabel *et al.* 2011*a*). Also, Munididae, despite being the most diverse family of squat lobsters (Baba *et al*. 2008), is much less speciose in the East Pacific than Munidopsidae in the EP with only 21 species described or reported to date.

Munidopsidae, with more representatives in abyssal depths than Munididae – that has a peak of diversity in the continental shelf – seems to be more prone to cosmopolitanism and have wider geographical ranges than the other families. For example, the recent finding of *M. lauensis* in the Indian Ocean suggests long distance dispersal among hydrothermal vents between the Indian and Pacific oceans (Borda *et al*. 2013; Hwang *et al.* 2022). This fact together with the shallow divergence between this species and *M. alvisca* could indicate the existence of a single, widely distributed taxon in which hydrothermal vents could facilitate a type of stepping-stone dispersal. Cosmopolitanism is known for many deep-sea invertebrate species, for example nematodes at both genus- and species-level (Miljutin *et al.* 2010; Zeppilli *et al.* 2011), echinoderms (Thomas *et al.* 2020) and molluscs (Oliver 2015), among others. The abyss has often been perceived as a homogenous habitat lacking horizontal barriers to dispersal (e.g. Etter *et al.* 2005, 2011) but the existence of species complexes in abyssal depths has challenged the traditional view of general cosmopolitanisms for abyssal taxa (Schornikov 2005; Raupach *et al.* 2007; McClain and Hardy 2010; Brandão and Yasuhara 2013). In cases of taxa with pan-abyssal distributions, horizontal (geographic) barriers to gene flow seem to be less determinant than vertical (bathymetric) barriers (Etter *et al.* 2005; Breusing *et al.* 2020; McCowin *et al.* 2020; Prada and Hellberg 2021).

In the case of *Munidopsis*, some species are apparently distributed across small areas, whereas others have a much wider spatial distribution. These restricted distributions are more common in species from bathyal depths than for abyssal species, as is the case for species in Clade II, e.g. *M. hystrix*, *M. scabra* and *M. depressa* (Fig. 2), all endemic to the northern East Pacific. These contrasting distribution patterns could be related to the biological cycles and dispersal strategies of each species, although this could also be related to the rarity of some species (e.g. *M. granosicorium* is only known for the holotype and from the specimen described here from Costa Rica). The entire larval cycle of *Munidopsis* is only known for a few species, mainly from the abyssal clade, e.g. *M. bermudezi*, *M. bairdii, M. curvirostra* Whiteaves, 1874 and *M. similis* (Wenner 1982), all with planktotrophic larvae (Baba *et al.* 2011) and therefore able to disperse over long distances (Baco *et al.* 2016). However, hydrothermal vent species such as *M. lentigo* and *M. subsquamosa* Henderson, 1885 have been suggested to possibly have a lecithotrophic larva (Van Dover *et al.* 1985). The larval cycle for most species is unknown (Baba *et al.* 2011), however, and the only biological data available are body size and the relation to the size and number of eggs (Van Dover *et al.* 1985). If size and number of eggs are indicative of the type of life cycle, some munidopsids with a low number of large eggs (for example *M. granosicorium*, here analysed) might likely also have a lecithotrophic larval cycle with limited long-distance dispersal (Baco *et al.* 2016). Several studies at the population level (Etter *et al.* 2005; Zardus *et al.* 2006) have shown that bathyal species exhibit greater population structure than abyssal species, usually characterised by low genetic divergences among populations. This phenomenon may be influenced by the dispersal abilities of the species but also because of constraints for abyssal species in terms of vertical barriers in the deep sea.

Deep-sea squat lobsters from the East Pacific will continue to surprise us in many ways, for example with new taxa such as the new species described here, that represent ancient and highly divergent lineages. Also, new records demonstrate that deep species of *Munidopsis* could have wider ranges than previously considered, some perhaps being cosmopolitan and some of which have been able to cross the eastern Pacific Barrier (Lessios and Robertson 2006). Taxonomic knowledge is fundamental for investigating evolutionary and biogeographical questions regarding deep-sea taxa, in an era where the deep sea has become a target of economic interests as a source of multiple natural resources. Now more than ever there is a need to explore and study deep-sea species diversity and to understand these unique ecosystems before human activity has an irreversible impact.

Supplementary material

Supplementary material is available online.

References

Ahyong ST, Schnabel KE, Maas EW (2009) Anomuran phylogeny: new insights from molecular data. In 'Decapod Crustacean Phylogenetics'. (Eds JW Martin, DL Felder, KA Crandall) *Crustacean Issues*, vol. 18, pp. 399–341. (CRC Press: Boca Raton, FL, USA)

Ahyong ST, Baba K, Macpherson E, Poore GCB (2010) A new classification of the Galatheoidea (Crustacea: Decapoda: Anomura). *Zootaxa* **2676**, 57–68. doi:10.11646/zootaxa.2676.1.4

Ahyong ST, Andreakis N, Taylor J (2011) Mitochondrial phylogeny of the deep-sea squat lobsters, Munidopsidae (Galatheoidea). *Zoologischer Anzeiger – a Journal of Comparative Zoology* **250**, 367–377. doi:10.1016/j.jcz.2011.06.005

Arnés-Urgellés C, Buglass S, Ahyong ST, Salinas-de-León P, Wicksten MK, Marsh L (2020) Arthropoda; crustacea; decapoda of deep-sea volcanic habitats of the galapagos marine reserve, tropical eastern pacific. *Biodiversity Data Journal* **8**, e54482. doi:10.3897/BDJ.8.e54482

Baba K (2005) Deep-sea chirostylid and galatheid crustaceans (Decapoda: Anomura) from the Indo-Pacific, with a list of species. *Galathea Report* **20**, 1–317.

Baba K, Wicksten MK (2019) Chirostyloidean squat lobsters (Crustacea: Decapoda: Anomura) from the Galapagos Islands. *Zootaxa* **4564**(2), 391–421. doi:10.11646/zootaxa.4564.2.5

Baba K, Macpherson E, Poore GCB, Ahyong ST, Bermudez A, Cabezas P, Lin C-W, Nizinski M, Rodrigues C, Schnabel KE (2008) Catalogue of squat lobsters of the world (Crustacea: Decapoda: Anomura – families Chirostylidae, Galatheidae and Kiwaidae). *Zootaxa* **1905**, 1–220. doi:10.11646/zootaxa.1905.1.1

Baba K, Macpherson E, Lin CW, Chan TY (2009) 'Crustacean Fauna of Taiwan. Squat lobsters (Chirostylidae and Galatheidae).' (National Taiwan Ocean University: Keelung, Taiwan)

Baba K, Ahyong ST, Macpherson E (2011) Morphology of marine squat lobsters. In 'The Biology of Squat Lobsters'. (Eds GCB Poore, ST Ahyong, J Taylor) pp. 1–38. (CSIRO Publishing: Melbourne, Vic., Australia)

Baco AR, Etter RJ, Ribeiro PA, von der Heyden S, Beerli P, Kinlan BP (2016) A synthesis of genetic connectivity in deep-sea fauna and implications for marine reserve design. *Molecular Ecology* **25**, 3276–3298. doi:10.1111/mec.13689

Bahamonde N (1964) Dos nuevos Munidopsis en aguas Chilenas *Boletín del Museo Nacional de Historia Natural* **28**, 157–170.

Benedict JE (1902) Descriptions of a new genus and forty-six new species of crustaceans of the family Galatheidae, with a list of the known marine species. *Proceedings of the United States National Museum* **26**, 243–334. doi:10.5479/si.00963801.26-1311.243

Blouin MS, Yowell CA, Courtney CH, Dame JB (1998) Substitution bias, rapid saturation, and the use of mtDNA for nematode systematics. *Molecular Biology and Evolution* **15**, 1719–1727. doi:10.1093/oxfordjournals.molbev.a025898

Borda E, Kudenov JD, Chevaldonné P, Desbruyères D, Blake JA, Fabri M-C, Hourdez S, Shank TM, Wilson NG, Pleijel F, Schulze A, Rouse GW (2013) Cryptic species of *Archinome* (Annelida: Amphinomida) from vents and seeps. *Proceedings of the Royal Society of London Series B: Biological Sciences* **280**, 20131876. doi:10.1098/rspb.2013.1876

Bouckaert R, Vaughan TG, Barido-Sottani J, Duchêne S, Fourment M, Gavryushkina A, Heled J, Jones G, Kühnert D, De Maio N, Matschiner M, Mendes FK, Müller NF, Ogilvie HA, du Plessis L, Popinga A, Rambaut A, Rasmussen D, Siveroni I, Suchard MA, Wu CH, Xie D, Zhang C, Stadler T, Drummond AJ (2019) BEAST 2.5: an advanced software platform for Bayesian evolutionary analysis. *PLoS Computational Biology* **15**, e1006650. doi:10.1371/journal.pcbi.1006650

Bracken-Grissom HD, Cannon ME, Cabezas P, Feldmann RM, Schweitzer CE, Ahyong ST, Felder DL, Lemaitre R, Crandall KA (2013) A comprehensive and integrative reconstruction of evolutionary history for Anomura (Crustacea: Decapoda). *BMC Evolutionary Biology* **13**, 128. doi:10.1186/1471-2148-13-128

Brandão SN, Yasuhara M (2013) Challenging deep-sea cosmopolitanism: taxonomic re-evaluation and biogeography of '*Cythere dasyderma* Brady, 1880' (Ostracoda). *Journal of Micropalaeontology* **32**, 109–122. doi:10.1144/jmpaleo2012-009

Breusing C, Johnson SB, Tunnicliffe V, Clague DA, Vrijenhoek RC, Beinart RA (2020) Allopatric and sympatric drivers of speciation in *Alviniconcha* hydrothermal vent snails. *Molecular Biology and Evolution* **37**, 3469–3484. doi:10.1093/molbev/msaa177

Cabezas P, Sanmartín I, Paulay G, Macpherson E, Machordom A (2012) Deep under the sea: unraveling the evolutionary history of the deep-sea squat lobster *Paramunida* (Decapoda, Munididae). *Evolution* **66**, 1878–1896. doi:10.1111/j.1558-5646.2011.01560.x

Coykendall DK, Nizinski MS, Morrison CL (2017) A phylogenetic perspective on diversity of Galatheoidea (Munida, Munidopsis) from cold-water coral and cold seep communities in the western North Atlantic Ocean. *Deep-Sea Research – II. Topical Studies in Oceanography* **137**, 258–272. doi:10.1016/j.dsr2.2016.08.014

Crandall KA, Fitzpatrick JF Jr (1996) Crayfish molecular systematics: using a combination of procedures to estimate phylogeny. *Systematic Biology* **45**, 1–26. doi:10.1093/sysbio/45.1.1

Cubelio SS, Tsuchida S, Hendrickx ME, Kado R, Watanabe S (2007) A new species of vent associated *Munidopsis* (Crustacea: Decapoda: Anomura: Galatheidae) from the Western Pacific, with notes on its genetic identification. *Zootaxa* **1435**, 25–36. doi:10.11646/zootaxa.1435.1.3

Dellicour S, Flot JF (2018) The hitchhiker's guide to single-locus species delimitation. *Molecular Ecology Resources* **18**, 1234–1246. doi:10.1111/1755-0998.12908

Dong D, Li X (2021) Two new species of the genus *Munidopsis* Whiteaves, 1874 (Crustacea: Anomura: Munidopsidae) from the Caroline Ridge, South of the Mariana Trench. *Journal of Oceanology and Limnology* **39**, 1841–1853. doi:10.1007/s00343-021-0385-6

Dong D, Xu P, Li XZ, Wang C (2019) *Munidopsis* species (Crustacea: Decapoda: Munidopsidae) from carcass falls in Weijia Guyot, West Pacific, with recognition of a new species based on integrative taxonomy. *PeerJ* **7**, e8089. doi:10.7717/peerj.8089

Dong D, Gan Z, Li X (2021) Descriptions of eleven new species of squat lobsters (Crustacea: Anomura) from seamounts around the Yap and Mariana Trenches with notes on DNA barcodes and phylogeny. *Zoological Journal of the Linnean Society* **192**, 306–355. doi:10.1093/zoolinnean/zlab003

Drummond AJ, Rambaut A (2007) BEAST: Bayesian evolutionary analysis by sampling trees. *BMC Evolutionary Biology* **7**(1), 214. doi:10.1186/1471-2148-7-214

Etter RJ, Rex MA, Chase MR, Quattro JM (2005) Population differentiation decreases with depth in deep-sea bivalves. *Evolution* **59**, 1479–1491. doi:10.1111/j.0014-3820.2005.tb01797.x

Etter RJ, Boyle EE, Glazier A, Jennings RM, Dutra E, Chase MR (2011) Phylogeography of a pan-Atlantic abyssal protobranch bivalve: implications for evolution in the deep Atlantic. *Molecular Ecology* **20**, 829–843. doi:10.1111/j.1365-294X.2010.04978.x

Faxon W (1895) XV. The stalk-eyed Crustacea. In 'Reports on an exploration off the west coasts of Mexico, Central and South America, and off the Galapagos Islands, in charge of Alexander Agassiz, by the U.S. Fish Commission Steamer "Albatross" during 1891, Lieut.-Commander Z.L. Tanner, U.S.N., commanding'. *Memoirs of the Museum of Comparative Zoology at Harvard College* **18**, 1–230.

Folmer O, Black M, Hoeh W, Lutz R, Vrijenhoek R (1994) DNA primers for amplification of mitochondrial cytochrome *c* oxidase subunit I from diverse metazoan invertebrates. *Molecular Marine Biology and Biotechnology* **3**, 294–299.

Fujisawa T, Barraclough TG (2013) Delimiting species using single-locus data and the Generalized Mixed Yule Coalescent approach: a revised method and evaluation on simulated data sets. *Systematic Biology* **62**, 707–724. doi:10.1093/sysbio/syt033

Gaither MR, Gkafas GA, de Jong M, Sarigol F, Neat F, Regnier T, Moore D, Gröcke DR, Hall N, Liu X, Kenny J, Lucaci A, Hughes M, Haldenby S, Hoelzel AR (2018) Genomics of habitat choice and adaptive evolution in a deep-sea fish. *Nature Ecology & Evolution* **2**(4), 680–687. doi:10.1038/s41559-018-0482-x

García Raso JE, García Muñoz JE, Manjón-Cabeza ME (2008) First record of *Munidopsis albatrossae* (Crustacea: Decapoda: Galatheidae) from Antarctic waters. *Polar Biology* **31**, 1281–1285. doi:10.1007/s00300-008-0476-2

Goffredi SK, Jones WJ, Erhlich H, Springer A, Vrijenhoek RC (2008) Epibiotic bacteria associated with the recently discovered Yeti crab,

Kiwa hirsuta. *Environmental Microbiology* **10**(10), 2623–2634. doi:10.1111/j.1462-2920.2008.01684.x
Guzman GL, Sellanes J (2015) A review of the Munidopsidae Ortmann, 1898 (Decapoda, Galatheoidea) in Chilean waters, including new records for the Southeastern Pacific. *Zootaxa* **4021**(2), 282–306. doi:10.11646/zootaxa.4021.2.3
Hansen HJ (1908) Crustacea Malacostraca. I. In 'The Danish-Ingolf Expedition. Volume III'. (H. Hagerup: Copenhagen, Denmark)
Hatch AS, Liew H, Hourdez S, Rouse GW (2020) Hungry scale worms: phylogenetics of Peinaleopolynoe (Polynoidae, Annelida), with four new species. *ZooKeys* **932**, 27–74. doi:10.3897/zookeys.932.48532
Henderson JR (1885) XXXIX. – Diagnoses of the new species of Galatheidea collected during the 'Challenger' expedition. *Annals and Magazine of Natural History* **16**, 407–421. doi:10.1080/00222938509459908
Hendrickx ME (2021) Squat lobsters (Crustacea: Decapoda: Anomura: Galatheoidea) from off the northwestern coast of the Baja California Peninsula, Mexico. *Zootaxa* **4965**, 375–384. doi:10.11646/zootaxa.4965.2.10
Hendrickx ME, Ayón-Parente M (2013) A new species of *Munidopsis* (Anomura, Galatheoidea, Munidopsidae) from the Gulf of California, Western Mexico. *Crustaceana* **86**, 1304–1315. doi:10.1163/15685403-00003241
Hendrickx ME, Ayón-Parente M, Serrano D (2011) Registro adicional de *Janetogalathea californiensis* (Anomura: Galatheidae) del Golfo de California central, México, con notas de su distribución. *Hidrobiológica* **21**, 89–94. [In Spanish]
Hudson RR (1991) Gene genealogies and the coalescent process. *Oxford Surveys in Evolutionary Biology* **7**, 1–44.
Huelsenbeck JP, Ronquist F (2001) MRBAYES: Bayesian inference of phylogenetic trees. *Bioinformatics* **17**, 754–755. doi:10.1093/bioinformatics/17.8.754
Hwang H, Cho B, Cho J, Park B, Kim T (2022) New record of hydrothermal vent squat lobster (*Munidopsis lauensis*) provides evidence of a dispersal corridor between the Pacific and Indian oceans. *Journal of Marine Science and Engineering* **10**(3), 400. doi:10.3390/jmse10030400
Jones WJ, Macpherson E (2007) Molecular phylogeny of the East Pacific squat lobsters of the genus *Munidopsis* (Decapoda: Galatheidae) with the descriptions of seven new species. *Journal of Crustacean Biology* **27**(3), 477–501. doi:10.1651/S-2791.1
Kahle D, Wickham H (2013) ggmap: spatial visualization with ggplot2. *The R Journal* **5**, 144–161. doi:10.32614/RJ-2013-014
Katoh K, Misawa K, Kuma K-i, Miyata T (2002) MAFFT: a novel method for rapid multiple sequence alignment based on fast Fourier transform. *Nucleic Acids Research* **30**, 3059–3066. doi:10.1093/nar/gkf436
Larsson A (2014) AliView: a fast and lightweight alignment viewer and editor for large datasets. *Bioinformatics* **30**, 3276–3278. doi:10.1093/bioinformatics/btu531
Lessios HA, Robertson DR (2006) Crossing the impassable: genetic connections in 20 reef fishes across the eastern Pacific barrier. *Proceedings of the Royal Society of London – B. Biological Sciences* **273**, 2201–2208. doi:10.1098/rspb.2006.3543
Luke SR (1977) Catalog of the benthic invertebrate collections of the Scripps Institution of Oceanography. I – Decapod Crustacea and Stomatopoda. *Scripps Institution of Oceanography Reference Series* **77-9**, 1–72.
McClain CR, Hardy SM (2010) The dynamics of biogeographic ranges in the deep sea. *Proceedings of the Royal Society of London – B. Biological Sciences* **277**, 3533–3546. doi:10.1098/rspb.2010.1057
McCowin MF, Feehery C, Rouse GW (2020) Spanning the depths or depth-restricted: three new species of *Bathymodiolus* (Bivalvia, Mytilidae) and a new record for the hydrothermal vent *Bathymodiolus thermophilus* at methane seeps along the Costa Rica margin. *Deep-Sea Research – I. Oceanographic Research Papers* **164**, 103322. doi:10.1016/j.dsr.2020.103322
Machordom A, Macpherson E (2004) Rapid radiation and cryptic speciation in squat lobsters of the genus Munida (Crustacea, Decapoda) and related genera in the South West Pacific: molecular and morphological evidence *Molecular Phylogenetics and Evolution* **33**(2), 259–279. doi:10.1016/j.ympev.2004.06.001
Macpherson E (2007) Species of the genus *Munidopsis* Whiteaves, 1784 from the Indian and Pacific Oceans and reestablishment of the genus *Galacantha* A. Milne-Edwards, 1880 (Crustacea, Decapoda, Galatheidae). *Zootaxa* **1417**, 1–135. doi:10.11646/zootaxa.1417.1.1
Macpherson E, Baba K (2011) Chapter 2. Taxonomy of squat lobsters. In 'The Biology of Squat Lobsters'. (Eds GCB Poore, ST Ahyong, J Taylor) pp. 39–71. (CSIRO Publishing: Melbourne, Vic., Australia)
Macpherson E, Segonzac M (2005) Species of the genus *Munidopsis* (Crustacea, Decapoda, Galatheidae) from the deep Atlantic Ocean, including cold-seep and hydrothermal vent areas. *Zootaxa.* **1095**, 1–60. doi:10.11646/zootaxa.1095.1.1
Macpherson E, Richer de Forges B, Schnabel K, Samadi S, Boisselier MC, Garcia-Rubies A (2010) Biogeography of the deep-sea galatheid squat lobsters of the Pacific Ocean. *Deep-Sea Research – I. Oceanographic Research Papers* **57**, 228–238. doi:10.1016/j.dsr.2009.11.002
Macpherson E, Beuck L, Freiwald A (2016) Some species of *Munidopsis* from the Gulf of Mexico, Florida Straits and Caribbean Sea (Decapoda: Munidopsidae), with the description of two new species. *Zootaxa* **4137**, 405–416. doi:10.11646/zootaxa.4137.3.7
Marin I (2020) Northern unicorns of the depths: diversity of the genus *Munidopsis* Whiteaves, 1874 (Decapoda: Anomura: Munidopsidae) in the northwestern Pacific Ocean, with descriptions of three new species along the Russian coast. *Progress in Oceanography* **183**, 102263. doi:10.1016/j.pocean.2020.102263
Marlow JJ, Anderson RE, Reysenbach AL, Seewald JS, Shank TM, Teske AP, Wanless VD, Soule SA (2022) New opportunities and untapped scientific potential in the abyssal ocean. *Frontiers in Marine Science* **8**, 798943. doi:10.3389/fmars.2021.798943
Miljutin DM, Gad G, Miljutina MM, Mokievsky VO, Fonseca-Genevois V, Esteves AM (2010) The state of knowledge on deep-sea nematode taxonomy: how many valid species are known down there? *Marine Biodiversity* **40**, 143–159. doi:10.1007/s12526-010-0041-4
Miller MA, Pfeiffer W, Schwartz T (2010) Creating the CIPRES Science Gateway for inference of large phylogenetic trees. In 'Proceedings of the Gateway Computing Environments Workshop (GCE)', 14 November 2010, New Orleans, LA, USA. INSPEC Accession Number 11705685. (IEEE) doi:10.1109/GCE.2010.5676129
Miranda I, Peres PA, Tavares MDS, Mantelatto FL (2020) New molecular data on squat lobster from the coast of São Paulo State (Brazil) (Anomura: *Munida* and *Agononida*) and insights on the systematics of the family Munididae. In 'Deep-Sea Pycnogonids and Crustaceans of the Americas'. (Ed. ME Hendrickx) pp. 343–356. (Springer: Cham, Switzerland)
O'Hara TD, Williams A, Ahyong ST, Alderslade P, Alvestad T, Bray D, Burghardt I, Budaeva N, Criscione F, Crowther AL, Ekins M, Eléaume M, Farrelly CA, Finn JK, Georgieva MN, Graham A, Gomon M, Gowlett-Holmes K, Gunton LM, Hallan A, Hosie AM, Hutchings P, Kise H, Köhler F, Konsgrud JA, Kupriyanova E, Lu CC, Mackenzie M, Mah C, MacIntosh H, Merrin KL, Miskelly A, Mitchell ML, Moore K, Murray A, O'Loughlin PM, Paxton H, Pogonoski JJ, Staples D, Watson JE, Wilson RS, Zhang J, Bax NJ (2020) The lower bathyal and abyssal seafloor fauna of eastern Australia. *Marine Biodiversity Records* **13**(1), 11. doi:10.1186/s41200-020-00194-1
Oliver PG (2015) Deep-water Thyasiridae (Mollusca: Bivalvia) from the Oman Margin, Arabian Sea, new species and examples of endemism and cosmopolitanism. *Zootaxa* **3995**, 252–263. doi:10.11646/zootaxa.3995.1.21
Palero F (2008) Genètica evolutiva en llagostes de l'infraordre Achelata. PhD thesis, Universitat de Barcelona, Barcelona, Spain.
Palero F, Rodríguez-Flores PC, Cabezas P, Machordom A, Macpherson E, Corbari L (2019) Evolution of squat lobsters (Crustacea, Galatheoidea): mitogenomic data suggest an early divergent Porcellanidae. *Hydrobiologia* **833**(1), 173–184. doi:10.1007/s10750-019-3898-7
Palumbi S (1991) 'Simple fool's guide to PCR.' (Department of Zoology and Kewalo Marine Laboratory, University of Hawaii: Hawaii, HI, USA)
Paradis E (2010) pegas: an R package for population genetics with an integrated–modular approach. *Bioinformatics* **26**, 419–420. doi:10.1093/bioinformatics/btp696
Prada C, Hellberg ME (2021) Speciation-by-depth on coral reefs: Sympatric divergence with gene flow or cryptic transient isolation? *Journal of Evolutionary Biology* **34**, 128–137. doi:10.1111/jeb.13731
Puillandre N, Lambert A, Brouillet S, Achaz G (2012) ABGD, Automatic Barcode Gap Discovery for primary species delimitation. *Molecular Ecology* **21**, 1864–1877. doi:10.1111/j.1365-294X.2011.05239.x

Puillandre N, Brouillet S, Achaz G (2021) ASAP: assemble species by automatic partitioning. *Molecular Ecology Resources* **21**, 609–620. doi:10.1111/1755-0998.13281

Rannala B, Yang Z (2020) Species delimitation. In 'Phylogenetics in the Genomic Era'. (Eds C Scornavacca, F Delsuc, N Galtier) pp. 5.5:1–5.5:18. (Celine Scornavacca, Frédéric Delsuc and Nicolas Galtier) Available at https://hal.inria.fr/PGE/

Raupach MJ, Malyutina M, Brandt A, Wägele JW (2007) Molecular data reveal a highly diverse species flock within the munnopsoid deep-sea isopod *Betamorpha fusiformis* (Barnard, 1920) (Crustacea: Isopoda: Asellota) in the Southern Ocean. *Deep-Sea Research – II. Topical Studies in Oceanography* **54**, 1820–1830. doi:10.1016/j.dsr2.2007.07.009

Reid NM, Carstens BC (2012) Phylogenetic estimation error can decrease the accuracy of species delimitation: a Bayesian implementation of the general mixed Yule-coalescent model *BMC Evolutionary Biology* **12**(1), 196. doi:10.1186/1471-2148-12-196

Rodríguez Flores PC (2021) Biodiversidad, biogeografía y patrones evolutivos en crustáceos (Anomura, Galatheoidea) de zonas tropicales y templadas. PhD thesis, Universitat de Barcelona, Barcelona, Spain.

Rodríguez-Flores PC, Macpherson E, Machordom A (2018) Three new species of squat lobsters of the genus *Munidopsis* Whiteaves, 1874, from Guadeloupe Island, Caribbean Sea (Crustacea, Decapoda, Munidopsidae). *Zootaxa* **4422**, 569–580. doi:10.11646/zootaxa.4422.4.7

Rodríguez-Flores PC, Machordom A, Abelló P, Cuesta JA, Macpherson E (2019*a*) Species delimitation and multi-locus species tree solve an old taxonomic problem for European squat lobsters of the genus *Munida* Leach, 1820. *Marine Biodiversity* **49**, 1751–1773. doi:10.1007/s12526-019-00941-3

Rodríguez-Flores PC, Macpherson E, Machordom A (2019*b*) Revision of the squat lobsters of the genus *Leiogalathea* Baba, 1969 (Crustacea, Decapoda, Munidopsidae) with the description of 15 new species. *Zootaxa* **4560**, 201–256. doi:10.11646/ZOOTAXA.4560.2.1

Rodríguez-Flores PC, Macpherson E, Machordom A (2021) Revision of the squat lobsters of the genus *Phylladiorhynchus* Baba, 1969 (Crustacea, Decapoda, Galatheidae) with the description of 41 new species. *Zootaxa* **5008**, 1–159. doi:10.11646/zootaxa.5008.1.1

Rodríguez-Flores PC, Buckley D, Macpherson E, Corbari L, Machordom A (2020) Deep-sea squat lobster biogeography (Munidopsidae: *Leiogalathea*) unveils Tethyan vicariance and evolutionary patterns shared by shallow-water relatives *Zoologica Scripta* **49**(3), 340–356. doi:10.1111/zsc.12414

Rodríguez-Flores PC, Macpherson E, Machordom A (2022*a*) New species of deep-sea squat lobsters (Decapoda: Anomura: Galatheoidea) from Guadeloupe, French West Indies, unveiled through integrative taxonomy. *Journal of Crustacean Biology* **42**(1), ruab070. doi:10.1093/jcbiol/ruab070

Rodríguez-Flores PC, Macpherson E, Schnabel K, Ahyong ST, Corbari L, Machordom A (2022*b*) Depth as a driver of evolution and diversification of ancient squat lobsters (Decapoda, Galatheoidea, *Phylladiorhynchus*). *Molecular Phylogenetics and Evolution* **171**, 107467. doi:10.1016/j.ympev.2022.107467

Roterman CN, Lee WK, Liu X, Lin R, Li X, Won YJ (2018) A new yeti crab phylogeny: vent origins with indications of regional extinction in the East Pacific. *PloS ONE* **13**, e0194696. doi:10.1371/journal.pone.0194696

Salinas-de-León P, Martí-Puig P, Buglass S, Arnés-Urgellés C, Rastoin-Laplane E, Creemers M, Cairns S, Fisher C, O'Hara T, Ott B, Raineault NA, Reiswig H, Rouse G, Rowley S, Shank TM, Suarez J, Watling L, Wicksten MK, Marsh L (2020) Characterization of deep-sea benthic invertebrate megafauna of the Galapagos Islands. *Scientific Reports* **10**, 13894. doi:10.1038/s41598-020-70744-1

Schmitt WL (1921) The marine decapod Crustacea of California with special reference to the decapod Crustacea collected by the United States Bureau of Fisheries Steamer *Albatross* in connection with the biological survey of San Francisco Bay during the years 1912–1913. *University of California Publications in Zoology* **23**, 1–470.

Schnabel KE, Cabezas P, McCallum A, Macpherson E, Ahyong ST, Baba K, Poore GCB (2011*a*) Worldwide distribution patterns of squat lobsters. In 'The Biology of Squat Lobsters'. (Eds GCB Poore, ST Ahyong, J Taylor) pp. 149–182. (CSIRO Publishing: Melbourne, Vic., Australia)

Schnabel KE, Ahyong ST, Maas EW (2011*b*) Galatheoidea are not monophyletic – molecular and morphological phylogeny of the squat lobsters (Decapoda: Anomura) with recognition of a new superfamily. *Molecular Phylogenetics and Evolution* **58**, 157–168. doi:10.1016/j.ympev.2010.11.011

Schornikov EI (2005) The question of cosmopolitanism in the deep-sea ostracod fauna: the example of the genus Pedicythere. *Hydrobiologia* **538**, 193–215. doi:10.1007/s10750-004-4963-3

Smith SI (1885) On some new or little known decapod Crustacea, from recent Fish Commission dredgings off the east coast of the United States. *Proceedings of the United States National Museum* **7**, 493–511. doi:10.5479/si.00963801.455.493

South A, South MA (2016) Package 'rworldmap'. Mapping global data. *The R Journal* **3**, 35–43.

Sukumaran J, Knowles LL (2017) Multispecies coalescent delimits structure, not species. *Proceedings of the National Academy of Sciences* **114**(7), 1607–1612. doi:10.1073/pnas.1607921114

Swofford DL (2003) PAUP*. Phylogenetic Analysis Using Parsimony (*and Other Methods). Version 4. (Sinauer Associates: Sunderland, MA, USA) Available at https://paup.phylosolutions.com/

Tan MH, Gan HM, Lee YP, Linton S, Grandjean F, Bartholomei-Santos ML, Miller AD, Austin CM (2018) ORDER within the chaos: Insights into phylogenetic relationships within the Anomura (Crustacea: Decapoda) from mitochondrial sequences and gene order rearrangements. *Molecular Phylogenetics and Evolution* **127**, 320–331. doi:10.1016/j.ympev.2018.05.015

Thomas EA, Liu R, Amon D, Copley JT, Glover AG, Helyar SJ, Olu K, Wiklund H, Zhang H, Sigwart JD (2020) *Chiridota heheva* – the cosmopolitan holothurian. *Marine Biodiversity* **50**, 110. doi:10.1007/s12526-020-01128-x

Tilesius G (1815) De cancris Camtschaticis, oniscis, entomostracis et cancellis marinis microscopicis noctilucentibus, Cum tabulis IV. Aeneis et appendice adnexo de acaris et ricinis Camtschaticis. *Mémoires de l'Académie Impériale des Sciences de St Pétersbourg* **5**, 331–405.

Trifinopoulos J, Nguyen LT, von Haeseler A, Minh BQ (2016) W-IQ-TREE: a fast online phylogenetic tool for maximum likelihood analysis. *Nucleic Acids Research* **44**, W232–W235. doi:10.1093/nar/gkw256

Van Dover CL, Factor JR, Williams AB, Berg CJ Jr (1985) Reproductive patterns of decapod crustaceans from hydrothermal vents. *Bulletin of the Biological Society of Washington* **6**, 223–227.

Wenner EL (1982) Notes on the distribution and biology of Galatheidae and Chirostylidae (Decapoda: Anomura) from the Middle Atlantic Bight. *Journal of Crustacean Biology* **2**, 360–377. doi:10.2307/1548053

Whitfield JB, Lockhart PJ (2007) Deciphering ancient rapid radiations. *Trends in Ecology & Evolution* **22**, 258–265. doi:10.1016/j.tree.2007.01.012

Wicksten MK (2012) Decapod Crustacea of the Californian and Oregonian zoogeographic provinces. *Zootaxa* **3371**, 1–307.

Williams AB, Baba K (1989) New squat lobsters (Galatheidae) from the Pacific Ocean: Mariana Back Arc Basin, East Pacific Rise, and Cascadia Basin. *Fishery Bulletin* **87**, 899–910.

Williams AB, Van Dover CL (1983) A new species of *Munidopsis* from submarine thermal vents of the east Pacific Rise at 21°N (Anomura: Galatheidae). *Proceedings of the Biological Society of Washington* **96**, 481–488.

Yule GU (1925) II. – A mathematical theory of evolution, based on the conclusions of Dr J. C. Willis, F. R. S. *Philosophical Transactions of the Royal Society of London – B. Biological Sciences* **213**, 21–87. doi:10.1098/rstb.1925.0002

Zardus JD, Etter RJ, Chase MR, Rex MA, Boyle EE (2006) Bathymetric and geographic population structure in the pan-Atlantic deep-sea bivalve *Deminucula atacellana* (Schenck, 1939). *Molecular Ecology* **15**, 639–651. doi:10.1111/j.1365-294X.2005.02832.x

Zeppilli D, Vanreusel A, Danovaro R (2011) Cosmopolitanism and biogeography of the genus *Manganonema* (Nematoda: Monhysterida) in the deep sea. *Animals* **1**, 291–305. doi:10.3390/ani1030291

Zhang J, Kapli P, Pavlidis P, Stamatakis A (2013) A general species delimitation method with applications to phylogenetic placements. *Bioinformatics* **29**, 2869–2876. doi:10.1093/bioinformatics/btt499

Data availability. All genetic data are publicly available on GenBank (https://www.ncbi.nlm.nih.gov/genbank/). Collecting information, images and life habitus pictures are available through the Harvard Museum of Comparative Zoology's MCZbase (https://mczbase.mcz.harvard.edu/) and the Scripps Institution of Oceanography Benthic Invertebrate Collection database (https://sioapps.ucsd.edu/collections/bi/).

Conflicts of interest. G. Giribet is the Editor-in-Chief of *Invertebrate Systematics* and G. W. Rouse is Associate Editor of *Invertebrate Systematics*. Despite this relationship, these editors did not at any stage have Editor-level access to this manuscript while in peer review, as is the standard practice when handling manuscripts submitted by an editor to this journal. *Invertebrate Systematics* encourages editors to publish in the journal and editors are kept totally separate from the decision-making process for their own manuscripts. The authors declare that they have no further conflicts of interest.

Declaration of funding. P. C. Rodríguez-Flores is funded by an E. O. Wilson Biodiversity Postdoctoral Fellowship at the Museum of Comparative Zoology, Harvard University. This project was partially funded by a LinnéSys Award (Systematic Association and Linnean Society). Shipping time, specimen collection or preliminary analyses were funded by the National Science Foundation (NSF) Office of Polar Programs Award 1043749 (N. Wilson, G. Rouse and R. Burton); NSF Division of Ocean Sciences Awards OCE-0826254 and OCE-1634172 (G. Rouse, L. Levin); the Monterey Bay Aquarium Research Institute; the Schmidt Ocean Institute; the Ocean Exploration Trust and National Oceanic and Atmospheric Administration Ocean Exploration and Research; and Scripps Institution of Oceanography.

Acknowledgements. We thank the staff of the Department of Invertebrate Zoology in the MCZ, especially J. Trimble and A. Baldinger, for support provided during the revision of the MCZ collection. We also thank C. Piotrowski from the California Academy of Sciences, San Francisco, for facilitating loans of specimens for this study, and K. Reed and M. Nizinski from the USNM for facilitating loans and hosting the corresponding author at the museum support centre of the Smithsonian Institution. We thank the captains, crew, submersible pilots, technicians and scientific participants on all research cruises who contributed to this study. We are grateful to E. Recuero, S. Derkarabetian, E. Macpherson, the Associate Editor and one reviewer for helpful comments on the manuscript draft.

Author affiliations
[A]Department of Organismic and Evolutionary Biology, Museum of Comparative Zoology, Harvard University, 26 Oxford Street, Cambridge, MA 02138, USA.
[B]Scripps Institution of Oceanography, University of California San Diego, La Jolla, CA 92093, USA.